

INFORMATION TO USERS

This manuscript has been reproduced from the microfilm master. UMI films the text directly from the original or copy submitted. Thus, some thesis and dissertation copies are in typewriter face, while others may be from any type of computer printer.

The quality of this reproduction is dependent upon the quality of the copy submitted. Broken or indistinct print, colored or poor quality illustrations and photographs, print bleedthrough, substandard margins, and improper alignment can adversely affect reproduction.

In the unlikely event that the author did not send UMI a complete manuscript and there are missing pages, these will be noted. Also, if unauthorized copyright material had to be removed, a note will indicate the deletion.

Oversize materials (e.g., maps, drawings, charts) are reproduced by sectioning the original, beginning at the upper left-hand corner and continuing from left to right in equal sections with small overlaps.

Photographs included in the original manuscript have been reproduced xerographically in this copy. Higher quality 6" x 9" black and white photographic prints are available for any photographs or illustrations appearing in this copy for an additional charge. Contact UMI directly to order.

ProQuest Information and Learning
300 North Zeeb Road, Ann Arbor, MI 48106-1346 USA
800-521-0600

UMI[®]

University of Alberta

Targeting of Biotinylated Long-Circulating Liposomes to Human Ovarian Cancer

By

Chris Zhiming Fan



**A thesis submitted to the Faculty of Graduate Studies and Research in partial
fulfillment of the requirement for the degree of Master of Science**

In

Pharmaceutical Sciences

Faculty of Pharmacy and Pharmaceutical Sciences

Edmonton, Alberta

Spring 2002



**National Library
of Canada**

**Acquisitions and
Bibliographic Services**

**395 Wellington Street
Ottawa ON K1A 0N4
Canada**

**Bibliothèque nationale
du Canada**

**Acquisitions et
services bibliographiques**

**395, rue Wellington
Ottawa ON K1A 0N4
Canada**

Your file Votre référence

Our file Notre référence

The author has granted a non-exclusive licence allowing the National Library of Canada to reproduce, loan, distribute or sell copies of this thesis in microform, paper or electronic formats.

The author retains ownership of the copyright in this thesis. Neither the thesis nor substantial extracts from it may be printed or otherwise reproduced without the author's permission.

L'auteur a accordé une licence non exclusive permettant à la Bibliothèque nationale du Canada de reproduire, prêter, distribuer ou vendre des copies de cette thèse sous la forme de microfiche/film, de reproduction sur papier ou sur format électronique.

L'auteur conserve la propriété du droit d'auteur qui protège cette thèse. Ni la thèse ni des extraits substantiels de celle-ci ne doivent être imprimés ou autrement reproduits sans son autorisation.

0-612-69707-X

Canada

University of Alberta

Library Release Form

Name of Author: Chris Zhiming Fan

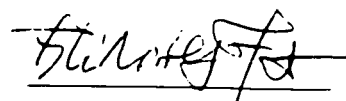
Title of Thesis: Targeting of Biotinylated Long-Circulating Liposomes to Human Ovarian Cancer

Degree: Master of Science

Year This Degree Granted: 2002

Permission is hereby granted to the University of Alberta Library to reproduce single copies of this thesis and to lend or sell such copies for private, scholarly or scientific research purpose only.

The author reserves all other publication and other rights in association with the copyright in the thesis, and except as herein before provided, neither the thesis nor any substantial portion thereof may be printed or otherwise reproduced in any material form whatever without the author's prior written permission.



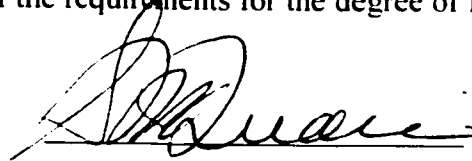
3B, 8914—112ST, NW
Edmonton, AB, T6G2C5
Canada

Date: Jan. 4, 2002

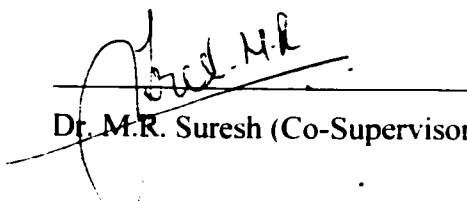
University of Alberta

Faculty of Graduate Studies and Research

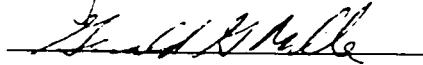
The undersigned certify that they have read, and recommend to the Faculty of Graduate Studies and Research for acceptance, a thesis entitled "Targeting of biotinylated long-circulating liposomes to human ovarian cancer", submitted by Chris Zhiming Fan in partial fulfillment of the requirements for the degree of Master of Science in Pharmaceutical Sciences.



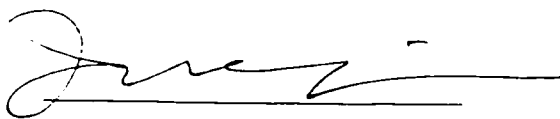
Dr. S.A. McQuarrie (Supervisor)



Dr. M.R. Suresh (Co-Supervisor)



Dr. G.G. Miller (Committee Member)



Dr. J.S. Sim (External Examiner)

Date: 4 Jan 2002

Dedicated

To

**My dear parents, Yuan Dasheng and Fan Zailan, my sister Yuan Zhiqun for their
endless love accompanying me all the times.**

Abstract

Our project is a novel multistep radioimmunotherapeutic approach to be used as an adjuvant treatment for ovarian cancer. The CA-125 antigen is located on the surface of ovarian cancer cells. First, anti-CA125 monoclonal antibodies (Mabs) B43.13 and B27.1 were purified and labeled with a long-armed biotin. Secondly, the free biotin concentration was less than 10nM as determined by a sensitive ELISA and may not significantly compromise the strategy of biotinylated liposome targeting. The biotin transport mechanism was studied to understand the inhibition of transporting and the potential non-specific binding of biotinylated liposomes. Finally, biotinylated liposomes were prepared and a preliminary *in vitro* study was performed to demonstrate the targeting of liposomes to ovarian cancer cells using confocal laser scanning microscopy (CLSM). The results indicated that biotinylated liposomes specifically bound to NIH OVCAR-3 human ovarian cancer cells via biotinylated monoclonal antibodies and a streptavidin-biotin system.

Acknowledgements

I would like to express my sincere appreciation to my supervisor Dr. SA McQuarrie for his kindness, understanding, and encouragement. Without his insight to direct and supervise, this project would not have been possible. I would also like to thank my co-supervisor Dr. MR Suresh for his full knowledge, valuable suggestions, and kindly supplied reagents. My appreciation will be extended to Dr. GG Miller for his kind words and suggestions in my thesis and project, to Dr. JR Mercer for his kind help during my study here. Additionally, I would also like to thank all the colleagues in Dr. Suresh's lab at present and in the past, including Dr. Ashok Kumar, Soraya Shahhosseinei, Rajesh Vij, Trivikram Chebrolu *et al.* for their direct help and friendship. Finally, I would like to thank many friends of mine at the University of Alberta for their friendship and help in my life. I do experience a lot. I would like to take this opportunity to thank all of you and wish you all the best.

CHAPTER 1.....	1
LITERATURE REVIEW	1
1.1 CANCER	1
1.2 CANCER THERAPY	2
1.3 OVARIAN CANCER.....	4
1.3.1 CA-125 Antigen.....	8
1.4 RADIOIMMUNOTHERAPY	8
1.4.1 Radioimmunotherapy in Ovarian Cancer	11
1.5 MONOCLONAL ANTIBODIES	14
1.5.1 Production of Monoclonal Antibodies	14
1.5.2 Structure and Function of Monoclonal Antibodies	15
1.5.3 Applications of Monoclonal Antibodies	17
1.5.4 Anti-CA125 Monoclonal Antibodies B43.13 and B27.1	17
1.5.5 Bispecific Monoclonal Antibodies.....	18
1.6 LIPOSOMES	19
1.6.1 Advantages of Liposomes.....	21
1.6.2 Different Types of Liposomes and Their Applications	22
1.7 BIOTIN-AVIDIN/STREPTAVIDIN SYSTEM	23
1.7.1 Biotin.....	23
1.7.3 Streptavidin.....	25
1.7.4 Biotin-Avidin/Streptavidin System and Its Application	25
1.8 HYPOTHESES AND OBJECTIVES.....	27
CHAPTER 2.....	30
PRODUCTION AND PURIFICATION OF BIOTINYLATED MAB B43.13 AND B27.1	30
2.1 INTRODUCTION	30
2.1.1 Tissue Culture	30
2.1.2 Purification Techniques	31
2.1.3 ELISA and Affinity Study.....	32
2.1.4 SDS-PAGE	34
2.1.5 Biotinylated Antibodies	35
2.2 MATERIALS AND METHODS.....	40
2.2.1 Tissue Culture and Storage.....	40
2.2.2 Purification of Mabs B43.13 and B27.1	42
2.2.3 ELISA and Relative Affinity Study.....	44
2.2.4 SDS-PAGE	45
2.2.5 Production of Biotinylated Monoclonal Antibodies	47
2.2.6 Characteristics of Biotinylated Monoclonal Antibodies	48
2.3 RESULTS AND DISCUSSION	52
2.3.1 Growth of Mabs B43.13 and B27.1 Cell Lines.....	52
2.3.2 Purification of Mabs B43.13 and B27.1	52
2.3.3 ELISA and Affinity Study.....	54
2.3.4 SDS-PAGE	59
2.3.5 Production of Biotinylated Monoclonal Antibodies	61
2.3.6 Confirmation of Biotinylation Using an ELISA Technique.....	63
2.3.7 In Vitro Confirmation of Biotinylation Using CLSM	65

CHAPTER 3.....	67
BIOTIN TRANSPORT IN OVARIAN CANCER CELLS.....	67
3.1 INTRODUCTION	67
3.1.1 Quantitative Measurement of Biotin Content.....	67
3.1.2 Biotin Transport.....	68
3.2 MATERIALS AND METHODS.....	71
3.2.1 Determination of Biotin Content Using HABA Assay.....	71
3.2.2 Determination of Biotin Content Using an ELISA Technique.....	73
3.2.3 Biotin Uptake As a Function of the Biotin Concentration.....	75
3.2.4 Protein Assay.....	78
3.2.5 Calculation of the Counting Efficiency of a Liquid Scintillation Counter	79
3.2.6 Calculation of the Counting Efficiency of a Microbeta.....	79
3.2.7 Biotin Uptake As a Function of the Incubation Time	80
3.2.8 Determination of V_{max} and K_m	81
3.3 RESULTS AND DISCUSSION	81
3.3.1 HABA Assay.....	81
3.3.2 Determination of Biotin Content Using an ELISA Technique.....	85
3.3.3 Biotin Uptake As a Function of the Biotin Concentration.....	90
3.3.4 Protein Assay With Bio-Rad Reagent.....	95
3.3.5 Biotin Uptake As a Function of the Incubation Time	96
3.3.6 Determination of V_{max} and K_m	100
CHAPTER 4.....	103
BIOTINYLATED LONG-CIRCULATING LIPOSOMES AND <i>IN VITRO</i> TARGETING STUDIES USING CONFOCAL LASER SCANNING MICROSCOPY	103
4.1 INTRODUCTION	103
4.1.1 Liposomes.....	103
4.1.2 Confocal Laser Scanning Microscopy	104
4.2 MATERIALS AND METHODS.....	108
4.2.1 Preparation of Biotinylated Liposomes Encapsulated with Sulforhodamine B	108
4.2.2 Purification of Liposomes Using a Sephadex G50 Column	109
4.2.3 Stability of Liposomes	110
4.2.4 <i>In Vitro</i> Targeting via the Biotin-Streptavidin System Using CLSM.....	110
4.3 RESULTS AND DISCUSSION	112
4.3.1 Preparation of Liposomes	112
4.3.2 <i>In Vitro</i> Targeting Study.....	116
CHAPTER 5.....	121
SUMMARY AND FUTURE WORK.....	121
REFERENCES	127

LIST OF TABLES

Table 1.1	FIGO staging system for cancer of the ovary	6
Table 1.2	Characteristic of radionuclides	11
Table 1.3	Structure and classification of monoclonal antibodies	16
Table 3.1	Km values of biotin transport in different cell lines	69
Table 3.2	Determination of the biotin concentration in unknown samples using a HABA assay	84
Table 3.3	Comparison of the formula and R^2 value in different ranges of biotin standard curve using an ELISA technique	89
Table 3.4	Determination of biotin concentration in unknown samples using an ELISA technique	89
Table 3.5	Calculation of the counting efficiency of a liquid scintillation counter	90
Table 3.6	Calculation of the uptake efficiency in SKOV cells	91
Table 3.7	Original data for biotin uptake amount vs. biotin concentration in SKOV cells using a liquid scintillation counter	93
Table 3.8	Original data for biotin uptake amount vs. incubate time in OVCAR cells	96
Table 3.9	Original data for biotin uptake amount vs. incubation time in SKOV cells using a liquid scintillation counter	98

LIST OF FIGURES

Figure 1.1	A schematic representation of a biotinylated long-circulating liposome target ovarian cancer cells via a bispecific monoclonal antibody	12
Figure 1.2	The basic structure of an antibody	15
Figure 1.3	A schematic representation of liposome bilayer structure and a phospholipid molecule	20
Figure 1.4	Structure of D-biotin	24
Figure 1.5	A schematic representation of a biotinylated long-circulating liposome target ovarian cancer cells via a biotinylated Mab	29
Figure 2.1	Structure of Sulfo-NHS-LC-Biotin and NHS-Biotin	36
Figure 2.2	Sulfo-NHS-LC-Biotin reacts with a primary amine	38
Figure 2.3	Biotin hydrazide reacts with a carbohydrate group	39
Figure 2.4	Purification of Mab B43.13 using a Protein G column	53
Figure 2.5	Comparison of different incubation times of Mab B27.1 with CA125 antigen using an ELISA technique	55
Figure 2.6	Comparison of different incubation times of Mab B43.13 with CA125 antigen using an ELISA technique	56
Figure 2.7	Comparison of the relative affinity of Mabs B43.13 and B27.1	58
Figure 2.8	SDS-PAGE result	60
Figure 2.9	Confirmation of biotinylation of Mab B27.1 using an ELISA technique	64
Figure 2.10	<i>In vitro</i> confirmation of biotinylation of Mab B27.1 using CLSM	66
Figure 3.1	Enzyme velocity as a function of the concentration of a substrate	70
Figure 3.2	The 1/velocity as a function of the 1/[substrate]	71
Figure 3.3	Biotin standard curve using HABA assay	82
Figure 3.4	Biotin standard curve using an ELISA technique for 0.4pM–4μM	86
Figure 3.5	Biotin standard curve using an ELISA technique for 10–35nM	87
Figure 3.6	Biotin standard curve using an ELISA technique for 17.5–27.5nM	88
Figure 3.7	Biotin uptake rate vs. biotin concentration in SKOV cell lines	92

Figure 3.8	Biotin uptake vs. biotin concentration in SKOV cell lines (with cold biotin)	94
Figure 3.9	Standard curve for protein assay using Bio-Rad reagent	95
Figure 3.10	Biotin uptake rate vs. incubation time in OVCAR cell lines using a 1450 Microbeta	97
Figure 3.11	Biotin uptake kinetics vs. incubation time in SKOV cells using a liquid scintillation counter	99
Figure 3.12	Determination of K_m and V_{max} in SKOV cell lines	101
Figure 3.13	Determination of K_m and V_{max} in OVCAR cell lines	102
Figure 4.1	A schematic representation of confocal laser scanning microscopy	105
Figure 4.2	Purification of liposomes using a Sephadex G50 column	114
Figure 4.3	Stability of liposomes for storage at room temperature for 4 days	115
Figure 4.4	Biotinylated antibody specifically binds to the surface of OVCAR cells	117
Figure 4.5	Biotinylated liposomes specifically bind to the surface of OVCAR cells	119
Figure 4.6	Preliminary internalized results of botinylated monoclonal antibody and biotinylated liposomes	120

ABBREVIATIONS AND SYMBOLS

ΔA	Delta A; change in absorbancy
[A]	Concentration of A
ADCC	Antibody dependent cell mediated cytotoxicity
Ag	Antigen
BSA	Bovine serum albumin
BsMab	Bsipecific monoclonal antibody
Bq	Becquerel (unit of radioactivity)
CDC	Complement dependent cytotoxicity
CH	Cholesterol
CLSM	Confocal laser scanning microscope
Ci	Curie
Conc.	Molar concentration (M or moles/L)
Cpm	Counts per minute
CTL	Cytotoxic T lymphocytes
Da	Dalton
DMSO	Dimethyl sulfoxide
DNA	Deoxyribonucleic acid
dps	Disintegration per second (unit of radioactivity) 1 dps=1 Bq
DSPC	Distearoyl phosphatidylcholine
DSPE	Distearoyl phosphatidylethanolamine
EDTA	Etylenediaminetetraacetic acid
ELISA	Enzyme linked immunosorbent assay
Fab	Fragment of antigen binding
FACS	Fluorescence activated cell sorter
FBS	Fetal bovine serum
Fc	Crystallizable fragment

FITC	Fluorescein isothiocyanate
HAMA	Human antimouse antibody
HABA	4-hydroxyazobenzene - 2' - carboxylic acid
HAT	Hypoxanthine, Aminopterin, and Thymidine
HBSS	Handk's balanced salt solution
HEPES	N-(2-hydroxyethyl)piperazine-N'-(2-ethanesulfonic acid)
HPLC	High performance liquid chromatography
HRPO	Horseradish peroxidase
IgG	Immunoglobulin G
i.p.	Intraperitoneal
i.v.	Intravenous
K_d	Dissociation constant
LUV	Large unilamellar vesicles
NHS	N-hydroxysuccinimide
Mab	Monoclonal antibody
2-ME	2-mercaptoethanol
MEM	Eagle's minimum essential medium
MLV	Multilamellar vesicles
MW	Molecular weight
OD	Optical density
rbc	Red blood cell
RES	Reticuloendothelial system
RIT	Radioimmunotherapy
RP-HPLC	Reversed phase high performance liquid chromatography
rpm	Revolutions per minute
RPMI 1640	Roswell Park Memorial Institute medium number 1640
PBS	Phosphate buffered saline
PI	Isoelectric point
PEG	Polyethylene glycol

SA	Streptavidin
SD	Standard deviation
SDS	Sodium dodecyl sulfate
SDS-PAGE	Sodium dodecyl sulfate polyacrylamide gel electrophoresis
SUV	Small unilamellar vesicles
T_c	Transition temperature
TEMED	N,N,N,N-tetramethylenediamine
TMB	3, 3', 5, 5' - tetramethylbenzidine
TPBS	Phosphate buffered saline containing Tween 20
Tris	Tris (hydroxymethyl) aminoethane
ULV	Unilamellar vesicles
UV	Ultraviolet
10⁶	Mega (symbol = M)
10³	Kilo (symbol = k)
10⁻³	Milli (symbol = m)
10⁻⁶	Micro (symbol = μ)
10⁻⁹	Nano (symbol = n)
10⁻¹²	Pico (symbol = p)
10⁻¹⁵	Femto (symbol = f)

CHAPTER 1

LITERATURE REVIEW

1.1 CANCER

Cancer is the second leading fatal disease in America, second only to cardiovascular disease (Goldsby RA *et al.*, 2000). Every year, more than 6 million lives are lost worldwide from cancer, which has a tremendous impact on society and human beings. To date, more than 900 drugs have been developed in the world for various cancer therapies. Although every year, many novel approaches are continuing to be discovered, designing an effective and convincing clinical trial for cancer therapy is a demanding task (Goldsby RA *et al.*, 2000; Berghammer P *et al.*, 2001).

Many causes and mechanisms of cancer are still unknown. However, we know that cancer cells arise from normal cells. Cancer cells multiply in an uncontrolled way, resulting in a tumor. A benign tumor will not spread from the original site to other parts of the body and is noncancerous. On the other hand, a malignant tumor is a cancerous tumor, which can spread to surrounding tissue and even go further to the whole body through the bloodstream or lymphatic system, resulting in the production of metastatic tumors. Normally, the metastatic tumor will elevate the potential for mortality and render cancer therapy more difficult (Pratt WB *et al.*, 1994).

There are about 200 different kinds of cancer in different parts of the body. Almost all the parts of the body (skin, tissue, organ, etc.) can develop cancer (Ayre SG *et al.*, 2000). We can directly classify cancers into organ-based categories with their names, including lung cancer, breast cancer, ovarian cancer, prostate cancer, etc. On the

other hand, cancer can be classified into four major groups as shown below (Goldsby RA *et al.*, 2000).

- Carcinomas are the most common types of cancer (80-90%) and arise from the epithelial system, including skin, lungs, ovaries, and other organs.
- Sarcomas are found in the connective tissue, including bones, muscles, fibrous tissues, and fat.
- Leukemias are the cancers of white blood cells in the bloodstream and bone marrow.
- Lymphomas arise from the lymphatic system, such as the spleen and the lymph nodes.

Many factors can trigger cancer, including cigarette smoking, unhealthy diet, sun exposure, viruses and some chemicals, which normally disrupt the DNA or genetic code of a cell. Some transformed cells are not dangerous immediately, while others multiply uncontrollably, resulting in a tumor (Pratt WB *et al.*, 1994; Ayre SG *et al.*, 2000). It may take years for a malignant tumor to produce clinically detectable symptoms. Cancer is common in people above the age of 50, although young people can also develop the disease (Ayre SG *et al.*, 2000).

1.2 CANCER THERAPY

Since cancer cells develop from normal cells, the similarity between cancer cells and normal cells can cause problems in cancer therapy and diagnosis in the early stages. The other reason that causes problems in cancer therapy is due to cancer invasion and metastatic spreading. Metastatic cancer can increase the risk of mortality (Pratt WB *et al.*, 1994; Stockler M *et al.*, 2000). To date, early detection provides the best chance for recovery from cancer, indicating that we should develop cancer therapy and early cancer diagnosis together.

To date, surgery, radiotherapy, and chemotherapy play important roles in cancer therapy. They have their advantages and limitations. These methods are often used together to deal with the malignant tumors to increase therapeutic efficacy.

Surgery is used to remove the primary tumor while radiotherapy kills the cancer cells with penetrating streams of photons, such as γ -rays. Radiotherapy is often used together with surgery to control the tumor growth and kill residual cancer cells after surgery (Leibel SA *et al.*, 1998). However, the side effects of radiation to the other normal cells, especially to the blood producing cells in bone marrow, may result in low levels of white blood cells and platelets (Leibel SA *et al.*, 1998). Common side effects in radiotherapy are nausea, fatigue, skin irritation, and hair loss (Leibel SA *et al.*, 1998). Side effects of radiotherapy are dependent on the radiation dose, treatment site and the disease that is treated (Russell NS *et al.*, 1999). Surgery and site-directed radiotherapy are both local treatments, which fail to deal with distant metastatic cancer (Russell NS *et al.*, 1999).

Chemotherapy, using anticancer drugs in treatment, can deal with both local and metastatic cancer. Most of the time chemotherapy is used with surgery, radiotherapy or other kinds of therapeutic approaches instead of using it alone. It can shrink a tumor before surgery or radiotherapy, which is called neo-adjuvant therapy. Additionally, it can kill cancer cells that may remain after surgery or radiotherapy (Tannock IF *et al.*, 2001). Different anticancer drugs have their own anticancer mechanism. Most anticancer drugs play a role in interfering with different stages of cell division to kill cancer cells (Pratt WB *et al.*, 1994). Therefore, anticancer drugs are most useful against rapidly dividing cells, however, they can also cause side effects on the bone marrow and GI tract, since the stem cells in these organs have a high cellular proliferation rate (Jeyakumar A *et al.*, 2001). Unfortunately, there are many kinds of cancer cells. Some vigorously divide while others are dormant and will vigorously divide later. The anticancer drugs can kill the vigorously dividing cells but are less efficient in killing the dormant cells, which will vigorously divide later and lead to recurrent problems (Pratt WB *et al.*, 1994). Additionally, the most

common malignant tumors, including prostate, lung, and colon cancer, usually have a low rate of dividing cells which makes them less susceptible to anticancer drugs (Pratt WB *et al.*, 1994; Jeyakumar A *et al.*, 2001).

From the above description, we know that surgery, radiotherapy, and chemotherapy are important approaches for current cancer therapy. However, much work on improving current therapies and discovering new approaches are still required because millions of lives are still lost due to this second leading killer. Many cancers are found to be metastatic at the time of presentation and cannot be easily cured. Furthermore, radiotherapy and chemotherapy can cause problems in bone marrow and rapid dividing cells, resulting in low level of white blood cells and interference of normal cell division (Leibel SA *et al.*, 1998; Brian EH *et al.*, 1994). In recent years, more effort has been directed to the research related to the molecular mechanisms of cancer therapy. Research has been done related to immunotherapy, gene therapy, antisense oligonucleotides, cytokines, drug targeted delivery, growth factor, angiogenesis inhibitors (drugs that block the nutrition of tumors) and tumor vaccines (signal transduction inhibitors) (Brian EH *et al.*, 1994). Many new approaches and new drugs are discovered every year (Harrington KJ *et al.*, 2000; Ernest J *et al.*, 2001). With the development of molecular biology and biotechnology, we will know more about the mechanism of cancer development.

1.3 OVARIAN CANCER

Ovarian cancer is the second leading gynaecologic malignancy and the fourth leading cause of cancer death in the United States (Parkin DM *et al.*, 1993). Approximately 70% of women have already developed the advanced stage malignancy at the time of diagnosis (Tenereillo MG *et al.*, 1995). This high mortality rate is due to lack of symptoms in early stages and lack of effective screening tools. Ovarian cancer has only vague clinical symptoms, even when it invades the upper abdomen and develops towards an advanced stage. The CA125 serum test is used to monitor ovarian cancer in high-risk groups and monitor disease progression in

therapy. However, this test has its limitations and many other diseases also contribute to elevated CA125 levels, such as pregnancy, hepatitis and endometriosis (Bast RC *et al.*, 1983; Nouwen EJ *et al.*, 1987). Improving diagnostic techniques to detect early stages is critical to increase survival, because 5 years survival of early stage is high up to 50-90%, while 5 year survival of advanced stages is only 15-20% (Landis SH *et al.*, 1999; Michale C *et al.*, 1994).

The ovaries are composed of germ cells, stromal cells, and epithelial cells. Each of these cell types can develop cancer, resulting in many different types of ovarian cancer. To date, at least 10 different types of ovarian cancer have been discovered. Among these, ovarian cancer in epithelial cells is the most common (Gershenson DM *et al.*, 1998). Women have a 1.4% chance of getting ovarian cancer during their life time. The risk will increase in high risk groups, including family history of breast cancer, ovarian cancer and colon cancer, older women above age 50, and high dietary fat.

Epithelial cancers begin on the surface of an ovary and then spread to the tissues around the ovary, including the uterus, bladder, and peritoneum. Tumor cells in the peritoneum may cause abdominal swelling, which is due to formation of ascites fluid. Tumor cells can also spread to the lymphatic system and nodes around the ovaries. Vascular spread is minimal and results in little distant spread rather than the phenomenon of peritoneal carcinomatosis (McGinn KA *et al.*, 1998). According to the International Federation for Gynecology and Obstetrics (FIGO), ovarian cancer can be classified in four stages as shown in Table 1.1.

Stage	Description
I	Tumor limited to the ovaries
II	Tumor invades to pelvic extension
III	Tumor invades to pelvis, retroperitoneal nodes, small bowel, and omentum.
IV	Tumor forms to distant metastases.

Table 1.1 FIGO staging system for cancer of the ovary. Stage I can be further subclassified into IA, IB and IC categories. Stage II can be further subclassified into IIA, IIB, and IIC categories. Stage III can be further subclassified into IIIA, IIIB, and IIIC categories (McGinn KA *et al.*, 1998).

In 2001, approximately 2,500 Canadian women will develop ovarian cancer and 60% of these women will die as estimated in Canadian Cancer Statistics 2001. Approximately 27,000 women develop ovarian cancer every year and 14,000 women die of this each year in the United States (McGinn KA *et al.*, 1998). The 5 year survival of early stage, Stage I and II, is as high as 50-90% while 5 year survival of advanced stages, III and IV, is only 15-20% (Landis SH *et al.*, 1999; Michael C *et al.*, 1994). High risk groups include those with a family history of breast cancer, ovarian cancer, and colon cancer, as well as delayed pregnancy beyond age 30, exposure to high levels of radiation, and high dietary fat (Parkin DM *et al.*, 1993; Gershenson DM *et al.*, 1998).

The traditional treatments, surgery, chemotherapy, and radiotherapy play important roles in ovarian cancer treatment. Current regimens for advanced epithelial ovarian cancer are surgical debulking, followed by chemotherapy with platinum and paclitaxel (Taxol) as the first line therapy. Platinum is a conventional first line chemotherapy drug while paclitaxel was approved by Food and Drug Administration in 1992 (Michelle C *et al.*, 1994; Giorgio B *et al.*, 2001). The alternative first line chemotherapy drugs are carboplatin and cisplatin (Roland PY *et al.*, 1998). If the first line chemotherapy fails or patients experience recurrence after the first line therapy, secondary/salvage treatment regimens will be considered, which include topotecan (Hycamtin), doxorubicin (Doxil) (Hakes TB *et al.*, 1992; Kudelka A *et al.*, 1996; Giorgio B *et al.*, 2001) and intraperitoneally delivered radiolabeled monoclonal antibodies (Alvarez R *et al.*, 1997).

Due to low long-term survival (below 20%) with current treatments, numerous novel therapeutic approaches for ovarian cancer have been studied by several investigators, including immunotherapy (Hedda H *et al.*, 1994; Han X *et al.*, 1997), targeted approaches (Harrington KJ *et al.*, 2000; Ernest J *et al.*, 2001) and gene therapy (Wang MH *et al.*, 1998; Rosenfeld ME *et al.*, 1995; Vivian E *et al.*, 1998).

1.3.1 CA-125 Antigen

CA125 (cancer antigen 125), an ovarian cancer associated antigen, is a high molecular weight glycoprotein that is located on the surface of ovarian cancer cells and is also shed into the blood and ascite (Bast RC *et al.*, 1983; O'Brien TJ *et al.*, 1986). CA125 is a heterogeneous molecular mixture containing primarily O-linked glycosylated chains and minor N-linked chains (Fendrick JL *et al.*, 1993). Electrophoresis on polyacrylamide gels without sodium dodecyl sulfate (SDS) shows that the CA125 antigen has a molecular weight above 1MDa. Electrophoresis with SDS under non-reducing conditions shows a subfraction at 200-250KDa (O'Brien TJ *et al.*, 1986; Masuho Y *et al.*, 1984; Matsuoka Y. 1987). The antigen is sensitive to protein denaturing reagents, which result in the loss of binding activity. It was discovered by Bast RC (Bast RC *et al.*, 1981) and normally exists in the body in a very low concentration (under 35U/mL) (David M *et al.*, 1998). CA125 has been proposed as a screening tool to diagnose ovarian cancer, however, because CA125 levels can change during menstruation, pregnancy, hepatitis, and endometriosis (Bast RC *et al.*, 1983; Nouwen EJ *et al.*, 1987; Zurawski VR *et al.*, 1988), its presence is not specific to ovarian cancer. Because no reliable screening tool is available for ovarian cancer, serum CA125 levels are still used to test women who are in a high risk category (Kenemans P *et al.*, 1993; Tuxen MK *et al.*, 1995).

1.4 RADIOIMMUNOTHERAPY

Radioimmunotherapy (RIT) involves the use of intact Mabs or their fragments to selectively direct cytotoxic radionuclides or other effectors to the site of disease. This therapeutic approach is particularly useful for cancer therapy because selectively killing cancer cells without harming normal cells is the main challenge in cancer therapy.

RIT was first used to treat melanoma with radioiodinated polyclonal antiserum in 1956 (Abrams G *et al.*, 2000). The invention of monoclonal antibodies by Kohler

and Milstein in 1975 (Kohler and Milstein, 1975) held great promise for RIT because of the high specificity and high affinity of the Mabs to tumor-associated antigens (TAAs). Numerous tumor-associated antigens, growth factors, and altered glycoproteins have been identified for Mab targeting (Jurcic JG *et al.*, 1996). Various Mabs labeled with different radionuclides, including ^{131}I , ^{90}Y and ^{186}Re , have been used for cancer therapy (Mach JP *et al.*, 1981; Finkler NJ *et al.*, 1989; Stewart JSW *et al.*, 1990; Meredith RF *et al.*, 1996; Nicholson S *et al.*, 1995). However, several obstacles need to be overcome before this kind of approach can be successfully realized. Targeted antigens may not be expressed on all the malignant cells. Antigen size, density may be changed and antigens may be shed from the cell surface (Strand SE *et al.*, 1993). Approximately 20% accumulation in mouse tumor models and less than 0.1% accumulation in human beings via intravenous injection are found in the RIT targeting (Mann BD *et al.*, 1984; Abrams G *et al.*, 2000). This low accumulation in human beings is probably due to blood supply, a high interstitial pressure, poor vascularization in the solid tumor, which cause problems in antigen accessibility. Additionally, the HAMA (human antimouse antibody) response in human beings result in compromised pharmacokinetic distribution. This low uptake, combined with inappropriate accumulation in organs, such as the liver, spleen and bone marrow are some of the main problems in RIT (McQuarrie SA *et al.*, 2001).

Another problem occurs when murine antibodies are recognized as foreign proteins and are rapidly cleared from bloodstream by human antimouse antibodies (HAMA). Approximately 40% of patients develop the HAMA response after a single injection while this proportion increases up to 90% with repeated administrations (Dillman RO *et al.*, 1994; Khazaeli MB *et al.*, 1994). Since single dose therapy generally elicits no significant response in cancer therapy, the HAMA problem needs to be overcome before RIT can be effectively used (Abrams G *et al.*, 2000). To overcome these delivery problems, various efforts have been made as described below.

- In order to increase tumor-to-normal tissue ratios, pre-targeting strategies involving unlabeled Mabs and radiolabeled effector molecules have been studied.

First, the unlabeled Mabs are administered to achieve the maximum accumulation in a tumor site expressing the antigen. Normally, it takes 1 day to complete Mab accumulation at the tumor site and several days are required to remove the residual Mab from the bloodstream and other normal tissues (Goodwin DA *et al.*, 1997). After residual Mabs on the other normal tissues have been removed, a radiolabeled effector, such as liposomes, are administered to target the unlabeled Mab. The Mab should be retained on the surface of tumor without shedding and internalization to facilitate the second targeting. The ideal radiolabeled effector should have high selectivity to the tumor sites and high affinity to unlabeled Mab. Through this pretargeting strategy, better tumor-to-normal tissue ratios are expected. Several different types of pretargeting strategies have been described, including Mab/hapten, Mab/biotin-avidin system, BsMab, and Mab/oligonucleotide (Goodwin DA *et al.*, 1997). The Mab should retain its immune specificity after modification and have high affinity to tumor associated antigen without significant shedding or internalization. Additionally, Mabs should have high affinity to the radiolabeled effector. Several studies confirm enhanced tumor-to-normal tissue ratios using pretargeting agents in multistep therapeutic approaches (Goodwin DA *et al.*, 1988, 1997; Sung C *et al.*, 1995; Paganelli G *et al.*, 1990; Gestin JF *et al.*, 2001).

- In order to increase targeting and achieve better tumor-to-normal tissue ratios, regional administration, including intraperitoneal administration and intrathecal administration have been studied (Mezzanzanica D *et al.*, 1991).
- In order to reduce the HAMA response, Mab fragments, including Fab, F(ab')₂, and single chain Fv (sFv) have been developed. Since the mouse Fc portion is the main factor to trigger the HAMA response, Mab fragments that do not contain mouse Fc portion are less immunogenic. However, Mab fragments are cleared more rapidly from the plasma and may not accumulate sufficiently to the tumor (Milenic DE *et al.*, 1991; Schreiber GJ *et al.*, 1995). Several biotechnological engineering techniques have been studied to achieve chimeric and humanized antibodies because these antibodies do not produce a HAMA response. Mouse/human chimeric Mabs containing the human constant regions may be less

immunogenic and retain antigenic recognition while fully humanized Mabs are also being studied (Liu AY *et al.*, 1987; Kashmiri SVS *et al.*, 1995; Dianne MF *et al.*, 1999).

To date, radioimmunotherapy is still at a preliminary stage and many challenges remain in this approach. Radioimmunotherapy has been investigated to treat different diseases, including lymphoma, leukemia, breast, ovarian, and lung cancer. There are some encouraging results in treating lymphoma and leukemia, however there has been limited success in treatment of solid tumors because antigen accessibility is difficult (Abrams G *et al.*, 2000). RIT for Hodgkin's lymphoma is near approval (Abrams G *et al.*, 2000). The increasing volume of research data on RIT show a potential for future cancer therapy (Gestin JF *et al.*, 2001; Abrams G *et al.*, 2000; Chetanneau A *et al.*, 1994; Breitz HB *et al.*, 1993).

1.4.1 Radioimmunotherapy in Ovarian Cancer

RIT has been investigated as a potential adjuvant therapy for ovarian cancer by several investigators (Andersson H *et al.*, 2001; McQuarrie SA *et al.*, 2001; Markman M 1998; Malik J *et al.*, 1997). Numerous monoclonal antibodies labeled with different radioisotopes, including ^{131}I , ^{90}Y and ^{186}Re have been intraperitoneally injected to patients and clinical results were promising in dealing with early stage ovarian cancer (Epenetos AA *et al.*, 1987; Finkler NJ *et al.*, 1989; Stewart JSW *et al.*, 1990).

Radionuclide	Half-life	Major emissions
^{131}I	8 days	Beta, gamma
^{90}Y	2.5 days	Beta
^{186}Re	3.5 days	Beta, gamma

Table 1.2 Characteristic of radionuclides

Our project utilizes a novel multistep radioimmunotherapeutic approach to be used as an adjuvant treatment for ovarian cancer. Bispecific monoclonal antibody (BsMab) with anti-CA125 and anti-biotin paratopes will direct cytotoxic radionuclides encapsulated in liposomes to the site of ovarian cancer. The BsMab is intraperitoneally administered to target ovarian cancer cells as a pretargeting agent. At a later time, biotinylated liposomes containing cytotoxic radionuclides will be directed to the anti-biotin binding sites of BsMab. The schematic representation of the strategy is shown in Figure 1.1.

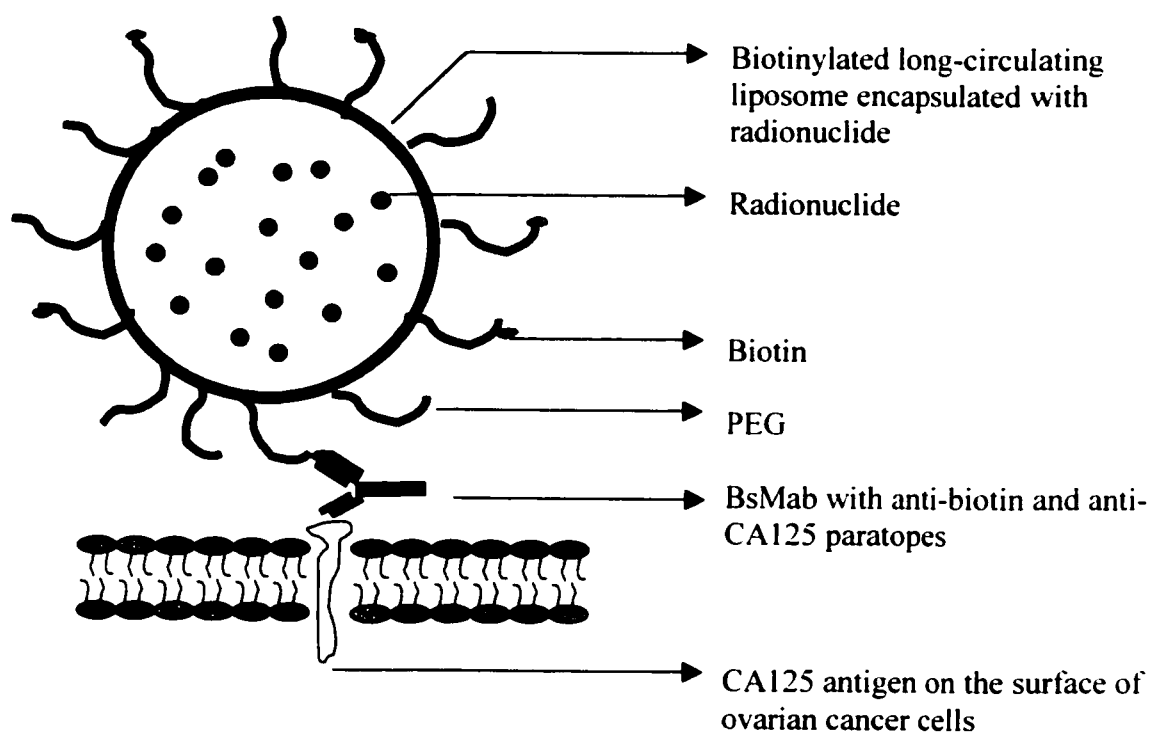


Figure 1.1 A schematic representation of a biotinylated long-circulating liposome target ovarian cancer cells via a bispecific monoclonal antibody

Many challenges still exist in this RIT approach. To overcome the low tumor-to-normal tissue ratios, pretargeting strategies involving unlabeled Mabs and radiolabeled molecules have been studied by several investigators (Goodwin DA *et al.*, 1988, 1997; Sung C *et al.*, 1995; Paganelli G *et al.*, 1990), resulting in enhanced tumor-to-normal tissue ratios. In our project, we propose to use a multistep protocol to increase the radiation delivered to the cancer, while sparing normal tissue. The rationale for this approach is described below.

Ovarian cancer is a disease with a poor prognosis. Approximately 70% of women have already developed advanced stage malignancy at the time of diagnosis. The 5 year survival of advanced stage patients is only 15-20% (Landis SH *et al.*, 1999; Michale C *et al.*, 1994) with the current treatment. Therefore, it is important to find a new therapeutic approach to treat these patients. Ovarian cancer cells remain in the peritoneal cavity for most of the natural history of the disease (McGinn KA *et al.*, 1998) and several studies suggest that intraperitoneal administration provides optimum treatment for patients with ovarian carcinomatosis (Garrido MA *et al.*, 1990; Mezzanzanica D *et al.*, 1991). Therefore, we propose to use intraperitoneal administration to deal with ovarian cancer patients. Our approach can be used to treat Stages I, II and III patients. This protocol is not intended for Stage IV patients that have systemic metastatic cancer. However, since systemic spread is uncommon and carcinomatosis is usually confined to the peritoneal cavity, our approach may benefit most patients, if successful. Furthermore, the i.p. route results in better pharmacokinetic distribution and a greater tumor-to-normal ratio and low toxicity. The majority of antibody accumulation is found on free-floating cells in the ascites (Klein JL *et al.*, 1986; Abrams PG *et al.*, 2000). There is almost no Mab uptake in tumor masses greater than 8 gram because of high interstitial pressures, less lymphoid vessels, and poor vascularization (Jain RK 1990). The advantages of treating micrometastases within the peritoneal cavity with intraperitoneal RIT are high antibody accessibility, high antibody penetration, and high-energy beta particles penetration (Jain RK 1990). The disadvantage of targeting to free-floating cells

expressing the CA125 may be avoided by tapping the ascitic fluid to facilitate the antibody accumulation in the micrometastases (Abrams PG *et al.*, 2000).

Liposomes were selected to carry the cytotoxic radionuclides, ^{188}Re , to the site of disease. This delivery vehicle was chosen because liposomes can encapsulate more radioactivity than Mabs that are typically used in RIT, resulting in an adequately radiolabeled effector system. Intraperitoneal administration will also benefit liposome targeting in ovarian cancer metastases. Liposomes with a diameter greater than 110nm are retained in the peritoneal cavity for about 24hr (Nassander UK *et al.*, 1992). The Mab should remain on the surface of tumor without shedding and internalization to facilitate the liposome targeting. Since our CA125/antibody conjugate is slowly internalized by 12–24hr, and antibody shedding was happened by 5–20hr (Xiao Z *et al.*, 2001), the optimal time to deliver the biotinylated liposomes may be 4hr.

1.5 MONOCLONAL ANTIBODIES

1.5.1 Production of Monoclonal Antibodies

A monoclonal antibody (Mab) may have high specificity and affinity to a particular determinant on an antigen. In 1975, G. Kohler and C. Milstein first introduced a revolutionary technique to produce Mabs (Kohler and Milstein, 1975). They used red blood cells (rbc) from sheep as a source of antigen to immunize mice and then obtained the anti-sheep rbc B cells that were harvested from the spleens of the mice. Next, spleen cells and immortalized myeloma cells were fused to obtain a hybridoma, which produces monoclonal antibody. The positive hybridoma that produced the desired Mab was obtained through cloning and recloning techniques. The discovery of the Mab was an important invention, which brought a great potential in cancer diagnosis and cancer therapy.

1.5.2 Structure and Function of Monoclonal Antibodies

A Mab is composed of four polypeptide chains, two identical heavy chains (molecular weight 55,000-90,000) and two identical light chains (molecular weight 25,000). These four polypeptide chains form a Y-shaped structure as shown in Figure 1.2.

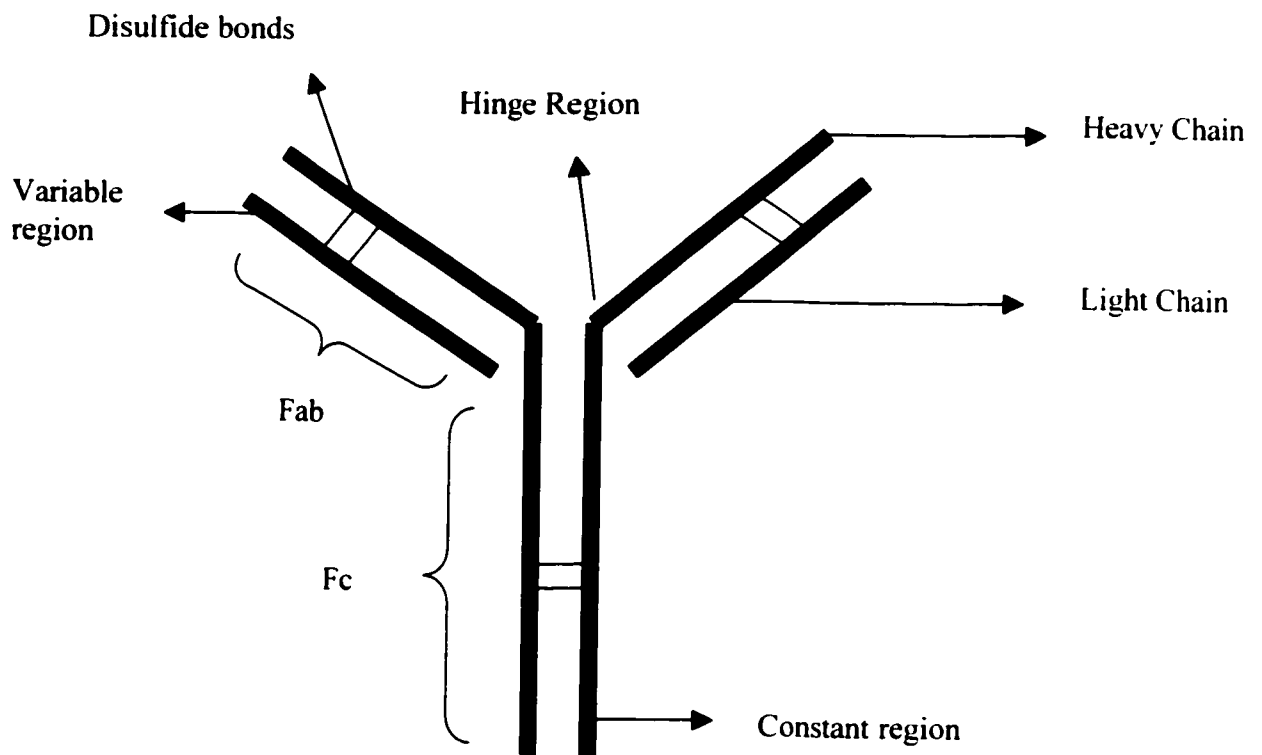


Figure 1.2 The basic structure of an antibody

The two identical heavy chains and light chains are linked with disulfide bonds. The amino terminal on the Fab outer portion is known to exhibit sequence variation and is called the variable region. The carboxy terminal on the Fc portion remains fairly consistent and is called the constant region.

The Fab (fragment of antigen binding) portions of the immunoglobulin contain variable regions of amino acids. Its function is to bind the specific antigen. The Fc (crystallizable fragment) portions of the immunoglobulin contain constant regions of carbohydrate groups. Its normal function is to induce antibody-dependent cell-mediated cytotoxicity (ADCC), complement-dependent cytotoxicity (CDC), antigen aggregation, and precipitation. The Fc portions of the immunoglobulin are used to classify antibodies. The five different classes of antibodies (IgG, IgA, IgD, IgE, IgM) are different by unique amino acid sequences in the heavy chain constant regions. The letter gamma, alpha, delta, epsilon and mu stand for them respectively. IgG and IgA can be further classified as IgG1 to 4 and IgA1 to 2. There are only two types of light chains, kappa and lambda. The hinge region is a flexible area, which can change the distance between the two antigen-binding sites and facilitate binding to different agents. The Table 1.3 and Figure 1.2 provide additional information about antibodies (Goldsby RA *et al.*, 2000).

	Ig G	IgM	IgA	IgE	IgD
Heavy chains	γ	μ	α	ϵ	δ
Light chains	κ or λ	κ or λ	κ or λ	κ or λ	κ or λ
Subclasses	1,2,3,4	1,2	1,2	None	None
MW (Da)	150,000	900,000	350,000	190,000	180,000

**Table 1.3 Structure and classification of monoclonal antibodies
(Goldsby RA *et al.*, 2000)**

1.5.3 Applications of Monoclonal Antibodies

Monoclonal antibodies have been extensively used in immunoassay and diagnosis of diseases (Bodey B *et al.*, 1996; Divgi CR *et al.*, 1996). Mabs are used in many ELISA techniques to determine the level of antigens, including viral and bacterial antigens (Winkelstein A *et al.*, 1997). Additionally, Mabs have been used to monitor normal components in human serum (Rose N *et al.*, 1997). Mabs can also be coupled to an affinity column to purify desired molecules and cells. For example, anti-CD34 Mab was used to harvest CD34 stem cells, resulting in purification of CD34 stem cell to reconstitute the hematopoietic stem cells of cancer patients (Goldsby RA *et al.*, 2000). Fluorescently labeled Mabs are used in confocal laser scanning microscopy (CLSM) and fluorescence activated cell sorter (FACS) techniques (Goldsby RA *et al.*, 2000).

The clinical uses of Mabs are still in the beginning stages. Radiolabeled Mabs are used to target disease and are visualized using a gamma camera in a technique known as radioimmunoimaging. When used in radioimmunotherapy, Mabs labeled with appropriate radionuclides can direct cytotoxic radiation to the cancer (Stewart JSW *et al.*, 1990; Nicholson S *et al.*, 1995). Additionally, Mabs can be used as a pretargeting agent to target the disease, followed by attracting anticancer drugs or cytotoxic radionuclides to the tumor sites (Goodwin DA *et al.*, 1997; Gestin JF *et al.*, 2001). For example, Mabs OKB7, LLB, IF5, and C2B8 have been used in clinical trials to treat Non-Hodgkin's lymphoma (Scheinberg DA *et al.*, 1990; Abrams PG *et al.*, 2000).

1.5.4 Anti-CA125 Monoclonal Antibodies B43.13 and B27.1

A total of 26 monoclonal antibodies against CA125 have been studied (Nustad K *et al.*, 1996). CA125 has three main antigenic domains, one is OC125-like (group A), the other two are M11-like (group B) and OV197-like (group C). The OC125-like domain has four subgroups, with different binding specificities. Mabs B43.13 and

B27.1 are mouse IgG1 anti-CA125 monoclonal antibodies, which we used in our project. Mab B43.13 belongs to the A3 subgroup and Mab B27.1 belongs to the A4 subgroup.

Monoclonal antibodies B43.13 and B27.1 were developed by Biomira Inc. and have affinities of 10^9 M^{-1} for CA125 (Capstick V *et al.*, 1991; McQuarrie SA *et al.*, 1998). The affinity of Mab B27.1 is 1.6 times higher than the affinity of Mab B43.13 (Nustad K *et al.*, 1996). The hybridoma was produced by immunization of a mouse with CA125 antigen to obtain antibody-producing mouse spleen cells. After fusing these spleen cells with malignant myeloma cells, the mixture was transferred to HAT (Hypoxanthine, Aminopterin and Thymidine) selective medium or a FACS (fluorescence activated cell sorter) to select the appropriate hybridoma. Cloning and recloning techniques were used to select the positive clones with good antibody characteristics. ELISA and SDS-PAGE were used to evaluate the Mabs' specificity and purity.

1.5.5 Bispecific Monoclonal Antibodies

Although bispecific monoclonal antibodies (BsMab) were not used in my work, they will be briefly reviewed as they are one of the keys of the overall project. BsMabs have two different antigen binding paratopes capable of binding two different antigens. They can be produced by three ways:

- Chemical cross-linking of two antibodies (Dijk J *et al.*, 1989; Perez P *et al.*, 1986).
- Fusion of two hybridomas or fusion of hybrid cells with spleen cells to obtain a quadroma or trioma (Milstein C *et al.*, 1984; Lanzavecchia A *et al.*, 1987).
- Genetic engineering technology (Shalaby MR *et al.*, 1992).

The two antigen binding sites of the BsMab lend it to applications in immunoassay and in *in vitro* targeting (Milstein *et al.*, 1983; Suresh MR *et al.*, 1986). Several

studies relating their uses in ovarian cancer have been documented (Mezzanzanica D *et al.*, 1988; Kriangkum J *et al.*, 2000; Pupa SM *et al.*, 1988; Moller SA *et al.*, 1991). For example, Mezzanzanica *et al.* used BsMabs to direct lysis of ovarian carcinoma by activated human cytotoxic T lymphocytes and Fc receptor-mediated lysis. Their results were promising.

1.6 LIPOSOMES

Liposomes were introduced by Alec Bangham in 1965 (Bangham AD *et al.*, 1965). Phospholipids were put in an aqueous solution and spontaneously formed spherical vesicles named liposomes. The Figure 1.3 shows the structure of a liposome and a phospholipid molecule. Phospholipids are composed of one hydrophilic head and two hydrophobic tails. When dispersed in water, the phospholipid molecules are arranged in a sphere, where heads join together on the outside while tails join together on the inside. The major forces that form a stable bilayer are hydrophobic interactions, van der Waals' forces and hydrogen bonding. Thus, liposomes consist of one or more lipid bilayers that encapsulate an aqueous interior. As is commonly known, the basic structure of a biomembrane is the phospholipid bilayer. Thus, liposomes mimic the biomembrane, resulting in its initial use as a model for biological membranes (Kinsky *et al.*, 1977). The first liposome product appeared on the market in 1986 as a skin cosmetic product and liposomes were used successfully in cosmetic formulations for some years (Mayhew E *et al.*, 1984; Egbaria K *et al.*, 1991). Since then, researchers realized the importance of liposomes and their enormous potential as a drug delivery system. Liposomes have four ways to deliver their contents, including endocytosis, fusion with the cell membrane, lipid exchange with the cell membrane, and adsorption due to their special phospholipid bilayer structure. To date, more than one hundred different liposomal formulations have been found. Among these, the most important application of liposomes is as a controlled drug delivery for cancer therapy and gene therapy (Allen TM *et al.*, 1993; Kim S 1993; Cullis, PR *et al.*, 1989; Ostro MJ *et al.*, 1989; Lasic DD 1992).

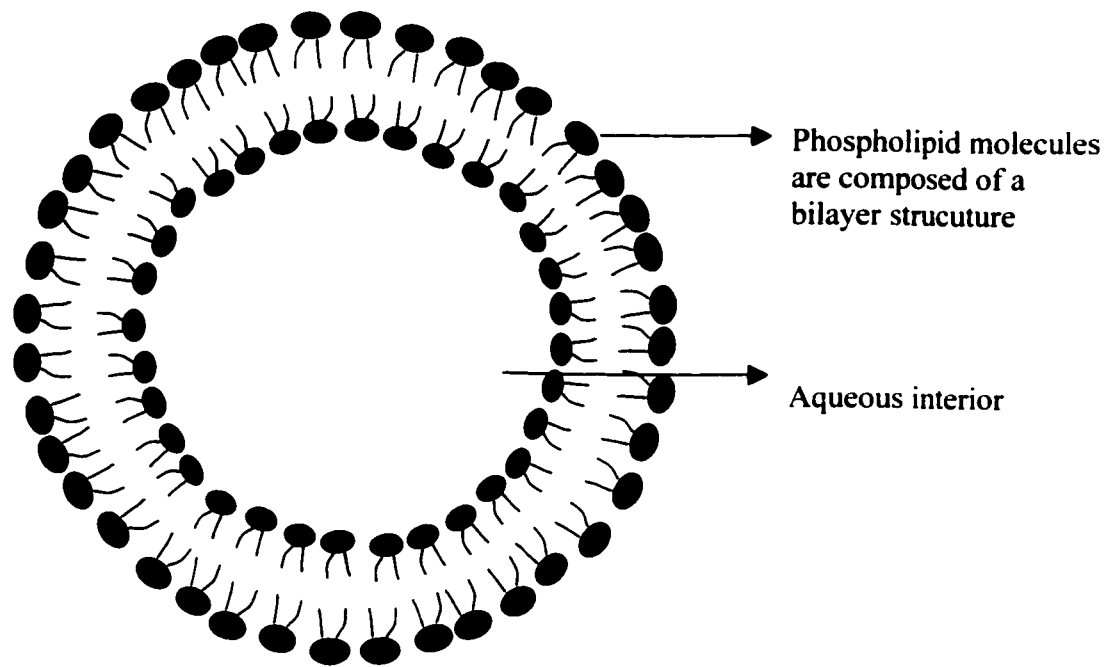


Figure 1.3a A schematic representation of liposome bilayer structure, which is formed by phospholipids.

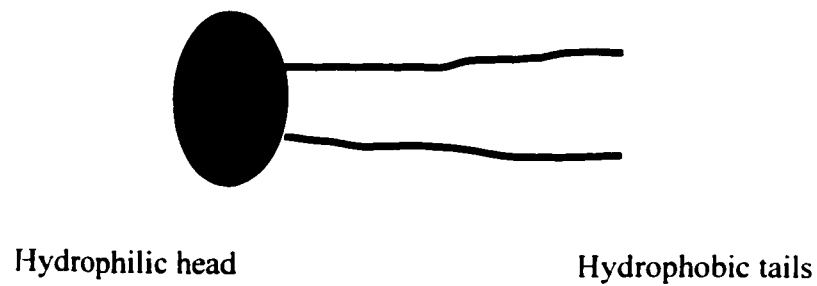


Figure 1.3b A schematic representation of a phospholipid molecule

1.6.1 Advantages of Liposomes

The first liposomes were prepared by putting phospholipids in an aqueous solution, which then spontaneously formed spherical vesicles (Bangham AD *et al.*, 1965). Liposomes consist of one or more lipid bilayers, and are a promising drug delivery system. Liposomes are prepared from natural phospholipids, thus are biodegradable, non toxic, and non immunogenic (Gregoriadis G *et al.*, 1993; Kim S 1994). Liposomes have different sizes, compositions, charges, and lamellarity according to the method of preparation (Olson F *et al.*, 1979; Szoka F *et al.*, 1980; Gruner SM *et al.*, 1985). This flexibility makes them a promising controlled delivery system to carry many different kinds of compounds, including anticancer drugs, peptides, and DNA. Liposomes can encapsulate both water-soluble and water-insoluble drugs because of their structure (Talsma H *et al.*, 1992). Water-soluble drugs are encapsulated in the aqueous interior while water-insoluble drugs are encapsulated in the lipid bilayer.

In addition to liposomes affecting the pharmacokinetics and the biodistribution of encapsulated drugs, their own half-life in circulation can be increased by PEGylation (Juliano RL *et al.*, 1978; Allen TM *et al.*, 1991; Webb MS *et al.*, 1995). Conventional liposomes without polyethylene glycol (PEG) are easily taken up by the reticuloendothelial system (RES) while the PEGylated liposomes, named "stealth liposomes", can avoid RES uptake and have a long circulating half-life.

Liposomes can provide passive targeting to tumour sites through extravasation from leaky vasculature (Leserman L *et al.*, 1990; Dewhirst MW *et al.*, 1989; Gabizon A *et al.*, 1988). When conjugated with antibodies, liposomes can provide active targeting to specific antigen binding sites (Zigterman GJ *et al.*, 1987; Matthay KK *et al.*, 1984; Wolff B *et al.*, 1984). Therefore, liposomes can accumulate in specific disease sites and increase therapeutic efficacy. Through their specific targeting ability, liposomes can reduce the toxicity of encapsulated drugs, especially for antimicrobial, antiviral, and anticancer drugs (Juliano RL *et al.*, 1978; Forssen EA *et*

al., 1981; van Hoesel *et al.*, 1984). In addition, liposomes increase the stability of encapsulated drugs, especially for peptides and DNA used in gene therapy (Fleisher D *et al.*, 1995; Shek PN *et al.*, 1986).

1.6.2 Different Types of Liposomes and Their Applications

Liposomes consist of multilamellar vesicles (MLV, more than one lipid bilayer) and unilamellar vesicles (ULV, only one lipid bilayer). ULV are further subclassified as small unilamellar vesicles (SUV, diameter less than 100nm) and large unilamellar vesicles (LUV, diameter great than 100nm) (Rongen H *et al.*, 1997; Hope MJ *et al.*, 1985). There are many different types of liposomes based on different compositions. The main types are conventional and special liposomes. Conventional liposomes are made of phospholipids, cholesterol, and charged lipids. On the basis of conventional liposomes, many kinds of special liposomes are made. For example, stealth liposomes containing polyethylene glycol (PEG) are used to avoid clearance by macrophages and the reticuloendothelial system (RES) (Allen TM *et al.*, 1987; Holland JW *et al.*, 1996), thus increasing their circulation time in the bloodstream. Biotinylated liposomes containing biotinylated phospholipid components are used in immunoassay and in *in vitro* targeting studies (Bayer EA *et al.*, 1979; Hashimoto K *et al.*, 1986). Immunoliposomes coupled with antibodies are used in cancer therapy (Zigterman GJ *et al.*, 1987; Matthay KK *et al.*, 1984; Wolff B *et al.*, 1984) and cationic liposomes are used in gene therapy (Stamatos L *et al.*, 1988; Behr JP *et al.*, 1989; Felgner JH *et al.*, 1994). For example, Liposomes coupled with Fab' fragment against the OA3 antigen is used to target the ovarian cancer and liposomes coupled with anti-CD19 Mab is used to target a human B lymphoma (Gregoriadis G *et al.*, 1998).

Different types of liposomes have their own specific targeting ability to different cell lines *in vivo* and *in vitro* (Jan AA *et al.*, 1999). Liposomes coupled with Mab have been extensively used *in vitro* and *in vivo* (Ahmad I *et al.*, 1992; Ahmad I *et al.*, 1993). Various endogenous ligands, like biotin, folate, transferrin, growth factor

receptors etc. have been coupled to liposomes for targeting specific cells, including peptides, protein, carbohydrates, and growth factors on their surface (Allen TM *et al.*, 1998; Hofland H *et al.*, 1995; Vingerhoeds MH *et al.*, 1994).

1.7 BIOTIN-AVIDIN/STREPTAVIDIN SYSTEM

1.7.1 Biotin

The D-isomer of biotin (Figure 1.4) is a small, hydrophobic molecule with a molecular weight of 244.31 Dalton. It exists in every living cell, blood, and tissue in low concentration (0.5nM–10nM) (Guilarte TR *et al.*, 1985; Mock DM *et al.*, 1992, 1996). Liver, kidney, pancreas, and cancerous tumours have a higher biotin content than other tissues (Krieg PA *et al.*, 1987; Merck Index 1989). Biotin is also known as vitamin H and coenzyme R. It functions as an essential cofactor for four carboxylases (acetyl-CoA carboxylase, pyruvate carboxylase, methylcrotonyl-CoA carboxylase, propionyl-CoA carboxylase) that catalyze metabolic reactions. Thus, biotin plays a very important role in the formation and metabolism of fatty acids, glucose, leucine, amino acids, and cholesterol (Zempleni J *et al.*, 1999). Biotin is required by all living cells to maintain basic physiological functions, but can only be synthesized by bacteria, yeasts, algae, and some plants (Mock DM *et al.*, 1996). Humans have to obtain biotin from the diet. Otherwise, they will develop biotin deficiency symptoms, including hair loss and depression. Biotin deficiency is very rare. Normally 30 mg of biotin per day is enough for a human being. Biotin is found in many kinds of foods. Normally, egg yolks and liver are rich sources of biotin (Mock DM 1999; Baumgartner ER *et al.*, 1999; Bonjour JP 1991)

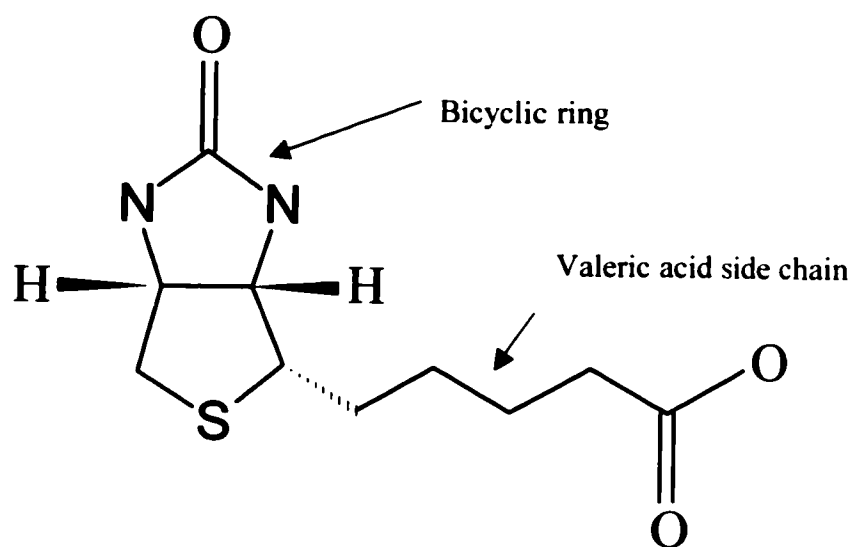


Figure 1.4 Structure of D-biotin (MW 244.31 Dalton)

1.7.2 Avidin

Avidin was originally isolated from a hen's egg-white. It has an isoelectric point (pI) of approximately 10 (Woolley DW *et al.*, 1942; Green NM 1975) and has a molecular weight of about 68,000 Dalton (Dayhoff MO 1972). Avidin is a tetrameric glycoprotein composed of four identical subunits, which have the capability to bind biotin. The oligosaccharide on each subunit is an important characteristic of avidin where asparagine-17 is glycosylated (Delange RJ *et al.*, 1971). Due to its positive charge and carbohydrate characteristics, avidin can nonspecifically bind to charged molecules, membrane sugar receptors, and result in background problems.

1.7.3 Streptavidin

Streptavidin, the bacterial analog of avidin, is a 60,000 Dalton, tetrameric protein isolated from *streptomyces avidinii* (Chalet L *et al.*, 1963). It is similar to avidin and consists of four identical subunits that bind biotin. However, streptavidin is non-glycosylated and nearly neutral protein (pH about 5-6), resulting in reduced nonspecific binding to charged molecules and membrane sugar receptors. Therefore, streptavidin is a popular interchangeable reagent for avidin in many applications, such as localization of antigens on the surface of the cells, and confocal microscope image analysis (Wilchek M *et al.*, 1988; Meier T *et al.*, 1996).

1.7.4 Biotin-Avidin/Streptavidin System and Its Application

The biotin-avidin system is used as a widespread noncovalent biological binding system between a protein and a ligand. Biotin has an extremely strong binding affinity to avidin ($K_d = 1.3 \times 10^{-15}$ M at pH 5) (Green NM 1963). The bicyclic ring of biotin slides inside the avidin binding pocket while the carboxyl group on the valeric acid side chain of biotin is not involved in this interaction between biotin and avidin (Mattaj IW 1993; Lain S *et al.*, 1991). The high affinity between biotin and avidin is probably due to the network of hydrogen bonding, proper hydrophobic residues, and

an elegant binding pocket (Wei R *et al.*, 1964; Weber *et al.*, 1992; Freitag S *et al.*, 1997).

Biotin can react with avidin very quickly with the association constant $7 \times 10^7 \text{ M}^{-1} \text{S}^{-1}$. The biotin-avidin complex is extremely resistant to many types of denaturing agents and extreme conditions, including wide pH 2–13 range, temperature up to 132°C, and organic solvents (Donovan JW *et al.*, 1973; Ross SE *et al.*, 1986). Therefore, the biotin-avidin system is very popular in biological research to cross-link two biotinylated molecules. Its extremely high affinity makes it a valuable tool in affinity chromatography, immunoblotting, ELISA, localization of antigens on cells and tissues, confocal microscope image analysis, flow cytometry, and genetic mapping (Berger M *et al.*, 1975; Wilchek M *et al.*, 1988; Wilchek M *et al.*, 1990; Armstrong R *et al.*, 1990).

Many advantages exist in the application of the biotin-avidin system, including

- The bond formation is fast between biotin and avidin while the affinity is the strongest known noncovalent biological binding.
- It can increase sensitivity in enzyme or fluorescent immunoassays because of four binding sites.
- Avidin is easily covalently linked to different ligands, including fluorochromes and enzymes. These conjugated agents are readily available from many commercial suppliers.
- Biotinylated reagents are also readily available from many commercial suppliers. Biotinylation procedures are relatively simple and inexpensive. When used under gentle conditions, they can preserve the biological activity of the associated protein.

1.8 HYPOTHESES AND OBJECTIVES

This thesis describes some preliminary results for this project, including the *in vitro* targeting ability of liposomes to ovarian cancer. Since the BsMab remains under development, a biotinylated anti-CA125 Mab was first used to target the ovarian cancer cells, followed by attracting biotinylated liposomes to the ovarian cancer cells. The biotin-streptavidin system was used to connect these two biotinylated agents. As a pretargeting step, biotinylated anti-CA125 monoclonal antibody was incubated with ovarian cancer cells. Mab targeting was monitored with FITC (green) labeled streptavidin bound to the biotinylated Mab. Next, biotinylated long-circulating liposomes encapsulated with sulforhodamine B (red dye) was added. The red dye was used to monitor the binding localization of the liposomes and was used as a surrogate for radionuclides. Confocal laser scanning microscopy was used to monitor *in vitro* targeting. The schematic representation of this *in vitro* targeting is shown in Figure 1.5.

On the basis of the above discussion, the following hypotheses were tested in this thesis:

- Biotinylated anti-CA125 monoclonal antibody can specifically target ovarian cancer cells with CA125 antigen on its surface.
- Through the biotin-streptavidin system, biotinylated anti-CA125 monoclonal antibody can direct biotinylated liposomes to specifically bind to ovarian cancer cells.
- Exogenous biotin in mouse ascites will not inhibit the pretargeting strategy.

To test the above hypotheses, we prepared purified biotinylated anti-CA125 Mabs and biotinylated liposomes. We also need to know whether or not exogenous biotin inhibits this targeting. The following detailed objectives were completed in this thesis.

- Anti-CA125 monoclonal antibodies B43.13 and B27.1 were obtained from the growth of the appropriate hybridomas and were purified using a Protein G column.
- Purified Mab B43.13 and B27.1 were labeled with a long-armed biotin and their characteristics were confirmed using HABA assay, ELISA, and CLSM techniques.
- A sensitive ELISA was developed to determine biotin concentration in mouse ascites for the future *in vivo* application.
- The biotin transport mechanism in ovarian cancer cells was studied to understand the exogenous biotin inhibition of targeting and nonspecific binding.
- Biotinylated long circulating liposomes containing sulforhodamine B were prepared using a commercial extruder.
- Preliminary *in vitro* targeting ability of liposomes to ovarian cancer cells was studied using CLSM.

The following chapters discuss these hypotheses and objectives in detail.

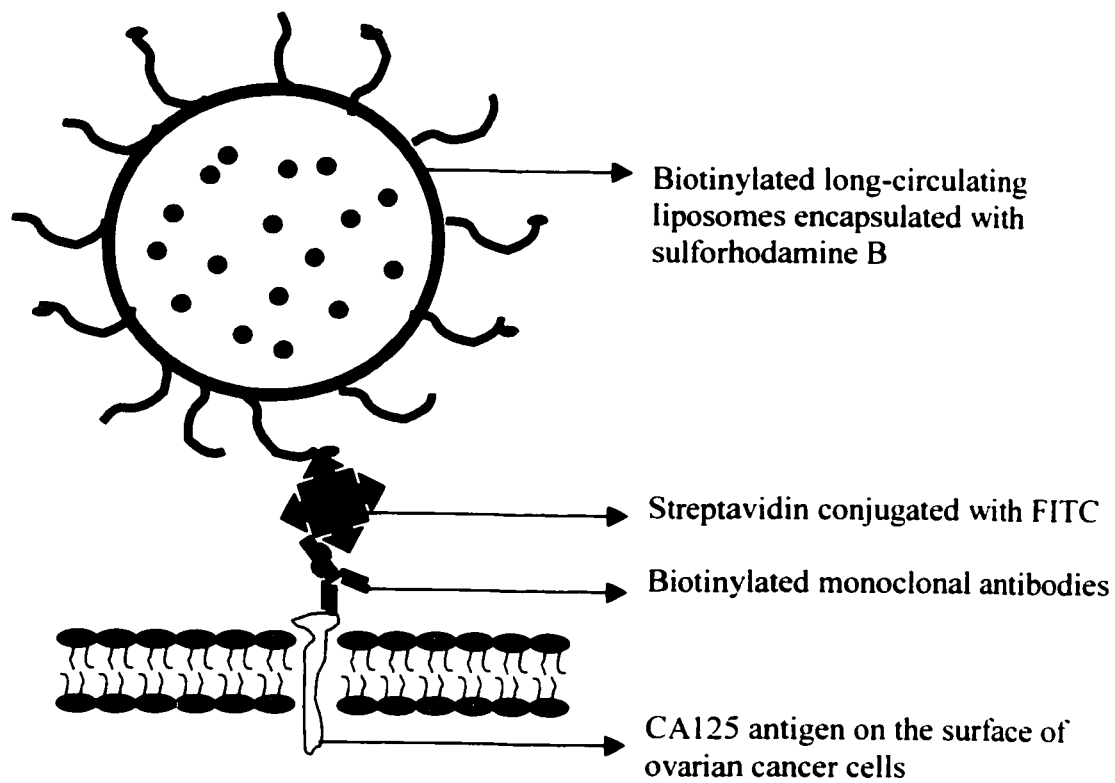


Figure 1.5 A schematic representation of a biotinylated long-circulating liposome target ovarian cancer cells via biotinylated monoclonal antibody

CHAPTER 2

PRODUCTION AND PURIFICATION OF BIOTINYLATED MAB B43.13 AND B27.1

2.1 INTRODUCTION

Biotinylated Mab was used as a pretargeting agent in our *in vitro* targeting study. Therefore, this chapter describes the production and purification of biotinylated anti-CA125 monoclonal antibodies (Mabs) B43.13 and B27.1. The Mabs B43.13 and B27.1 were obtained from the growth of the appropriate hybridomas using RPMI-1640 medium containing 8% fetal bovine serum (FBS). The antibodies were harvested and purified using a Protein G column. A modified ELISA technique was used to evaluate the specificity and the relative affinity of the Mabs. An SDS-PAGE technique was used to determine the purity of the Mabs. Purified Mabs B43.13 and B27.1 were labeled with a long-armed biotin and their characteristics were evaluated using HABA assay, ELISA, and confocal laser scanning microscopy (CLSM) techniques.

2.1.1 Tissue Culture

RPMI-1640 medium was developed by Moore GE and coworkers, and has a wide application for many types of cell lines (Moore GE *et al.*, 1967, 1976). Sterile conditions were employed and cells were grown in an incubator at 37°C, 5% carbon

dioxide with 100% humidity. To obtain enough quantity of antibodies, the cells were grown to a sufficient density prior to harvest.

2.1.2 Purification Techniques

There are many different ways to purify monoclonal antibodies as described by Voet and Coligan (Voet D *et al.*, 1999; Coligan JE *et al.*, 1998). The purification procedure should be performed under mild conditions (near pH 7) to retain Mab activity because the Mab is easily destroyed by strong acid (pH 2), strong base (pH 12) or high temperature conditions (above 50°C). Differential salt concentrations, solvents, temperature, and pH can be used to precipitate the antibodies as a first step, followed by differential chromatography to further purify to obtain relatively pure Mabs. Many commercial columns are available and their principles are described below.

- Affinity chromatography is an adsorption method of separation (Voet D *et al.*, 1999). The immobilized ligands are coupled to a column's matrix and will only bind to a specific antibody. Other proteins will remain unbound and are eluted. The antibody is eluted with 0.1 M glycine, which is removed by dialysis in an appropriated buffer.
- Gel filtration chromatography is also called size-exclusion chromatography (Voet D *et al.*, 1999). The column is packed with a hydrophilic polymeric gel with many pores that is formed from cross-linked dextran beads. It is useful to separate different sizes of the antibodies and antibody fragments. Small size molecules will diffuse into the gel pores and pass through the column slowly. The large molecules, which do not diffuse into the pores, will elute quickly.
- Ion exchange chromatography is used for protein purification as the most common technique because of its high capacity (Voet D *et al.*, 1999). The ion exchange column temporarily binds chloride and sodium ions. When the protein sample passes through the column, the desired protein will displace the ions and

bind to the column. Later, an elution buffer is used to release desired protein to yield a relatively pure product.

- Ultrafiltration is another method for protein purification. Different membranes are used to separate different size proteins (Voet D *et al.*, 1999; Coligan JE *et al.*, 1998).

A Protein G column (affinity chromatography) was used in our project to purify the Mabs B43.13 and B27.1. HiTrap® Protein G column (Sepharose HP 1mL) was purchased from Sigma, St. Louis, MO. The column matrix is originally made from the Type G *Streptococci*, which can specifically bind to the Fc portion of the immunoglobulin G (IgG). The protein G column binds only to the Fc receptor and does not bind to an albumin or a Fab receptor binding site. Approximately 20% ethanol is commonly used to store the column to avoid bacterial growth. 0.02% sodium azide or 0.02% thimerosal may be used if necessary.

2.1.3 ELISA and Affinity Study

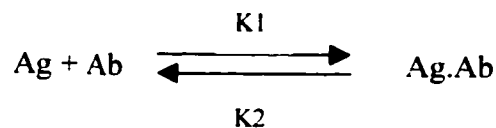
Enzyme-linked immunosorbent assay (ELISA) is a standard analytical technique to quantify the antigens and antibodies with high sensitivity and high specificity. There are many different kinds of ELISA techniques. The most commonly used techniques are indirect ELISA, sandwich ELISA, and residual titration ELISA (Goldsby RA *et al.*, 2000). The methods summarized below were obtained from Coligan *et al.* (Coligan JE *et al.*, 1998).

- Indirect ELISA is used to detect specific antibodies. The microtiter plate is coated with an antigen, followed by addition of a specific antibody. After washing away the first antibody, the second antibody conjugated with an enzyme is added to develop a color, whose intensity is proportional to the amount of the test antibody in solution.
- Sandwich ELISA is the most useful to detect soluble antigens because it has high sensitivity (2–5 times) compared to direct ELISA. The plate is coated with the

purified antibody and is then incubated with a solution containing its antigen. After washing away the unbound antigen, the second antibody conjugated with an enzyme that reacts with the same antigen is added for the second incubation. Finally, the substrate is added to develop a color, whose intensity is proportional to the amount of the antigen.

- The residual titration ELISA is also called competitive indirect ELISA. An antibody is incubated with an antigen and then this mixture is transferred to an antigen pre-coated ELISA plate for a second incubation. The residual antibody, which is not bound in the first incubation, will bind to the ELISA plate. After washing away the unbound reagent, the second antibody conjugated with an enzyme is added to develop a color, whose intensity is inversely proportional with the antigen in the original sample.

The antibody-antigen binding equation is a reversible reaction as shown below.



Where:

$\text{K}_1/\text{K}_2 = \text{K}_a = 1/\text{K}_d = \text{Affinity}$

K_a = association rate constant

K_d = dissociation rate constant

Determination of the affinity of antibodies requires the measurement to be made at molar equilibrium. Numerous methods have been studied to measure the affinity of antibodies, including equilibrium dialysis, electrophoresis, radioimmunoassay, and ELISA (Heegaard NHH *et al.*, 1991; Friguet B *et al.*, 1985; Nimmo GR *et al.*, 1984). Equilibrium dialysis is a commonly accepted technique to determine the affinity of antibodies. The antibody and radiolabeled antigen are separated into two chambers by a semi-permeable membrane, which only allows the movement of unbound antigen, not the antigen-antibody complex. At equilibrium, the bound antigen and unbound antigen can be determined by counting radioactivity in two chambers and

the affinity can be calculated using a Scatchard equation (Scatchard G 1949; Steward MW *et al.*, 1985). The plot of bound/free antigen against bound antigen is linear, in which affinity can be calculated from the slope that is equal to $-K_a$. The major drawback of the equilibrium dialysis is that it is not useful for macromolecular antigens.

ELISA is a popular technique for affinity measurements because of its ease and simplicity. Many different ELISA methods of affinity measurements have been studied by several investigators (Friguet B *et al.*, 1985; Beatty JD *et al.*, 1987; Li CK 1985; Nimmo GR *et al.*, 1984). Variable antigen concentrations are used to react with constant antibody concentrations until an equilibrium is reached. At a later time, the unbound antibody is transferred to a pre-coated ELISA plate to be measured.

2.1.4 SDS-PAGE

Polyacrylamide gel electrophoresis (PAGE) is a widely used technique for analyzing protein. It is a rapid and sensitive method to characterize a protein's size and charge. Without sodium dodecyl sulphate (SDS), the gel is referred to as an undenaturing gel, which is used to resolve natural proteins. With SDS, the gel is a denaturing gel. SDS is a negatively charged ionic detergent, which is used to denature the 3D structure of the antibody and to bind tightly to the antibody. Whereas the reducing agent (2-mercaptoethanol or dithiothreitol) is used to reduce disulfide bonds of the antibody, resulting in obtaining individual heavy and light chains. When this mixture is added to a polyacrylamide gel matrix, the protein-SDS that has a constant negative net charge per mass migrates toward the anode under an electric field. The heavy and light chains are separated by their molecular sizes because the different sized proteins move at different speeds in the gel. Alternatively, both the charge and the size information of the proteins can be determined using a two-dimensional gel electrophoresis technique. Two-dimensional gels are superior to separate protein and determine protein purity to one-dimensional gels (Coligan JE *et al.*, 1998; Goldsby RA *et al.*, 2000).

TEMED (N,N,N,N-tetramethylethylenediamine) and ammonium persulphate are used as an initiator and a catalyst respectively in the SDS-PAGE technique. In the presence of an initiator and a catalyst, the polyacrylamide gels are formed by polymerizing acrylamide with a cross-linking agent (bis acrylamide) (Goldsby RA *et al.*, 2000; Goers J *et al.*, 1993). Since oxidizing agents, such as O₂ inhibit polymerization of polyacrylamide, butanol saturated water is used to cover the gel to separate the gel from the air. In addition, the gel solution is degassed before polymerization to avoid producing bubbles in the gel. The speed of gel formation is controlled by varying the concentration of TEMED and ammonium persulphate. The pore size of the gel is controlled by varying the concentration of acrylamide monomer and cross-linking agent. 5-15% separating gel (Total concentration of acrylamide monomer and bis-acrylamide) is used for most of the protein separation. The higher concentrations result in smaller pore sizes to separate small molecular weight proteins. The stacking gel has different buffer ions from the reservoir buffer and has a few large pore sizes, which provides a sample band before the sample reaches the separating gel, resulting in better resolution (Goldsby RA *et al.*, 2000; Goers J *et al.*, 1993).

2.1.5 Biotinylated Antibodies

Biotin is a hydrophobic molecule with a molecular weight 244.31 Da. Biotin is easily attached to proteins (Bartoli M *et al.*, 1999), antibodies (Lgnatowski TA 1999), enzymes (Rao SV *et al.*, 1999) and nucleic acids (Wilchek M *et al.*, 1988; Levi M *et al.*, 1990). Biotinylated agents are detected using avidin conjugated with an enzyme or fluorescent dye. The biotin-avidin system is the strongest known noncovalent biological interaction between a protein and a ligand ($K_d = 1.3 \times 10^{-15} \text{M}$ at pH 5) (Green NM 1963).

Varieties of biotinylation reagents are commercially available. Normally, a bicyclic ring of biotin slides in the avidin binding pocket and plays an important role in the reaction between the biotin and avidin while the carboxyl group on the valeric acid

side chain is not involved in the interaction (Green NM 1975; Wilchek M *et al.*, 1988) (see Figure 1.3). Therefore, biotin derivatives that modify the carboxyl group on the valeric acid side chain are called biotinylation reagents.

2.1.5.1 Biotinylation Reagents

When bound to antibodies, the biotin can hide in the hydrophobic pocket of an antibody and become inaccessible to avidin. Therefore, it is better to use spacer biotin to enhance efficiency in the formation of the biotin-avidin complex and to avoid inducing changes in the antibody structure (Gretch DR *et al.*, 1987; Hnatowich DJ *et al.*, 1987). Many companies supply the biotin containing a spacer between the protein-binding site and the avidin-binding site (known as long-armed or spacer biotin). Commonly available biotinylation reagents are NHS-biotin and sulfo-NHS-LC-biotin (Figure 2.1).

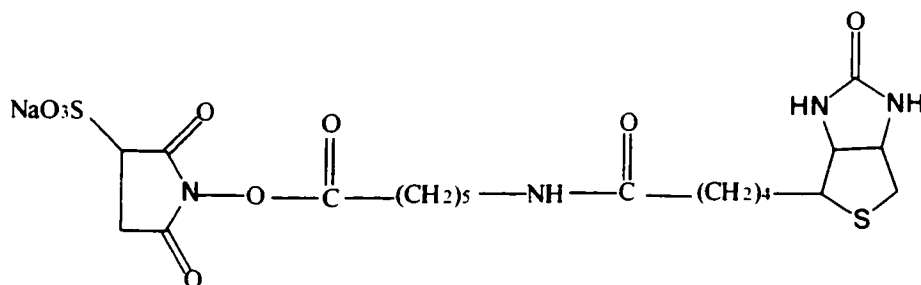


Figure 2.1a Structure of Sulfo-NHS-LC-Biotin (MW 556.58)

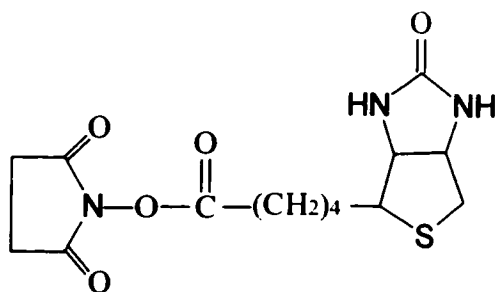


Figure 2.1b Structure of NHS-Biotin (MW 341.38)

NHS-Biotin, a water-insoluble biotin, is a N-hydroxysuccinimide derivative of biotin. NHS ester is the most popularly used reagent to label antibodies containing primary amino groups of lysine residues. The biotinylation procedure is simple and takes place under mild alkaline conditions, which do not interfere with the antibody structure. Sulfo-NHS-LC-biotin, a water-soluble biotin, is a sulfonated derivative of NHS-biotin. The polar characteristics are due to the sulfonate ($-\text{SO}_3$) group on the N-hydroxysuccinimide ring and the compound is impermeable to the cell membrane. Figure 2.2 shows the reaction of sulfo-NHS-LC-biotin with a primary amine (Meier T *et al.*, 1996).

Generally, water soluble and long-armed biotinylation reagents are preferred because they are more easily detected and handled. Biotin is covalently coupled to the primary amines (lysines) of IgG. Only the epsilon amine of the lysine residue can be effectively biotinylated with NHS esters (Lomant AJ 1976). Critical amino acid residues in the antigen-binding site should be avoided with the biotinylation reagent to preserve the biological activity of the antibodies. Sometimes, the biotinylation protocol may modify the antigen-binding site and result in the loss of its activity. In this case, carbohydrate directed biotinylation reagents are used. The principle of this reaction is shown in Figure 2.3. Carbohydrate directed biotinylation reagents, biotin hydrazide, biotin-LC-hydrazide or biocytin hydrazide are used to conjugate biotin to carbohydrate groups. The bond is stable between pH 2-10 (Hoffman WL *et al.*, 1988) and is particularly suitable for biotinylating antibody because the carbohydrate groups are localized on the Fc region, which is far away from the antigen-binding sites. Biotinylation of the amino group sites occurs at room temperature while biotinylation of the carbohydrate sites occurs at 0–4°C and exposure to light should be avoided.

In addition to the amine-reactive biotinylation reagents and carbohydrate directed biotinylation reagents that are discussed above, many other biotinylation reagents are also in use, including carboxyl reactive biotinylation reagents (EDC) and sulfhydryl reactive biotinylation reagents (Biotin-HPDP) (Meier T *et al.*, 1996).

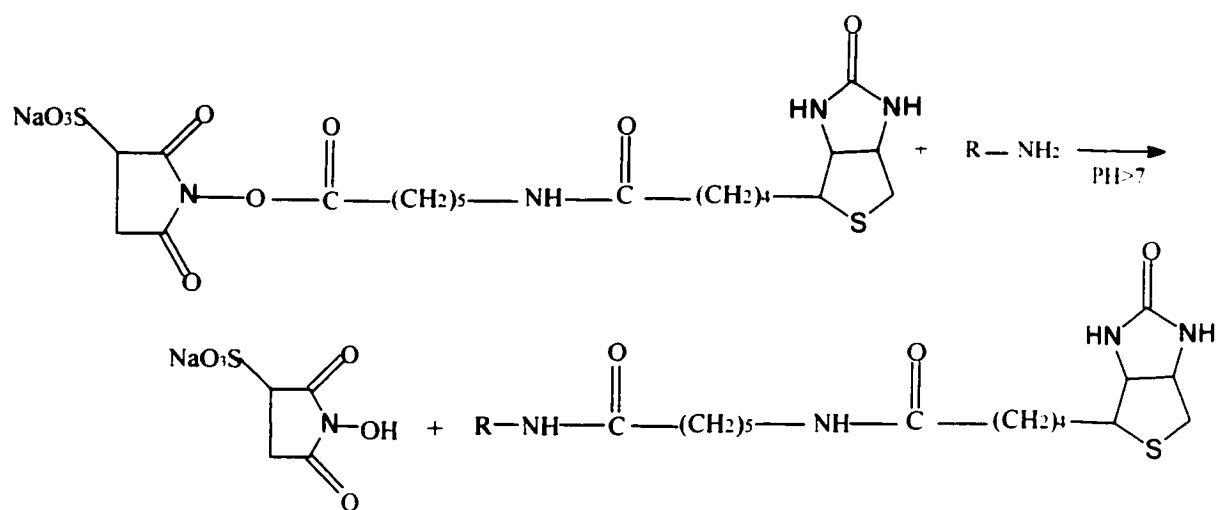


Figure 2.2 Sulfo-NHS-LC-biotin reacts with a primary amine

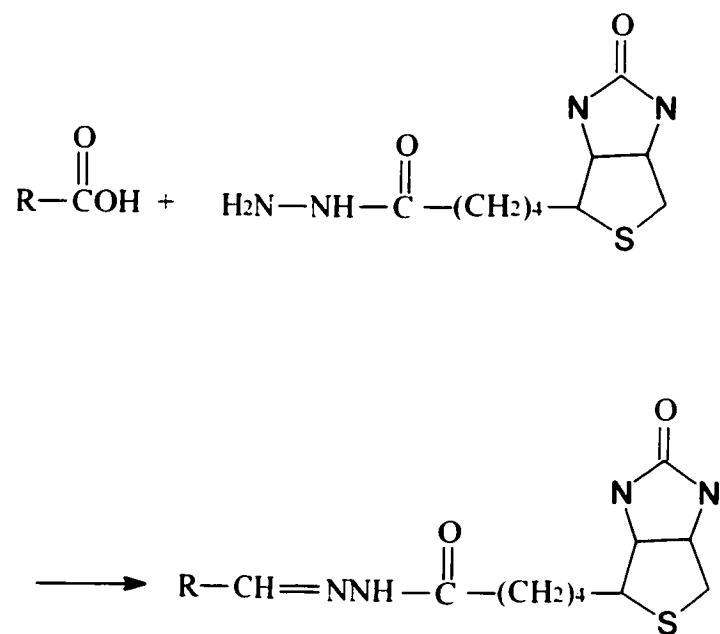


Figure 2.3. Biotin hydrazide reacts with a carbohydrate group.
 (Sources: Meier *et al.*, 1996)

2.2 MATERIALS AND METHODS

2.2.1 Tissue Culture and Storage

2.2.1.1 Materials

- *RPMI-1640 8% FBS medium (1L)*: One package of RPMI medium (10.4g) was dissolved in double distilled water with gentle stirring. 2.0g of sodium bicarbonate (NaHCO_3), 80mL of fetal bovine serum (FBS), 10mL of penicillin-streptomycin and 5mL of glutamine were added. The volume was adjusted to 1L with Millipore water and stirred until completely dissolved. The pH was adjusted to 7.2 using 1N NaOH or 1N HCl and the solution was immediately subjected to membrane filtration (0.22 μm). All of the above biological agents were purchased from GIBCO, Grand Island, NY.
- *Phosphate buffered saline (PBS)*: 0.41g of potassium phosphate (MW = 136.09), 1.14g of sodium phosphate (MW = 141.96) and 8.5g of sodium chloride (MW = 58.44) were dissolved in 1L of distilled water and the pH was adjusted to 7.2. (3 mM KH_2PO_4 , 8 mM Na_2HPO_4 and 0.145 M NaCl)
- *TPBS buffer*: 0.05% Tween was added to the above PBS buffer to obtain a phosphate buffered saline containing 0.05% Tween (TPBS). (3 mM KH_2PO_4 , 8 mM Na_2HPO_4 , 0.145 M NaCl and 0.05% Tween)

2.2.1.2 Methods

Mabs B43.13 and B27.1 hybridomas were kindly provided by Biomira Inc. Edmonton, Canada. The vials of cells were thawed in a 37°C water bath and resuspended in 10mL of RPMI-1640 medium containing 8% FBS (GIBCO, Grand Island, NY). After centrifuging at 1600rpm (260g) for 7 minutes, the cell pellet was resuspended in 10mL of fresh RPMI-1640 medium containing 8% FBS and

transferred to a 25cm² tissue culture flask (Costar Corporation, Cambridge, USA). The cells were incubated at 37°C, 5% carbon dioxide in 100% humidity incubator (Forma Scientific Inc, Ohio, USA) until the cells were vigorously growing (5–10 days). Most cell lines were split into fresh medium or new flasks when the cell density reached $1-2 \times 10^6$ cells/mL. The supernatant was collected when the appearance and the color of the medium became turbid and yellow. A hemocytometer and an inverted light microscope were used to monitor cell growth. Cells were counted using 0.4% trypan blue and the viability was calculated.

The hemacytometer has four counting squares in which each has a 1mm² area. The coverslip rests 0.1mm above the surface, resulting in the total volume of 0.1mm³. In our protocol, 100μL of cell suspension plus 100μL of 0.4% trypan blue resulted in obtaining the dilution factor equal to 2. The following formula was used to calculate cell density:

$$\text{Cell density (cells/mL)} = \text{cells \# in } 0.1\text{mm}^3 \times \text{dilution factor} \times 10^4$$

Under the microscope, the live cells did not take up dye while dead cells did and appeared blue.

The cells were split when necessary and recultured until 1–2L of supernatant were ready for use. The resultant supernatant containing the Mab was collected, followed by centrifuging at 3000rpm (1200g) at 4°C for 20min to remove the cell debris. The supernatant was collected for future purification while the pellet was discarded.

Vigorously growing cell lines were selected to freeze and store to preserve the cell lines. The supernatant was centrifuged at 1600rpm (260g) for 7minutes. The cell pellet was collected and 90% FBS plus 10% DMSO were added to it. FBS was added to maintain cells and DMSO was added to avoid crystallization. The concentration was adjusted to 3×10^6 cells/mL and 1.5 mL of cell suspension was pipetted into each vial. The vials were stored at 4°C for 20min, then in a -20°C

refrigerator for 20min and then stored in a -86°C freezer to avoid any damage to cells. Long term storage was in liquid nitrogen.

2.2.2 Purification of Mabs B43.13 and B27.1

2.2.2.1 Materials

- 0.1M sodium acetate pH 5.0: 8.2g of sodium acetate (MW 82.03) was dissolved in 1L of distilled water. The pH was adjusted to 5.0 using acetic acid.
- 0.1M glycine pH 2.8: 7.5g of glycine (MW 75.07) was dissolved in 1L of distilled water. The pH was adjusted to 2.8 using 1N HCl.
- 1M Tris-base buffer pH 8–9: 0.606g of Tris (MW=121.14) was dissolved in 5mL of distilled water. The pH was adjusted to 8–9 using 1N HCl.
- HiTrap® Protein G column (Sepharose HP 1mL) was purchased from Sigma, St. Louis, MO

2.2.2.2 Methods

Two purification methods were tested using a Protein G column. Either the supernatant was directly loaded on a Protein G column or ammonium sulfate was used to precipitate the antibody, followed by centrifuging to remove most of the albumin that came from the medium.

Ammonium sulfate was slowly added to the 500mL of supernatant to precipitate Mab B43.13 (or Mab B27.1) (50% solution precipitation). Most of the IgG was precipitated. The albumin that came from the RPMI medium was dissolved in the supernatant and was discarded. To enhance precipitation, the mixture was stirred at room temperature for 2hrs and then was stored overnight in a coldroom. The solution

was centrifuged at 3000rpm (1200g) at 4°C for 20min. The pellet containing the antibody was collected while the supernatant was discarded. The pellet was dissolved in 10mL of 0.1M sodium acetate at pH 5.0, and then dialyzed against 1L of sodium acetate in a coldroom to remove the ammonium sulfate. The dialysis solution was changed 3 times at 12hr intervals. Our sample was centrifuged at 1600rpm (260g) for 7 minutes and then the supernatant that contained the antibody was collected. The absorbance was monitored at 280nm using a spectrophotometer (DU®640, Beckman Instruments Canada Inc. Mississauga, Ontario) and the concentration of the protein was calculated using an extinction coefficient of 1.4 (Coligan JE *et al.*, 1998). Most of proteins containing three amino acids: tyrosine, phenylalanine, or tryptophan have a high absorbance at 280nm.

A HiTrap Protein G column (Sigma, St. Louis, MO) was used to separate the IgG from other proteins, especially from FBS that was added to the medium. The Protein G column (1mL) was equilibrated in 0.1M sodium acetate at a pH of 5.0. 10mL of the supernatant containing the desired antibody was loaded to the Protein G column and the unbound sample was collected. The column was washed with 0.1M sodium acetate at pH 5.0 and the wash sample was collected. At a later time, the desired antibody was eluted using 0.1M glycine at pH 2.8 with a flow rate of 0.5mL/min. The elutions were collected 1mL per fraction and 30 fractions were collected. 50µL of 1M Tris-based buffer was added to each fraction to minimize exposure to the low pH. At the end of the experiment, the column was recycled by washing it with 0.1M glycine at pH 2.8 and reequilibrated it to pH 5.0 with 0.1M sodium acetate. The fractions, wash samples, and unbound samples were monitored at UV_{280nm}. 0.1M glycine with 50µL of Tris-based buffer was used as a blank sample. The fractions, wash samples, and unbound samples were also monitored specifically using an ELISA technique.

2.2.3 ELISA and Relative Affinity Study

A modified ELISA method was developed to evaluate the specificity of Mabs B43.13 and B27.1. A standard 96 well ELISA plate (Nunc, Grand Island, NY) was coated with 100 μ L of CA125 antigen at 10 μ g/mL as a solid phase and then incubated overnight at 4°C. After washing with TPBS buffer 3 times, the nonspecific binding sites were blocked with 200 μ L of 2% BSA for 2hr in an incubator. After washing with the TPBS buffer 3 times, the 100 μ L of Mab B43.13 fractions, unbound sample, and negative controls were added to the plate and incubated at 4°C overnight. PBS buffer and anti-PSA Mab B87 were used as the negative controls. After washing 3 times to remove unbound antibody, 100 μ L of goat anti-mouse IgG conjugated with horseradish peroxidase (HRPO) at 1 μ g/mL was added and incubated at room temperature for 1hr on a shaker. After washing 3 times to remove the unbound antibody, the color was developed by adding TMB (3,3',5,5' – tetramethylbenzidine), H₂O₂ (hydrogen peroxide) and monitored at 650nm using an ELISA reader. HRPO is an enzyme that is extracted and purified from the root of horseradish. HRPO catalyzes TMB to produce a deep blue color in the presence of hydrogen peroxide.

2.2.3.1 Relative Affinity Study

Since a high affinity of Mab is generally better for *in vitro* and *in vivo* targeting study, the relative affinities of Mabs were compared using a modified ELISA method described above. A standard 96 well ELISA plate was coated with 100 μ L of CA125 antigen at 10 μ g/mL and incubated overnight at 4°C. After washing with the TPBS buffer 3 times, the plate was blocked with 200 μ L of 2% BSA for 2hr at an incubator. After washing with the TPBS buffer 3 times, 100 μ L of purified Mab B27.1, B43.13, serially diluted samples (1:1, 1:10, 1:100, 1:1000, 1:10,000, 1:100,000), and negative controls were added to the plate and incubated at room temperature for 6hr. After washing 3 times to remove the unbound antibodies, 100 μ L

of goat anti-mouse IgG conjugated with HRPO at 1µg/mL was added and incubated at room temperature for 1hr on a shaker. After washing 3 times to remove the unbound antibodies, the color was developed by adding TMB, H₂O₂ and monitored at 650nm using an ELISA reader. Instead of incubation at room temperature for 6hr, incubation at room temperature overnight and incubation at 37°C for 2hr were further studied using the similar procedure.

2.2.4 SDS-PAGE

2.2.4.1 Materials

1.5M Tris-HCl buffer, pH 8.8 with 0.4% SDS (100mL): 18.2g of Tris and 0.4g of SDS were dissolved in 80mL of water and the pH was adjusted to 8.8 using 1N HCl solution. The solution was diluted to a final volume of 100mL and filtered through a 0.45µm Millipore filter to obtain a clear solution.

Butanol saturated water (100mL): the butanol solution was diluted 1:1 using distilled water.

0.5M Tris-HCl buffer, pH 6.8 with 0.4% SDS (100mL): 6.06g of Tris and 0.4g of SDS were dissolved in 80mL of water and the pH was adjusted to 6.8 using 1M HCl. The solution was diluted to a final volume of 100mL and filtered through a 0.45µm Millipore filter.

Separating gel (10%) (16mL): 4mL of 40% Acrylamide, 4mL of 1.5M Tris buffer (pH 8.8), 8mL of water, 50µL of fresh ammonium persulphate (100mg in 1mL) and 10µL of TEMED were mixed together to obtain the separating gel for immediate use.

Stacking gel (4%) (5.0mL): 0.5mL of 40% Acrylamide, 1mL of 0.5M Tris buffer (pH 6.8), 3.5mL of water, 25µL of fresh ammonium persulphate (100mg in 1mL)

and 5 μ L of TEMED were mixed together to obtain the stacking gel for immediate use.

2 \times SDS/sample buffer (10mL): 2.5mL of 0.5M Tris buffer, 2mL of glycerol, 0.4g of SDS, 0.2mL of 2-ME, and 0.1mg of bromphenol blue were mixed together. The volume was adjusted to 10mL using distilled water and stored at -20°C in 1mL aliquots.

Tank buffer (Tris-glycine buffer, pH8.3) (1L): 15g of Tris, 72g of glycine and 5g of SDS were dissolved in 1L of water and the pH was adjusted to 8.3 using 1M HCL. It was diluted five times at the time of use.

Staining solution(200mL): 1 tablet of gel blue R (Pharmacia LKB, Biotechnology AB, Uppsala, Sweden) was dissolved in 120mL of water, 80mL of methanol and 20% acetic acid. The solution was filtered and stored at room temperature.

De-staining solution (500mL): 25% methanol and 7% acetic acid were mixed in water.

Sample preparation: 20 μ L of purified Mab B43.13, (or Mab B27.1) plus 20 μ L of 2 \times SDS/sample buffer were quickly mixed together in a microcentrifuge tube and heated for 5min at 100°C. A quick transition to 100°C was required to inactivate proteases that could degrade the sample protein, even after a few minutes at room temperature.

2.2.4.2 Methods

SDS-PAGE was used to determine the purity of antibodies. The SDS-PAGE sandwich was assembled and locked to the casting stand. The separating gel solution was carefully added to the sandwich along an edge until the height was about 8cm, followed by the slow addition of butanol saturated water (1cm thick) to cover the top

of the gel. The gel was polymerized for 1hr at room temperature. The butanol saturated water was poured off, followed by the slow addition of the stacking gel solution to fill the rest of the sandwich. A 0.75mm Teflon comb was inserted into the layer of stacking gel solution, followed by adding additional stacking gel to completely fill the spaces in the comb. The gel was polymerized for 1hr at room temperature

The Teflon comb was carefully removed and the wells were washed and filled with tank buffer. The samples were loaded to the wells and the SDS-PAGE sandwich was transferred to the chamber, followed by the filling of the chamber with tank buffer. The samples were run under a 10mA electric field for 45min until the bromphenol blue dye reached the bottom of the separating gel. The power supply was disconnected and the gel was washed with water. The gel was dipped into staining solution for 1hr to obtain color, followed by dipping it in a destaining solution for 2 days to remove the background. The gel was wrapped and dried using a porous plastic.

2.2.5 Production of Biotinylated Monoclonal Antibodies

2.2.5.1 Materials

- 10mg/mL Long-armed biotin in anhydrous DMSO: Long-armed biotin (biotinamidocaproic acid, 3-sulfo-N-Hydroxy-Succinimide ester, $C_{20}H_{29}N_4O_6S_2Na$ MW = 556.6 Da, Figure 2.1a) was dissolved in anhydrous DMSO. The Biotin/DMSO solution was prepared immediately before use. Reagent was purchased from Sigma, St. Louis. MO
- DMSO (anhydrous dimethyl sulfoxide): DMSO was kept under dessication.
- Biotin labeling buffer: 0.1M $NaHCO_3$ (sodium hydrogen carbonate) and 0.1M NaCl (sodium chloride) were dissolved in distilled water and the pH was adjusted to 8.4.

- Dialysis buffer: 0.1M Tris-Cl and 0.2M NaCl were dissolved in distilled water and the pH was adjusted to 7.4.

2.2.5.2 Methods

Mabs B43.13 and B27.1 were labeled with long-armed biotin for the *in vitro* targeting studies. 1mg/mL of purified Mab B27.1 was dialyzed using 1L PBS buffer for 2–3 days in a cold room to remove the ammonium sulfate, Tris, and glycine that may have been left behind by the purification procedure. The dialysis solution was changed 3 times at 12hr intervals. The Mab B27.1 continued to be dialyzed overnight using biotin labeling buffer at 4°C in order to adjust the pH to 8.4.

The protein concentration of Mab B27.1 was determined at 280nm using a spectrophotometer (Beckman DU®640, Beckman Instruments Canada Inc. Mississauga, Ontario). The extinction coefficient of 1.4 (Coligan JE *et al.*, 1998) was used to calculate the concentration of the antibody. 10µL of 10mg/mL biotin in DMSO was added to each milligram of antibody. The tube was wrapped in aluminum foil to protect the contents from light and incubated for 2hr at room temperature and then overnight at 4°C. The unbound biotin was removed by dialyzing against 1L of dialysis buffer or PBS buffer at 4°C for 2–3 days. The dialysis solution was changed 3 times at 12hr intervals. Similar procedures were used to label Mab B43.13.

2.2.6 Characteristics of Biotinylated Monoclonal Antibodies

2.2.6.1 Determination of the Biotin/Antibody Ratio Using a HABA Assay.

2.2.6.1.1 Materials

- 2mL HABA/avidin reagent: 0.121mg of 4-hydroxyazobenzene-2'-carboxylic acid (HABA) (MW 242.2D) and 0.4mg of avidin were dissolved in 2mL of PBS

buffer in a glass tube to obtain 0.25mM HABA in PBS containing 0.2mg/mL avidin. This reagent was purchased from Sigma. St. Louis MO.

2.2.6.1.2 Methods

A HABA assay was used to evaluate the degree of biotinylation. PBS buffer was used as a blank sample to establish the baseline in the spectrophotometer (Beckman DU®640, Beckman Instruments Canada Inc. Mississauga, Ontario) at 500nm. 1.0mL of HABA/avidin reagent (0.25mM HABA with 0.2mg/mL avidin) was pipetted to a 1cm cuvette and measured at 500nm to obtain the absorbance A_1 . 50 μ L of biotinylated antibodies at 1mg/mL concentration was added to this HABA/avidin reagent and was again measured at 500nm to obtain the absorbance A_2 . The detailed calculation of biotin concentration is shown in Chapter 3, Section 3.3.1.

2.2.6.2 Confirmation of Biotinylation Using an ELISA Technique

2.2.6.2.1 Materials

- 1% dialyzed BSA: 1mg of BSA was dissolved in 100mL of PBS and dialyzed against 1L of PBS buffer. The dialysis solution was changed 3 times at 12hr intervals.
- SA-HRPO solution: (streptavidin conjugated with horseradish peroxidase). The original concentration was 1mg/mL. Original streptavidin conjugated with HRPO solution was 1:1000 diluted using 1% dialyzed BSA. The reason for using 1% dialyzed BSA to dilute the sample was to reduce biotin content in the BSA and to avoid the SA-HRPO from binding to the glass wall.

2.2.6.2.2 Methods

Several different ELISA techniques were developed to confirm the immunoreactivity and biotinylation of the biotinylated Mabs. A standard 96 well ELISA plate was

coated with 100μL of CA-125 antigen at 1μg/well and incubated overnight at 4°C. The plate was washed with 200μL of TPBS 3 times and blocked with 200μL of 2% BSA for 2hr in a 37°C incubator. After washing, 100μL of biotinylated MAb B27.1 was added to the plate and incubated overnight at 4°C. After washing 3 times to remove the unbound Mab, 100μL of streptavidin conjugated with HRPO at 1μg/mL was added to the plate and incubated at room temperature for 1hr. After washing 3 times to remove the unbound reagent, the color reaction was developed by adding 100μL of TMB+H₂O₂ and monitored at 650nm. The positive controls and negative controls are shown below.

- Experiment sample: The plate was coated with the CA-125 antigen followed by adding biotinylated MAb B27.1 and then adding the SA-HRPO to develop the color.
- Positive control 1: The plate was coated with the CA-125 antigen followed by adding biotinylated MAb B27.1 and then adding goat anti-mouse IgG conjugated with HRPO to develop the color.
- Positive control 2: The plate was coated with the CA-125 antigen followed by adding MAb B27.1 without biotin and then adding goat anti-mouse IgG conjugated with HRPO to develop the color.
- Negative control 1: The plate was coated with the CA-125 antigen followed by adding MAb B27.1 without biotin and then adding the SA-HRPO to develop the color.
- Negative control 2: The plated was coated with CA-125 antigen followed by adding the PBS buffer and then adding the SA-HRPO to develop the color.

2.2.6.3 *In Vitro* Confirmation of Biotinylation Using CLSM

2.2.6.3.1 Materials

- *HBSS solution*: One package of HBSS powder (9.5g) (Sigma, St. Louis, MO) and 0.35g of NaHCO₃ were dissolved in 1L of distilled water and the pH was adjusted to 7.2. The solution was filtered through a 0.22µm membrane to obtain a sterile solution.
- *Glycerol /PBS solution*: The glycerol was 1:1 diluted using PBS buffer.

2.2.6.3.2 Methods

CLSM technique was used to further *in vitro* confirmation of immunoreactivity and biotinylation of the biotinylated Mabs. OVCAR-3 cancer cells (CA125 positive cell lines) were cultured in the 75cm² flask in RPMI-1640 medium. When the cells were in log phase growth, 5mL of trypsin-EDTA (GIBCO, Grand Island, NY) was used to suspend cells and the cell suspensions were centrifuged at 1600rpm (260g) for 7 minutes. The supernatant was discarded and the pellet was resuspended using a fresh RPMI 1640 medium. The cells were counted using 0.4% trypan blue and 10⁵ cells/well was transferred to the Lab-Tek slide (Nalge Nunc, Naperville, IL) to culture for 2–4 days. After cells were firmly confluent on the bottom of the slide, the cells were washed 3 times using a HBSS buffer. OVCAR cells were incubated with 2µg of biotinylated Mab B27.1 in 600µL HBSS buffer at 37°C for 1hr. After washing with the HBSS buffer 3 times to remove unbound Mab, 2µg of streptavidin conjugated with FITC (SA-FITC) in 400µL HBSS buffer was added and incubated at 37°C for 30 minutes. After washing 3 times, the 1:1 glycerol/PBS was dipped into the cells and the slides were coverslipped. The results were monitored using a confocal microscope (Zeiss, LSM510, Jean, Germany). For the negative control, the OVCAR cells were incubated with SA-FITC without adding biotinylated antibody. The other steps were similar to the experimental sample.

2.3 RESULTS AND DISCUSSION

2.3.1 Growth of Mabs B43.13 and B27.1 Cell Lines

Mabs B43.13 and B27.1 hybridoma cell lines were kindly provided by Biomira Inc. Edmonton, Canada. RPMI-1640 medium was developed by Moore GE *et al.* for tissue culture of many types of the cell lines (Moore GE *et al.*, 1967; Moore GE *et al.*, 1976). It was an optimum time to collect supernatant harvested antibodies when the medium began to turn yellow. Frequent splitting of cells at appropriate times would benefit the production of high titre antibody. A moderate cell density is beneficial in promoting a faster growth of cells. The optimum time to freeze cells was at the time the cells were vigorously growing. The cell densities of hybridomas B43.13 and B27.1 were 10^5 - 10^6 cells/mL and viabilities were about 80%. Mab B27.1 always grew more vigorously than Mab B43.13.

2.3.2 Purification of Mabs B43.13 and B27.1

A Protein G column was an affinity chromatography column which was used in the purification of IgG in our protocol. Normally 1mL volume of protein G can bind 20mg of antibodies. Approximately 30mL of 0.1M glycine at pH 2.8 was used to elute the desired antibody and fractions were collected at a 1mL/fraction. The purification results are shown in Figure 2.4.

The yield calculation was based on the Beer-Lamberts law, where the absorbance was proportional to the concentration. From the document, the extinction coefficient of 1.4 of antibody was used in my calculation (Coligan JE *et al.*, 1998), indicating that an absorbance of 1.4 was equal to 1.0mg/mL IgG. The antibody concentrations in the original supernatants of Mabs B27.1 and B43.13 were about 2.5mg/L. A total of 5mg of B27.1 and 5mg of B43.13 were harvested.

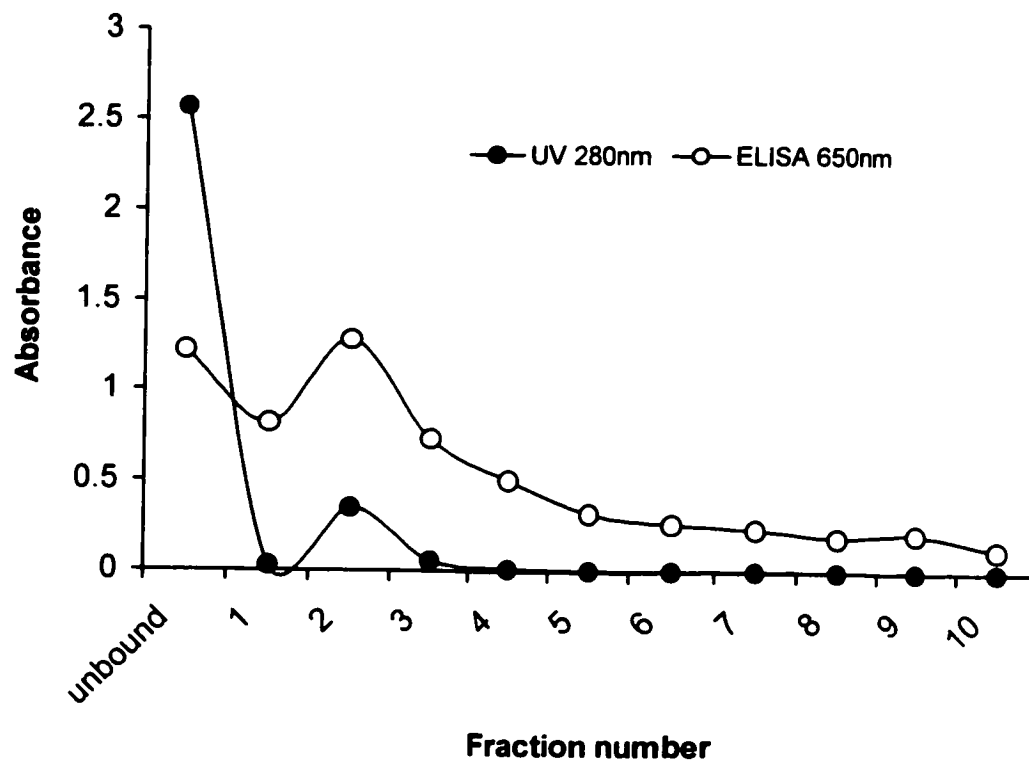


Figure 2.4: Purification of Mab B43.13 using a protein G column. Two assays were used to monitor the fractions. One was using UV_{280nm} to monitor the protein concentration. The other was using ELISA to monitor the immunoreactivity of the monoclonal antibody at OD_{650nm}. The fractions were eluted by 0.1M glycine buffer at pH 2.8 and purified Mab B43.13 were harvested in fraction 2 (1mL/fraction).

2.3.3 ELISA and Affinity Study

An indirect ELISA method was used to evaluate the specificity and the relative affinity of Mabs. Two negative controls (PBS buffer and anti-PSA Mab B87) were done together with the experimental samples and all negative controls gave low absorbances. Experimental samples yielded a signal that was 10–15 times higher than the negative controls. Different incubation times (overnight at room temperature, 6hrs at room temperature and 2hrs at 37°C) were further studied to evaluate the effects of a long incubation. The results are shown in Figure 2.5 and Figure 2.6. One way ANOVA assay ($p < 0.05$) shows that increasing incubation time significantly increases absorbance, resulting in high sensitivity. Additionally, selecting proper concentrations of the Mab were also critical to achieve optimal results in the ELISA technique. A concentration range from 10µg/mL–100µg/mL was used to calculate the relative affinity.

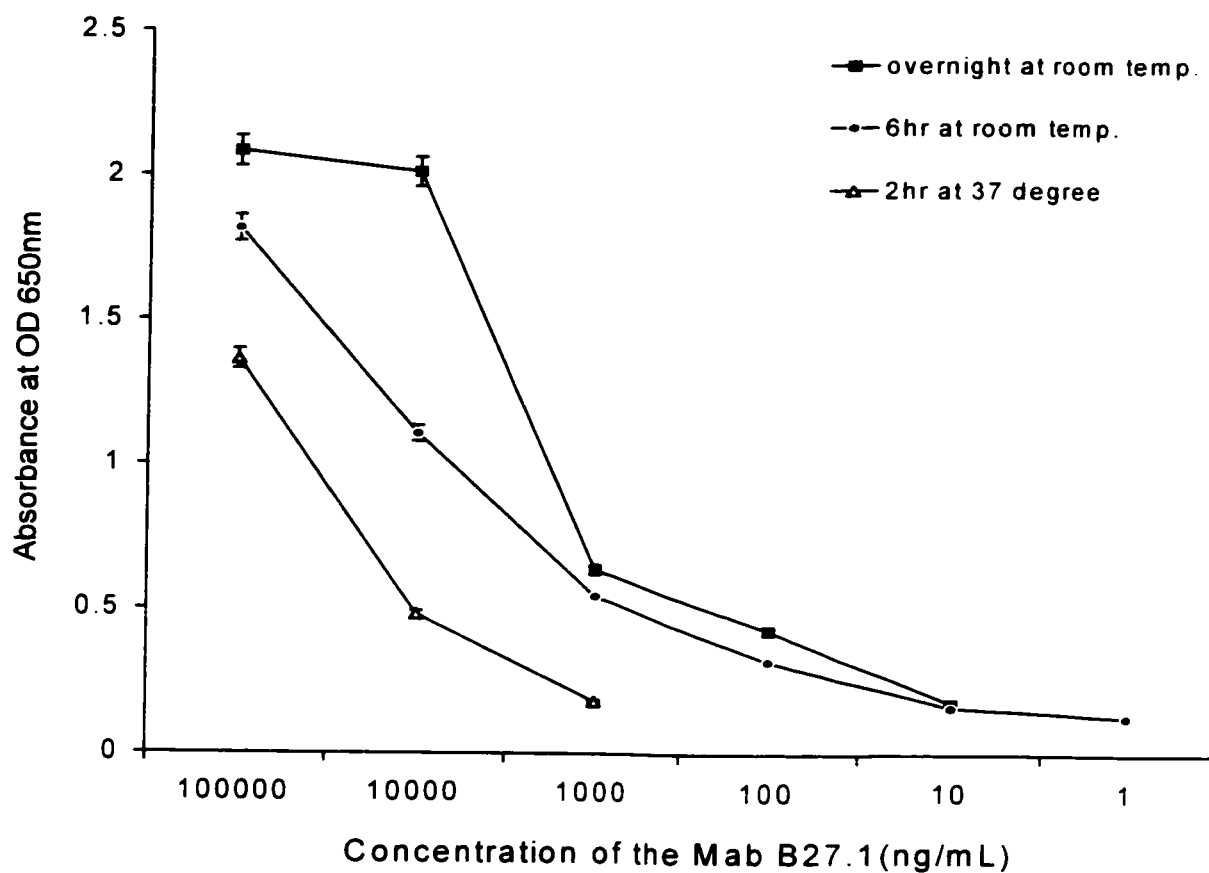


Figure 2.5 Comparison of different incubation times of Mab B27.1 with the CA125 antigen using an ELISA technique. When the incubation time increases, the absorbance also significantly increases. Each data point is the mean \pm SD. Error bars are not shown if they are smaller than the symbols.

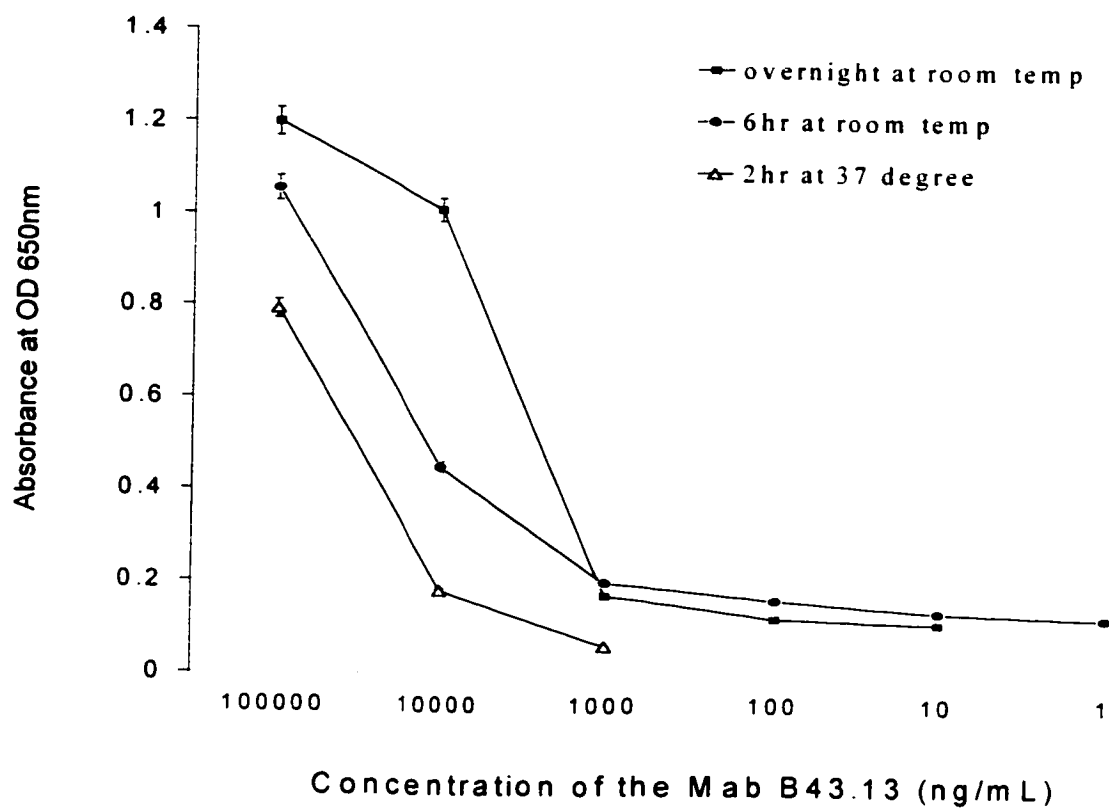


Figure 2.6 Comparison of different incubation times of Mab B43.13 with CA125 antigen using an ELISA technique. When the incubation time increases, the absorbance also significantly increases. Each data point is the mean \pm SD. Error bars are not shown if they are smaller than the symbols.

ELISA is a popular technique for affinity measurements because of its simplicity. Many different ELISA methods in the measurement of affinity have been studied by several investigators (Friguet B *et al.*, 1985; Beatty JD *et al.*, 1987; Nimmo GR *et al.*, 1984). The affinities of Mabs B27.1 and B43.13 had been measured by Capstick V *et al.* before, where the affinity constants of Mabs B27.1 and B43.13 were approximately 10^9 M^{-1} and the relative affinity of Mab B27.1 compared to that of Mab B43.13 was 1.6 (Capstick V *et al.*, 1991; Nustad K *et al.*, 1996; McQuarrie SA *et al.*, 1998). In order to select the proper antibody with a high affinity and to evaluate the characteristics of our antibodies for the future *in vitro* targeting study, the relative affinity of our Mabs B27.1 and B43.14 were studied using the simple modified ELISA method described in Section 2.2.3. Serial dilutions of the samples were incubated with an antigen pre-coated plate at different time intervals. The result is shown in Figure 2.7. Mab B27.1 had a 1.6 times higher affinity than Mab B43.13, which confirmed the result (1.6 times) found in literature (Nustad K *et al.*, 1996). The longer incubation time resulted in a higher signal, indicating that the CA125 antigen needed a longer time to react with the antibody or that the CA125 antigen may lose partial immunoreactivity during storage. The nominal sensitivities of Mabs B27.1 and B43.13 in ELISA were 10ng/mL and 100ng/mL respectively.

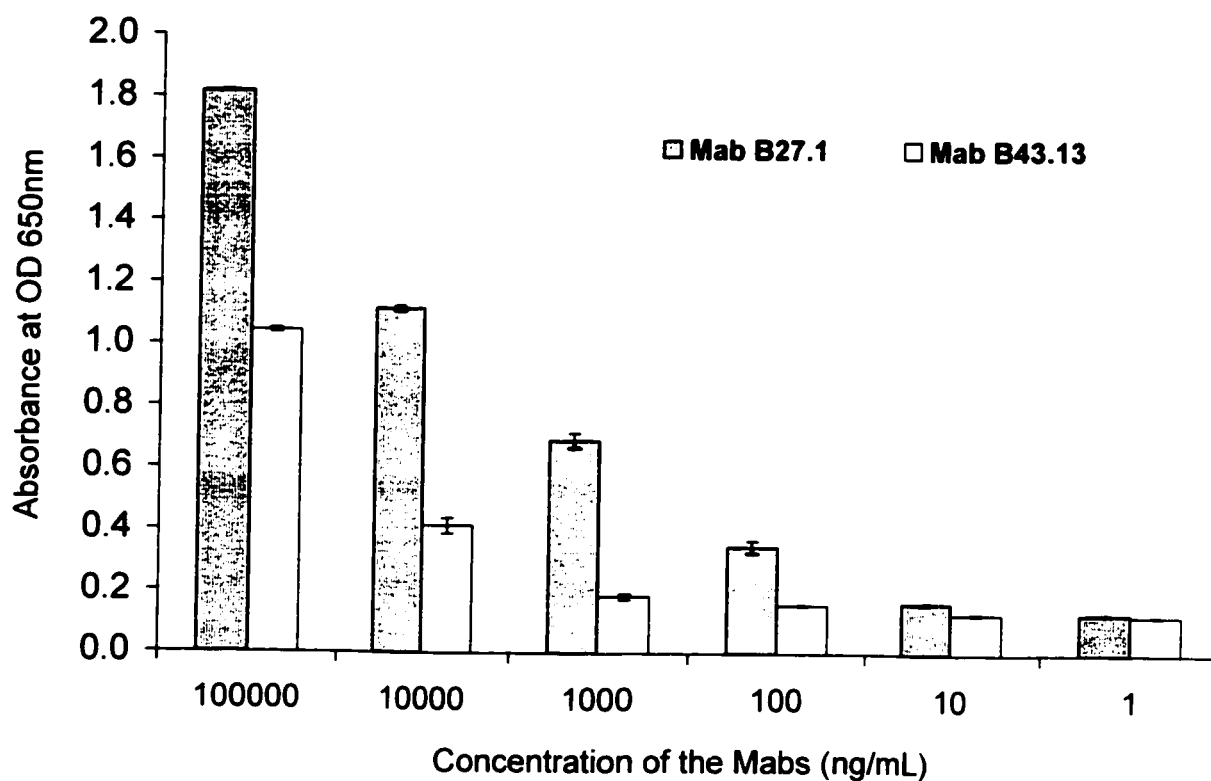


Figure 2.7 Comparison of the relative affinity of Mabs B43.13 and B27.1. The absorbance of Mab B27.1 is higher than that of Mab B43.13 at all concentrations. The relative affinity of Mab B27.1 is approximately 1.6 times higher than that of Mab B43.13.

2.3.4 SDS-PAGE

Sodium dodecyl sulphate-polyacrylamide gel electrophoresis (SDS-PAGE) is an electrophoresis technique, which is used to determine the purity of a protein. The principle involves using SDS to denature the antibody and then attach charges to it. The reducing reagent (2-mercaptoethanol) is used to break disulfide bonds between heavy and light chains. Both the heavy and light chains migrate under an electric field, resulting in separation by their sizes. The molecular weights of heavy and light chains in our Mabs, B27.1 and B43.13, were 55KD and 25KD respectively, as shown in Figure 2.8. The antibodies were relatively pure with only the two expected bands found. The density of the band to background has been calculated by ImageJ image analysis programs (Research Service Branch, National Institute of Mental Health, Bethesda, Maryland, USA) and results in approximately 88% and 91% for Mab B27.1 and B43.13 respectively. The molecular weights of the Mabs B27.1 and B43.13 were not significantly different. The supernatants containing many other proteins have many different bands. Since the hybridoma cell line only secretes one specific Mab, we can assume that no other Mabs exist in the supernatant. After purification using a Protein G column that can only bind IgG, the only Mab collected will be our desired Mabs B27.1 or B43.13.

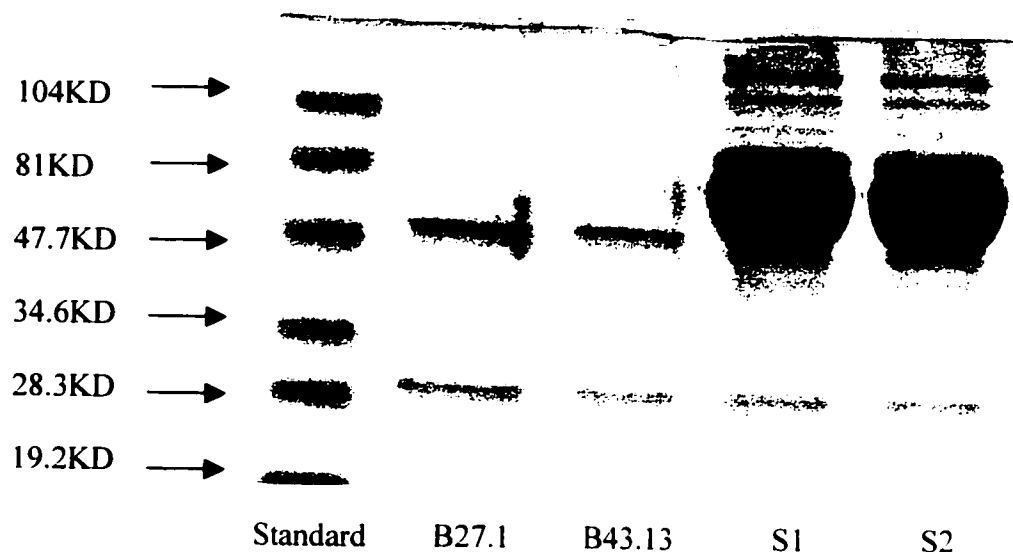


Figure 2.8 SDS-PAGE result. S1 is Mab B27.1 supernatant and S2 is Mab B43.13 supernatant. The result shows relative purity of Mabs B43.13 and B27.1 with two bands at about 55KD and 25KD. The molecular weights of the Mabs B27.1 and B43.13 are not significantly different. The standards from top to bottom are phosphorylase B (MW 104KD), bovine serum albumin (MW 81KD), ovalbumin (MW 47.7KD), Carbonic anhydrase (MW 34.6KD), soybean trypsin inhibitor (MW 28.3KD), and lysozyme (MW 19.2KD).

2.3.5 Production of Biotinylated Monoclonal Antibodies

The biotin-avidin system is the strongest known noncovalent biological interaction between a protein and a ligand ($K_d = 1.3 \times 10^{-15} \text{M}$ at pH 5) (Green NM 1963). Therefore, a biotin labeling technique is an important tool for many applications in biochemistry and cellular biology. Many different biotinylation reagents can be used to label the biotin to the antibody. My biotinylation protocol was modified on the basis of a protocol described by Coligan and his colleagues (Coligan JE *et al.*, 1998) and is described in section 2.2.5.

In order to effectively label the biotin to the antibody while preserving the biotin binding ability to the avidin, a long-armed biotin was used. The long-armed biotin has a spacer between the antibody-binding site (valeric acid side chain) and the avidin binding site (bicyclic ring). Normally, water soluble and long-armed biotinylation reagents are preferred for biotinylation (Gretch DR *et al.*, 1987; Meier T *et al.*, 1996). Sulfo-NHS-LC-biotin (MW 556.58), a water-soluble, long-armed NHS ester of biotin, was used in my biotinylation protocol for labeling antibodies containing primary amino groups of lysine residues. The reaction of sulfo-NHS-LC biotin with a primary amine is shown in Figure 2.2.

The biotinylation protocol is a simple and inexpensive protocol. It is optimal to have an antibody concentration at 2-5 mg/mL because the higher the concentration, the better the labeling efficiency. Normally a molar ratio higher than 15:1 of biotinylation reagent to antibody is used (David WC *et al.*, 1998). If the antibody concentration is lower than 1mg/mL, the amount of biotinylation reagent should be increased to obtain a similar degree of biotinylation when the higher concentration of antibody is used. Since the concentration of my Mab B27.1 was 1mg/mL, a 30:1 molar ratio of biotinylation reagent to antibody was used in my protocol. A formula was used to calculate the amount of a 10mg/mL biotinylation reagent needed to conjugate with the desired quantity of antibody (David WC *et al.*, 1998; Coligan JE *et al.*, 1998). For example, the ratio of biotinylation reagent/antibody = 30:1.

molecular weight of the antibody is 150,000, and the antibody concentration is 1mg/mL. Therefore, the volume of 10mg/mL biotinylation reagent is 11 μ L. The calculation is shown below.

$$\begin{aligned}
 & \text{(mL of 10mg/mL biotin-NHS)} \\
 &= (\text{mg antibody} \times 0.1 \times R \times \text{mol wt of biotin-NHS}) / \text{mol wt of antibody} \\
 &= 1 \times 0.1 \times 30 \times 556.6 / 150,000 \\
 &= 0.011\text{mL}
 \end{aligned}$$

Note: R = molar ratio of biotinylation reagent/antibody

(David WC *et al.*, 1998)

Due to the low concentration of Mabs B27.1 (1mg/mL) and the low binding ability, a long incubation time (2hr at room temperature and overnight at 4°C) between sulfo-NHS-LC-biotin and antibody was selected in my biotinylation protocol based on the protocol described by Coligan JE *et al.* (Coligan JE *et al.*, 1998). The biotinylation reagent is unstable in solution since the NHS esters hydrolyze quickly. Therefore, once the biotinylation reagent is dissolved in DMSO, it should be used immediately and the residual solution should be discarded. It is critical that the Tris, the glycine, the sodium azide, and the other ions are completely removed from the antibody using dialysis because the biotinylation reagent may react with them. This would result in the reduction of the labeling efficiency of the antibody. It is also necessary to remove gelatin or BSA, which are often used at 0.1–1% concentration to stabilize diluted antibodies. These proteins will also react with biotinylation reagents. When the pH increases, the reaction rate increases while the hydrolysis rate of the NHS ester increases too. Therefore, the optimum pH for biotinylating primary amines is pH 7–9 (Meier T *et al.*, 1996). Extra biotinylation reagents can be removed by dialysis or by a Gel-filtration column. A quench buffer may be optionally used to obtain a better degree of biotinylation. For instance, large amount of Tris or glycine can be used to terminate the biotinylation reaction at an optimum point to achieve proper molar ratio of biotin to antibody (Meier T *et al.*, 1996).

A HABA assay was selected to determine the degree of biotinylation following the protocol from Sigma, St. Louis MO. The HABA/avidin reagent was purchased from Sigma, St. Louis MO. The principle of this HABA assay was that HABA interacts with an avidin and provides a complex with maximum adsorption at 500nm. Additional information is provided in Chapter 3, Section 3.3.1. The biotin has an extremely high affinity with an avidin, thus replacing the HABA binding sites and results in decreasing absorbance at 500nm. The decrease is proportional to the biotin concentration. The degree of biotinylation of Mabs B27.1 and B43.13 are 7.4 and 5.9 respectively, which indicates that antibodies have been successfully labeled with biotin.

2.3.6 Confirmation of Biotinylation Using an ELISA Technique

Several positive and negative controls were tested simultaneously with the experimental samples. The results are shown in Figure 2.9. The ELISA method confirmed that the Mab had been successfully labeled with the long-armed biotin. The negative controls without biotinylated Mab did not show significant signals at 650nm. Comparing the positive control 1 with the positive control 2, the biotinylated antibody loses partial immunoreactivity during this biotinylation protocol (about 30%). Since we used an amine reactive biotinylated reagent, biotin is covalently coupled to the primary amines (lysines) of IgG. Thus critical amino acid residues in the antigen-binding site may be damaged with this kind of biotinylation reagent, resulting in the loss of partial immunoreactivity. Additionally, only the epsilon amine of the lysine residue can be effectively biotinylated with NHS esters (Lomant AJ *et al.*, 1976), which indicates that the epsilon amine bearing amino acid residue may be a critical feature of our Mabs.

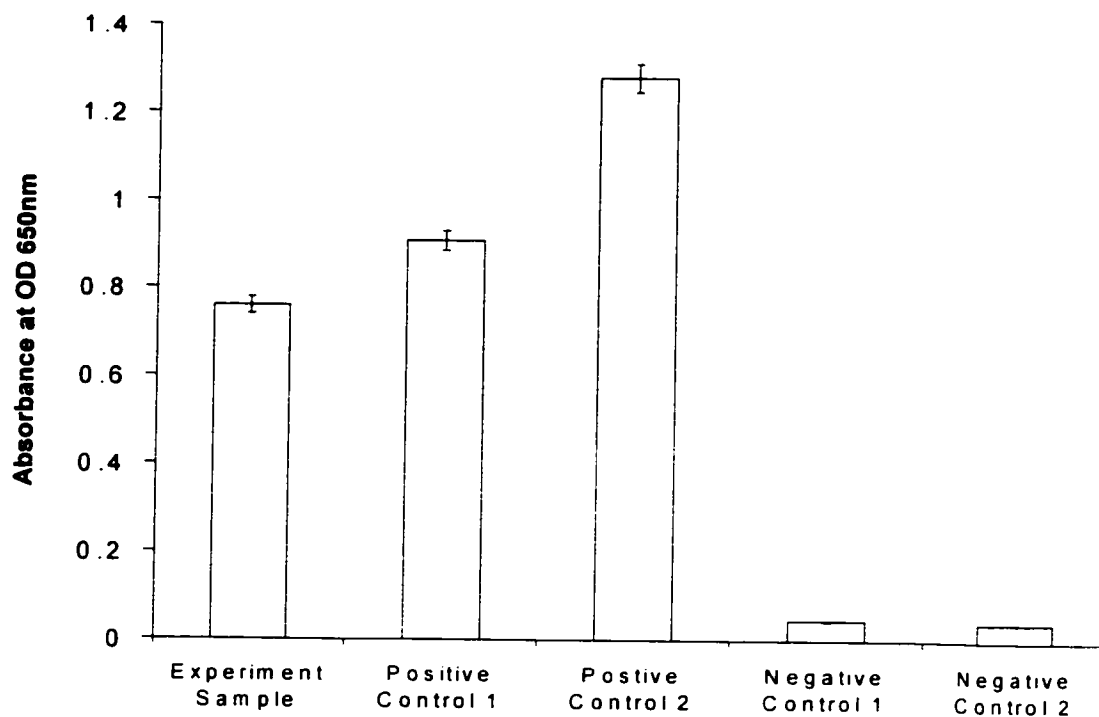


Figure 2.9 Confirmation of biotinylation of Mab B27.1 using an ELISA technique. The experiment sample is 15 times higher than the negative controls, indicating that antibodies have been successfully labeled with biotin. Comparing the positive control 1 with the positive control 2, the biotinylated Mab loses partial immunoreactivity during the biotinylation protocols (about 30%).

Experiment sample: CA-125 antigen + biotinylated Mab B27.1 + SA-HRPO

Positive control 1: CA-125 antigen + biotinylated Mab B27.1 + goat anti-mouse IgG-HRPO

Positive control 2: CA-125 antigen + Mab B27.1 + goat anti-mouse IgG-HRPO

Negative control 1: CA-125 antigen + Mab B27.1 + SA-HRPO

Negative control 2: CA-125 antigen + PBS + SA-HRPO

2.3.7 *In Vitro* Confirmation of Biotinylation Using CLSM

Streptavidin conjugated with SA-FITC instead of SA-HRPO was used to confirm biotinylation in an *in vitro* setting. Although losing partial binding activity of Mab, the biotinylated Mab B27.1 still had enough binding ability to the CA125 antigen on the surface of the OVCAR cancer cells, resulting in localization of the SA-FITC (green label) to the surface of the OVCAR cells (Figure 2.10). Without the biotinylated antibody, SA-FITC could not label the OVCAR cells directly by itself. Thus, the green label on the cell surface confirmed that the biotinylated antibody successfully targeted the OVCAR cells and that the biotinylation protocol was successful. Compared to the long incubation time (6hr or overnight) in the ELISA technique, only a 1hr incubation time was enough to achieve biotinylated Mab targeted the CA125 antigen *in vitro*. This indicates that the CA125 antigens on the living cells may have enhanced Ab binding ability (O'Brien TJ *et al.*, 1986; Masuho Y *et al.*, 1984; Matsuoka Y 1987). The concentration of the Mab in my CLSM experiments was 3.3µg/mL, compared with the 10µg/mL for the antibody in the ELISA technique. This indicates that the CLSM with fluorescence labeled technique was more sensitive than a normal ELISA technique (Coligan JE *et al.*, 1998).

In summary, biotinylated antibodies were evaluated by HABA assay, ELISA, and CLSM techniques, which indicates that antibodies were labeled with the biotin. The ratio of biotin/Mabs B27.1 and B43.13 are 7.4 and 5.9 respectively. Although losing partial binding activity of Mab (about 30%) during this biotinylation protocol with the amine reactive biotinylation reagent, the biotinylated antibodies still had enough affinity to bind the OVCAR cells at low concentrations and short incubation time (1hr) in *in vitro* targeting study. Long-armed carbohydrate directed biotinylation reagents that conjugate biotin to carbohydrate groups are particularly suitable for biotinylating antibodies because carbohydrate groups are located on Fc region that is far away from antigen-binding sites. Thus long-armed carbohydrate directed biotinylation reagents may be better to preserve immunoreactivity and avidin-binding sites of biotinylated Mabs.

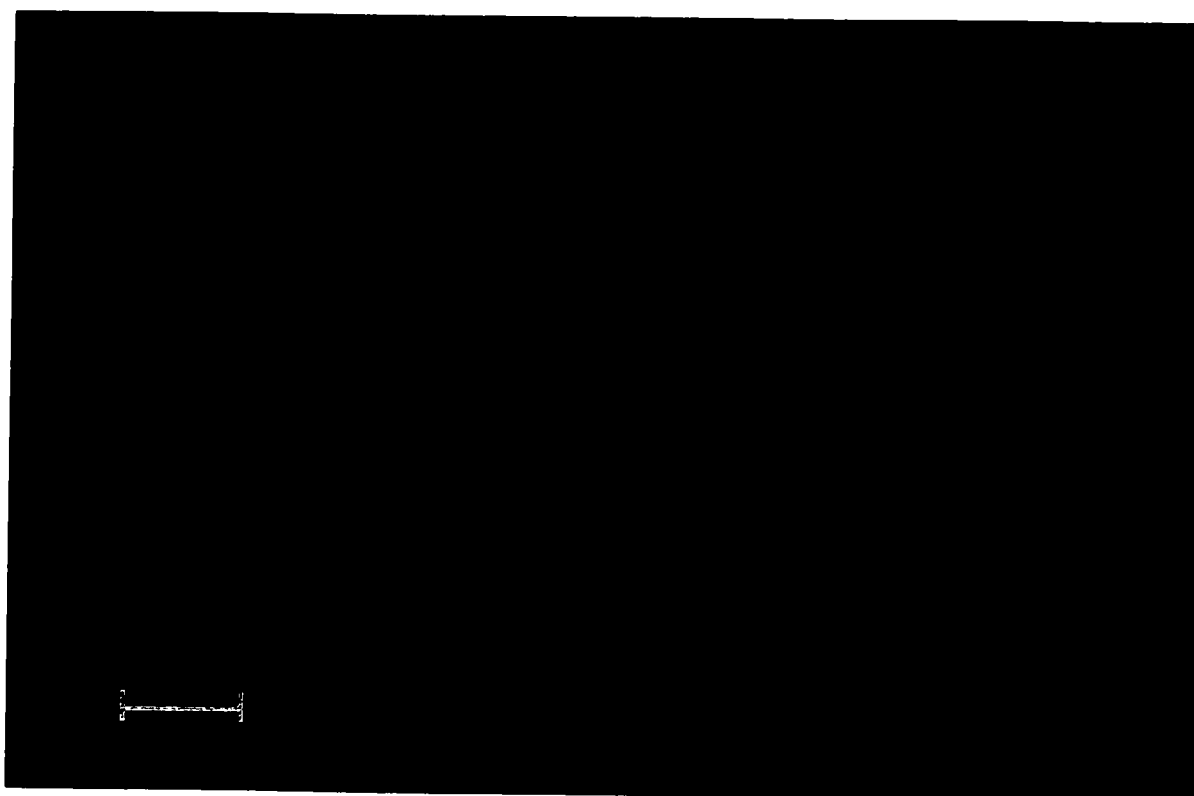


Figure 2.10. *In vitro* confirmation of biotinylation of Mab B27.1 using CLSM. The green label on the surface of the ovarian cancer cells confirms that the biotinylated Mab B27.1 targets OVCAR cells and directs SA-FITC (green label) to the surface of ovarian cancer cells via biotin-streptavidin cross-linking. Without the biotinylated antibody, the SA-FITC could not bind to the OVCAR cells by itself, resulting in no green fluorescence. Although losing partial binding activity (about 30%), biotinylated Mab B27.1 still targets the OVCAR cells under low concentration (3.3 μ g/mL) and short incubation time (1hr), indicating that the fluorescence technique is more sensitive than the normal ELISA technique.

CHAPTER 3

BIOTIN TRANSPORT IN OVARIAN CANCER CELLS

3.1 INTRODUCTION

Since the bispecific monoclonal antibody was under development, we planned to use a biotinylated monoclonal antibody as a pretargeting agent, followed by adding streptavidin conjugated with FITC and biotinylated liposomes to demonstrate the *in vitro* targeting. Thus exogenous free biotin may compete for the biotin binding sites, resulting in inhibition of liposome targeting. In order to estimate the effect of exogenous biotin and investigate the alternative transport mechanism of biotinylated liposomes to ovarian cancer cells, we first designed and studied a biotin transport experiment in ovarian cancer cells. Additionally, a simple ELISA method was developed to monitor very low biotin concentrations in mouse ascites for the future *in vivo* application to estimate the exogenous biotin effect on the inhibition of targeting.

3.1.1 Quantitative Measurement of Biotin Content

Several techniques are reported to determine biotin content, including radioassays, enzymatic assays, fluorescent assays, and chemiluminescent immunoassays (Lin HJ *et al.*, 1977; McCormick DB *et al.*, 1970; Mock DM *et al.*, 1985, 1996). The 2-(4'-hydroxyazobenzene)-benzoic acid (HABA) assay is a very common and traditional assay to determine biotin content with better reproducible results (Green NM 1970).

However, a HABA assay is not useful for determining biotin content in human plasma or mouse ascites with very low biotin concentration. Therefore, we developed a sensitive and simple ELISA method to determine biotin content at low concentration for the future *in vivo* application.

3.1.2 Biotin Transport

Biotin concentration in human plasma is very low (0.5nM–10nM, Guilarte TR 1985; Mock DM *et al.*, 1992; 1996). However, biotin plays an important role in carboxylase enzyme systems that catalyze metabolic reactions to produce carbohydrate, amino acid, and lipid. Thus biotin is a critical element for cellular function. Biotin transport mechanisms have been studied by many investigators in the intestine, kidney, and liver cell lines (Said HM *et al.*, 1998; Ma TY *et al.*, 1994; Debra W *et al.*, 1991; Ramaswamy K *et al.*, 1990; Chatterjee NS *et al.*, 1999), resulting in the following conclusions:

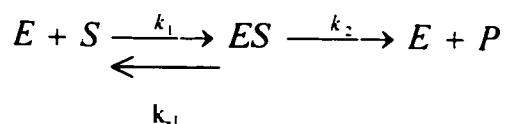
- Biotin uptake mechanism is Na⁺, temperature, and energy-dependent, a carrier mediated mechanism, and is saturable as a function of concentration.
- Biotin uptake inhibitors, including biotin analogs (biocytin, biotin methyl ester, diaminobiotin) with a free carboxyl group at the valeric acid moiety will greatly inhibit the biotin uptake.
- The V_{max} value is changed with different cell lines. However, the K_m value is relatively stable as listed in Table 3.1.
- If the cells are grown in a biotin-deficient medium, the V_{max} is 258% higher than the cells that are grown in a biotin-sufficient medium, perhaps due to upregulation of biotin transport. However, there are no significant differences between the K_m values.

Organs	Km Value
Intestine	5–15μM
Liver	1.2–20μM
Kidney	28–50μM
Placenta	21–26μM

Table 3.1 Km values of biotin transport in different cell lines. Sources: Said HM *et al.*, 1998; Ma TY *et al.*, 1994; Debra W *et al.*, 1991; Ramaswamy K *et al.*, 1990; Chatterjee NS *et al.*, 1999

Not much research has been done related to cancer cell lines with respect to biotin uptake. In our project, we plan to test if the same transport mechanism exists in ovarian cancer cells, to benefit further studies on the transport mechanism of biotinylated liposomes.

The simple way to determine the biotin kinetic data is to make a Michaelis-Menten plot, a commonly used method in enzyme kinetics. An enzyme catalyzes the chemical (the substrate) to produce another chemical (the product). The reaction equation is shown below.



E = Enzyme S = Substrate ES= E and S binding together P= Product

At the beginning of the reaction, the concentration of product increases quickly with the time and finally reaches a plateau. Some assumptions are identified to simplify analysis. For example, ES concentration is stable during the reaction, and the concentration of a substrate exceeds the concentration of an enzyme. On the basis of these assumptions, the Michaelis-Menten equation is used to plot a curve with enzyme velocity against the substrate concentration (see Figure 3.1).

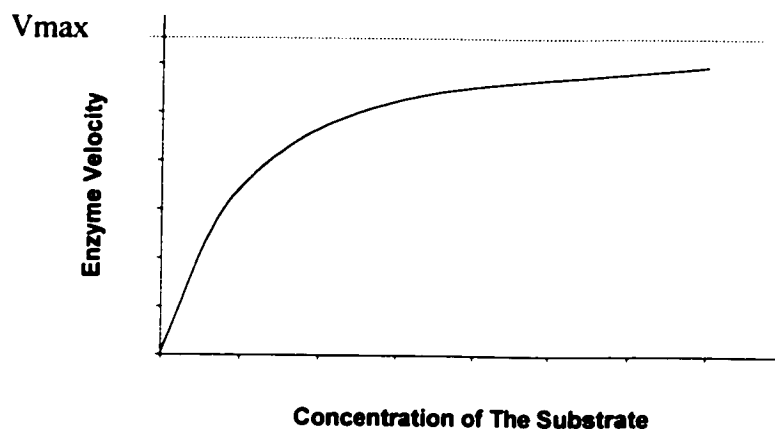


Figure 3.1 Enzyme velocity as a function of the concentration of a substrate

$$Velocity = V = \frac{V_{\max} [S]}{[S] + K_m}$$

[S] = Concentration of a substrate

Vmax = The largest velocity that substrate concentration can reach as it is shown in Figure 3.1. Usually Vmax is expressed in mol/mg protein/min

Km = The concentration of substrate that leads to half-maximal velocity. Usually Km is expressed in molar units.

To further simplify the procedure for calculating the Vmax and Km, Figure 3.2 is used for many kinds of enzymes and the parameters are shown in it. A plot of 1/velocity against 1/[substrate] is linear. Since a biotin is analogous to an enzyme, its transport kinetics can also be analyzed using the above approaches shown in Figure 3.1 and 3.2.

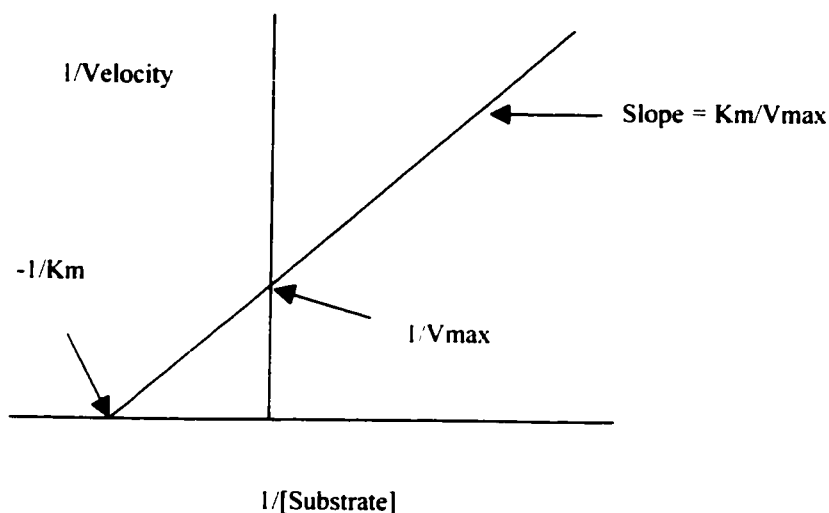


Figure 3.2 The 1/velocity as a function of the 1/[substrate]

3.2 MATERIALS AND METHODS

3.2.1 Determination of Biotin Content Using HABA Assay

3.2.1.1 Materials

- 2mL HABA/avidin reagent: 0.121mg of 4-hydroxyazobenzene-2-carboxylic acid (HABA) (MW 242.2D) and 0.4mg of avidin (one unit will bind 1.0 μ g of D-biotin) were dissolved in 2mL of PBS buffer in a glass tube to obtain 0.25mM HABA in PBS buffer containing 0.2 mg/mL of avidin. This reagent can be purchased from Sigma St. Louis MO.
- Serial biotin concentrations as standard samples: 1mg of biotin was dissolved in 1mL of PBS buffer as a stock biotin solution. Serial standard biotin concentrations were prepared in the range of 0–400 μ M.

- Unknown samples: RPMI-1640 medium, biotin-free medium and 4 samples from mouse ascites.

3.2.1.2 Methods

A HABA (4 - hydroxyazobenzene - 2' - carboxylic acid) assay was used to determine biotin contents in unknown samples. PBS buffer was put in a cuvette as a blank sample to establish the baseline in the spectrophotometer at 500nm. 1mL of HABA/avidin reagent was pipetted to 1cm cuvette and measured at 500nm to obtain absorbance A_1 . Subsequently, 50 μ L of serial biotin standard samples (range 0–400 μ M) were added to this HABA/avidin reagent to obtain the biotin test concentration at 0–20 μ M range. These test concentrations were measured at 500nm again to obtain absorbance A_2 . In the meantime, unknown samples and the negative control (PBS buffer) sample were monitored using the same method as for standard biotin samples. The biotin concentrations in unknown samples were calculated by interpolating from the biotin standard curve.

An alternative method to obtain a biotin standard curve is described below. After using a blank sample to establish the baseline in the spectrophotometer at 500nm, 2mL of HABA/avidin reagent was added to a 1cm cuvette and measured at 500nm to obtain A_1 . This HABA/avidin reagent was pipetted back to a glass tube and 1 μ L biotin stock solution at 1mg/mL was added using 5 μ L syringe (biotin test concentration is 2 μ M). After mixing it completely, this HABA/avidin reagent was pipetted to 1cm cuvette and measured to obtain A_2 . This HABA/avidin reagent was pipetted back to the glass tube again and another 1 μ L biotin stock solution at 1mg/mL was added (biotin test concentration is 4 μ M). After a thorough gentle mixing, this HABA/avidin reagent was pipetted to 1cm cuvette and measured to obtain A_3 . The procedure was repeated until biotin standard curve was finished to produce a 1–20 μ M range. The advantage of this procedure was that smaller amounts of HABA/avidin reagents were used and it was a simple operation. The disadvantage was that the error of small volume pipetting could be higher. However, the results

were quite similar, indicating this method was desirable and a HABA assay method was reproducible when sample volume was small.

3.2.2 Determination of Biotin Content Using an ELISA Technique

3.2.2.1 Materials

- 10 μ g/mL Biotin-BSA solution: Original biotin-BSA solution (1mg/mL) was 1:100 diluted using a PBS buffer to obtain 10 μ g/mL biotin-BSA solution.
 - 1% dialyzed BSA: 1mg of BSA was dissolved in 100mL of PBS and dialyzed against 1L of PBS buffer to reduce the biotin content. The dialysis solution was changed 3 times at 12 hr intervals.
 - SA-HRPO solution: (streptavidin conjugated with horseradish peroxidase). Original SA-HRPO solution (1mg/mL) was 1:1000 diluted using 1% dialyzed BSA. 1% dialyzed BSA was used to dilute the sample and avoid SA-HRPO binding to the glass wall.
 - TPBS buffer: 0.05% Tween was added to the PBS buffer to obtain a surfactant based phosphate-buffered saline solution (TPBS).
 - Biotin standard samples (serial concentrations)
 - 4pM–0.4 μ M series
- Stock biotin solution: 1mg of biotin was dissolved in 1mL of PBS buffer to obtain biotin concentration at 1mg/mL.
- The stock biotin sample was 1:1000 diluted to obtain the concentration at 1mg/L=4 μ M. Series were prepared using 10 fold dilutions to obtain biotin concentrations of 0.4 μ M, 0.04 μ M, until 0.4pM.

➤ 0.4nM–51.2nM series

128μL of 0.4μM biotin sample was dissolved in 1mL of PBS buffer to obtain the biotin concentration at 51.2nM. A series was prepared using doubling dilutions to obtain biotin concentrations of 51.2nM, 25.6nM, 12.8nM, until 0.4nM.

➤ 10nM–27.5nM series: 2.5 intervals

Biotin concentrations of 10, 12.5, 15, 17.5, 20, 22.5, 25, 27.5nM series were prepared.

➤ 10nM–45nM series: 5 nM intervals

➤ 1nM–8nM series: 1nM intervals

- Unknown samples

➤ Regular RPMI medium samples

1:1, 1:10, 1:100, 1:1000, 1:10000 dilution series

1:30, 1:50, 1:80 dilution series for the detailed studies

➤ Four mouse ascites samples named 2-1, 2-2, 3-1, 3-2

1:1, 1:10, 1:100 dilution series

- Positive control:

PBS buffer 160μL, instead of biotin samples, was incubated with 180μL of SA-HRPO and the other procedures were done the same as for the experimental samples.

- Negative control:

PBS buffer was used as a negative control. All the other procedures were done the same as for the experimental samples.

3.2.2.2 Methods

An ELISA technique was used to determine biotin contents in unknown samples. A standard 96-well ELISA plate (NUNC, Naperville, IL) was coated with 100 μ L of biotin-BSA at 10 μ g/mL and incubated overnight at 4°C. The plate was washed with TPBS buffer 3 times and blocked with 200 μ L of 1% BSA for 1hr at room temperature. After washing with TPBS buffer 3 times, 160 μ L of biotin standard samples or unknown samples were incubated with 180 μ L of SA-HRPO at room temperature for 1hr to ensure that biotin binding sites had already been completely bound to SA-HRPO. This mixture was added to the biotin-BSA pre-coated ELISA plate with 100 μ L/well in triplicate and incubated for 1hr to facilitate the free SA-HRPO to bind pre-coated biotin-BSA. After washing 3 times to remove the unbound SA-HRPO, the color was developed by adding TMB + H₂O₂ and monitored at 650nm using an ELISA reader. The absorbance has an inverse relationship with the biotin concentration. The biotin concentrations of unknown samples were determined by manually interpolating from the standard biotin curve.

3.2.3 Biotin Uptake As a Function of the Biotin Concentration

3.2.3.1 Materials

d-[8,9-³H(N)]-biotin reagent: ³H-biotin reagent was purchased from NEN Life Science Inc, Boston, MA with an activity of 1.0mCi/mL. Specific activity was 51.1Ci/mmol and total volume was 250 μ L. 50 μ L of aliquots were made and stored at -80°C. The concentration of this reagent was 20 μ M and molecular ratio of tritium/biotin was 1.8. This calculation is shown below. To confirm its value, we use the relationship between radioactivity and number of radioactive atoms.

$$1\text{mmol} = 6.02 \times 10^{20} \text{ atom biotin}$$

$$51.1\text{Ci equal to } 1.06 \times 10^{21} \text{ atom } ^3\text{H}.$$

$$\begin{aligned}
 N &= \frac{A}{\lambda} \\
 &= \frac{A \times t_{1/2}}{0.693} = 51.1 \times 3.7 \times 10^{10} \times 12.3 \times 365 \times 24 \times 60 \times 60 / 0.693 \\
 &= 1.06 \times 10^{21}
 \end{aligned}$$

Where:

A = activity in dps

λ = decay constant for ^3H (sec^{-1}) = $\ln 2/t_{1/2}$

Thus the atom ratio ^3H : biotin = $1.06 \times 10^{21} / 6.02 \times 10^{20} = 1.8$

HBSS buffer (Hanks' Balanced Salt Solution): One package of HBSS powder (9.5g) (GIBCO BRL, Grand Island, NY) and 0.35g of NaHCO_3 were dissolved in 1L of distilled water. The pH was adjusted to 7.2 and the solution was filtered through 0.22 μm membrane to obtain a sterile solution.

500nM ^3H -biotin reagent: 50 μL of original reagent was diluted 1:40 using a HBSS buffer to obtain 2mL of 500nM ^3H -biotin reagent. The activity in this 2mL aliquot was 50 μCi = 1.85×10^6 dps.

50nM ^3H -biotin reagent: 500nM ^3H -biotin reagent was 1:10 diluted.

5nM ^3H -biotin reagent: 50nM ^3H -biotin reagent was 1:10 diluted.

3.2.3.2 Methods

Experiment 1:

1. OVCAR-3 (CA125 positive) and SK-OV-3 (CA125 negative) cell lines (ATCC, Rockville, MD) were grown using RPMI 1640 medium in 75cm² flasks for 5–10 days until the cells were in their log phase of growth and confluent on the

bottom. 4mL of 0.25% trypsin-EDTA reagent (GIBCO, Grand Island, NY) was used to suspend the cells and cell suspension was then centrifuged at 1000rpm (95g) for 5 min. The cells were counted and viability was determined using 0.4% trypan blue. Approximately 10^5 cells/well were transferred to a 24-well plate to grow for about 2–4 days until the cells were firmly confluent to the bottom. During this time, a inverted light microscope was used to monitor cell growth and the medium was changed if necessary. Three wells of cell samples were reserved for future protein assays and the others were used to perform biotin uptake experiments at 37°C.

2. The cells were gently washed twice using a 4°C PBS or HBSS buffer. 200µL of cold biotin at 50nM–40µM range plus 200µL of 50nM ^3H -biotin reagent were added to prepare serial biotin concentrations in a 50nM–20µM range (50nM, 500nM, 5µM, 10µM, 20µM). Thus 400µL of different concentrations (50nM–20µM) of biotin containing 0.5µCi/well of radioactivity were incubated with OVCAR or SKOV cells for 1hr.
3. At the end of incubation, the incubation medium was pipetted out and the cells were gently washed with a 4°C PBS or HBSS buffer three times. The cells were digested using 0.5mL of 1N NaOH and incubated at 70°C for 1hr. The cells were then neutralized with concentration HCL (about 50–60µL) and 200µL of cell suspension was transferred to a liquid scintillation vial. 10mL of scintillation cocktail was added and the radioactivity was determined by a liquid scintillation counter (TRI-CARB 2000CA/LL, Canberra Packard, Canada).

Negative controls are listed below

- The Cells were incubated with no radioactivity, followed by counting in a liquid scintillation counter. All the other procedures were done the same as for the experimental samples.

- The wells with no cells were incubated with 0.5 μ Ci radioactivity, followed by counting in a liquid scintillation counter. All the other procedures were done the same as for the experiment samples.
- The wells with no cells were incubated with 1 μ Ci radioactivity, followed by counting in a liquid scintillation counter. All the other procedures were done the same as for the experimental samples.

Experiment 2:

Step 1 and step 2 procedures were done the same way as outlined for Experiment 1. At the end of incubation, the cells were washed three times using PBS or HBSS buffer. The cells were then resuspended using 0.5mL of 0.25% trypsin-EDTA and 200 μ L of cell suspensions were transferred to 96-well plate immediately. The Harvester 96 (TOMTEC INC, Hamden, CT) was used to harvest cells on a liquid scintillation film, followed by counting in a 1450 Microbeta (Liquid scintillation luminescence counter, Wallac TRILUX).

Experiment 3:

³H-biotin (5nM, 50nM, 500nM) without any cold biotin was incubated with ovarian cancer cells. Activities were 0.05 μ Ci/well, 0.5 μ Ci/well and 5 μ Ci/well respectively. The other procedures were done the same as in Experiment 1.

3.2.4 Protein Assay

3.2.4.1 Materials

Dye reagent: 1 part of original dye reagent (Bio-Rad, Hercules, CA) was diluted with 4 parts of distilled water.

BSA standard samples (50µg–500µg/mL serials): BSA serial concentrations were prepared using a PBS buffer at range 50µg–500µg/mL.

Unknown samples: The OVCAR or SKOV cells were resuspended using 0.5mL of PBS to obtain 1:1 dilution samples. 1:10 and 1:100 dilution samples were also prepared.

3.2.4.2 Methods

10µL of BSA standard samples and unknown samples were added to a 96-well ELISA plate, followed by addition of 200µL of dye reagent to develop the color. After 10min incubation on a shaker at room temperature, the color was determined at 595nm using an ELISA reader.

Five agents (0.25% trypsin-EDTA, 0.4% EDTA, HBSS, PBS or cell scraper) were tested to resuspend the cells respectively and monitored under a light microscope. Since 0.25% trypsin-EDTA and HBSS need to centrifuge to remove the extra protein, PBS buffer with the help of a scraper was chosen for protein assay in my experiment because of simplicity.

3.2.5 Calculation of the Counting Efficiency of a Liquid Scintillation Counter

Standard known activities (111dpm, 1110dpm and 11100dpm) of ^3H -biotin reagent were added to 10mL scintillation cocktail and counted using a liquid scintillation counter to calculate the counting efficiency.

3.2.6 Calculation of the Counting Efficiency of a Microbeta

Standard known activities (111dpm, 1110dpm and 11100dpm) of ^3H -biotin reagent were pipetted with a 5µL Hamilton syringe to the liquid scintillation film and counted using a 1450 Microbeta to calculate the counting efficiency.

3.2.7 Biotin Uptake As a Function of the Incubation Time

Experiment 1:

OVCAR cells were cultured and transferred to a 24-well plate in the same way as above. Biotin uptake experiments were performed at 37°C. Serial concentrations of biotin (50nM–500µM) containing 0.5µCi ³H-biotin were incubated with OVCAR cells for 1hr–4hr. At the end of incubation, the medium was removed and the cells were gently washed 3 times using PBS or HBSS buffer. The cells were resuspended using trypsin-EDTA and transferred to a 96-well plate. The Harvester 96 (TOMTEC INC, Hamden, CT) was used to harvest cells on a liquid scintillation film, followed by counting in a 1450 Microbeta (Liquid scintillation luminescence counter, Wallac TRILUX). Negative controls were same as before.

Experiment 2:

³H-biotin 5nM–500nM without any cold biotin was incubated with OVCAR cells for 0.5, 1.5, 4, 24 hr respectively. The other procedures were done the same as in Experiment 1.

Experiment 3:

SKOV cells were cultured and transferred to 24-well plate in the same way as described above. Biotin uptake studies were performed at 37°C using serial concentrations of ³H-biotin (5nM, 50nM) and incubated with SKOV cells for 0.5hr, 1hr, 2hr, 4hr respectively. At the end of incubation, the cells were washed, digested, neutralized, and counted using a liquid scintillation counter. Negative controls were same as before.

3.2.8 Determination of Vmax and Km

OVCAR and SKOV cell lines were cultured in the same way as above. However, 10^6 cells/well were transferred to a 6-well plate and were grown for 2–4 days. Biotin uptake experiments were performed at 37°C.

The cells were washed three times using PBS or HBSS buffer at 4°C. 400µL of different concentrations of biotin (50nM, 100nM, 200nM, 400nM, 800nM, 1600nM, 10µM, 20µM) with activity (1µCi/well) were incubated with OVCAR and SKOV cells for 10min. At the end of incubation, the cells were washed, digested, neutralized, and counted in a liquid scintillation counter using the same method as described before.

3.3 RESULTS AND DISCUSSION

3.3.1 HABA Assay

The HABA assay is commonly used to detect biotin at µM concentration. HABA can bind to avidin with an affinity constant of $6 \times 10^6 \text{ M}^{-1}$ to produce a maximum absorption at 500nm. When biotin exists in this HABA/avidin complex solution, biotin-avidin complex with high affinity (10^{15} M^{-1}) replaces the HABA binding sites and results in decreasing the absorbance proportionally to the biotin concentration. Thus a biotin standard curve is obtained by plotting absorbance against the biotin concentrations. The biotin concentration of the unknown sample was determined by interpolating the biotin standard curve. Without a biotin standard curve, biotin concentration of unknown samples can also be calculated using formula (1) below (Green NM 1970).

$$[biotin] = \frac{A_1 - A_2(V+2)/2}{34} mM \quad (1)$$

A_1 = absorbance of HABA/avidin reagent
 A_2 = absorbance of adding biotin samples
 V = volume of biotin samples

If $V < 0.2\text{mL}$, the factor $(V+2)/2$ may be ignored and formula (2) is obtained.

$$[biotin] = (A_1 - A_2)/34 = \Delta A/34 \text{ (mM)} = 10^3 \Delta A/34 \text{ (}\mu\text{M)} \quad (2)$$

Normally, when V is smaller than 0.2mL , formula (2) can be used to simply calculate biotin concentration. $1\mu\text{M}$ biotin decreasing absorbance 0.034 can be figured out from formula (2). The biotin standard curve is shown in Figure 3.3.

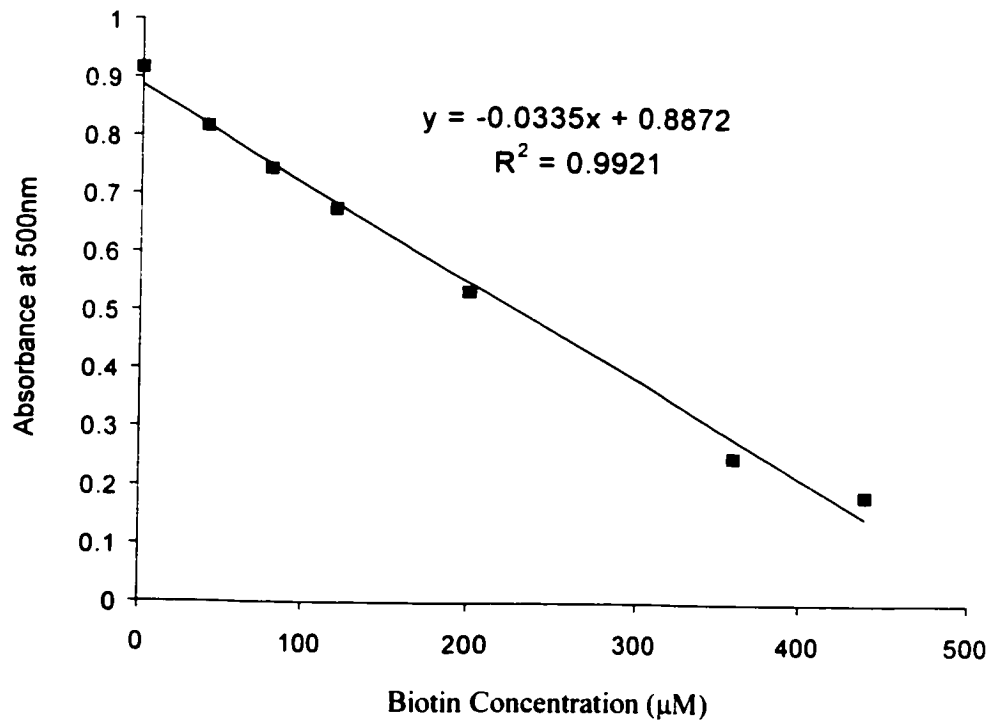


Figure 3.3 Biotin standard curve using HABA assay

HABA assay is used to detect biotin range at 1–20 μ M. When biotin concentration increases to 18 μ M, the color of HABA/avidin reagent is changed from orange to yellow, indicating that most of the HABA binding sites have been replaced by the biotin. The curve is linear at range 1–20 μ M and biotin concentration has a reverse relationship with the absorbance. The slope of the standard curve is 0.0335 indicating that 1 μ M biotin will decrease absorbance 0.0335, which matches with the result (0.034) from the formula (2).

The sensitivity of this method is 1 μ M (Green NM 1970) indicating that ΔA should be greater than 0.034 to be accurately calculated using this method. If 50 μ L of the biotin sample is added to 2mL of HABA/avidin reagent, then original unknown sample concentration should be greater than 40 μ M for accurate calculation. The calculation is shown below.

$$\text{Original Con.C} = 2\text{mL} \times 1\mu\text{M}/50\mu\text{L} = 40\mu\text{M}$$

Thus the lower detectable limit is 40 μ M in the 50 μ L sample volume.

If the ΔA is below 0.034 or if the biotin concentration of unknown samples is below the sensitivity (40 μ M), what will happen if we still use the HABA assay? Table 3.2 shows the results of unknown samples in mouse ascites using a HABA assay. Although we can obtain ΔA and calculate the biotin concentration using the formula (2), the results are not reliable compared with the following ELISA results (Table 3.4). An ELISA method was developed for low biotin concentrations.

Method	Mouse Ascites Samples	Mean Biotin ConC. (μ M)
1mL	2-1	35
HABA/avidin reagent	2-2	9
	3-1	40
	3-2	27
2mL	2-1	23
HABA/avidin	2-2	14
Reagent	3-1	18
	3-2	13

Table 3.2 Determination of the biotin concentration in unknown samples using a HABA assay. Although the biotin concentrations can be theoretically calculated, the results are not reliable compared with the following ELISA results (Table 3.4) because the biotin concentrations are below the sensitivity. Even the same method, different HABA/avidin reagent, we will obtain different results, indicating that the biotin content in mouse ascites are below the sensitivity of this HABA assay.

3.3.2 Determination of Biotin Content Using an ELISA Technique

Since the ELISA technique was found to be more sensitive than the UV spectrophotometer, a simple ELISA technique was developed to monitor the low biotin concentration in mouse ascites for the planned future *in vivo* applications. For this assay, biotin-BSA was used as a solid phase to capture agents. After blocking, the mixture of biotin samples with SA-HRPO were added, where only free SA-HRPO could bind to a precoated ELISA plate. After a washing step to remove the unbound reagent, the color was developed by adding TMB + H₂O₂, in which TMB reacts with HRPO to produce a deep blue color in the presence of H₂O₂. Thus the absorbance was proportional to free SA-HRPO and had an inverse relationship with the biotin content in the original samples. The method was simple and the results were reliable.

Figure 3.4 shows the first results of a standard curve with a wide range (4pM–0.4μM). When the biotin concentration was higher than 40nM, the absorbance had a low plateau. Similarly, when biotin concentration was lower than 4nM, the absorbance had a high plateau. Based on this preliminary data, narrow increasing ranges at 0.4nM–51.2nM, 10–30nM, 1–8nM were studied and the 10–30nM results are shown in Figure 3.5 and Figure 3.6. The figures show that biotin concentrations in the range of 17.5–25nM may be linear (Figure 3.6 and Table 3.3). A linear regression analysis was performed by selecting different data sets from the biotin concentration range of 17.5–30nM to find the linear portion of the curve. The R² value was used to locate the linear part of the curve, where R² is more close to 1, indicating that it is more linear.

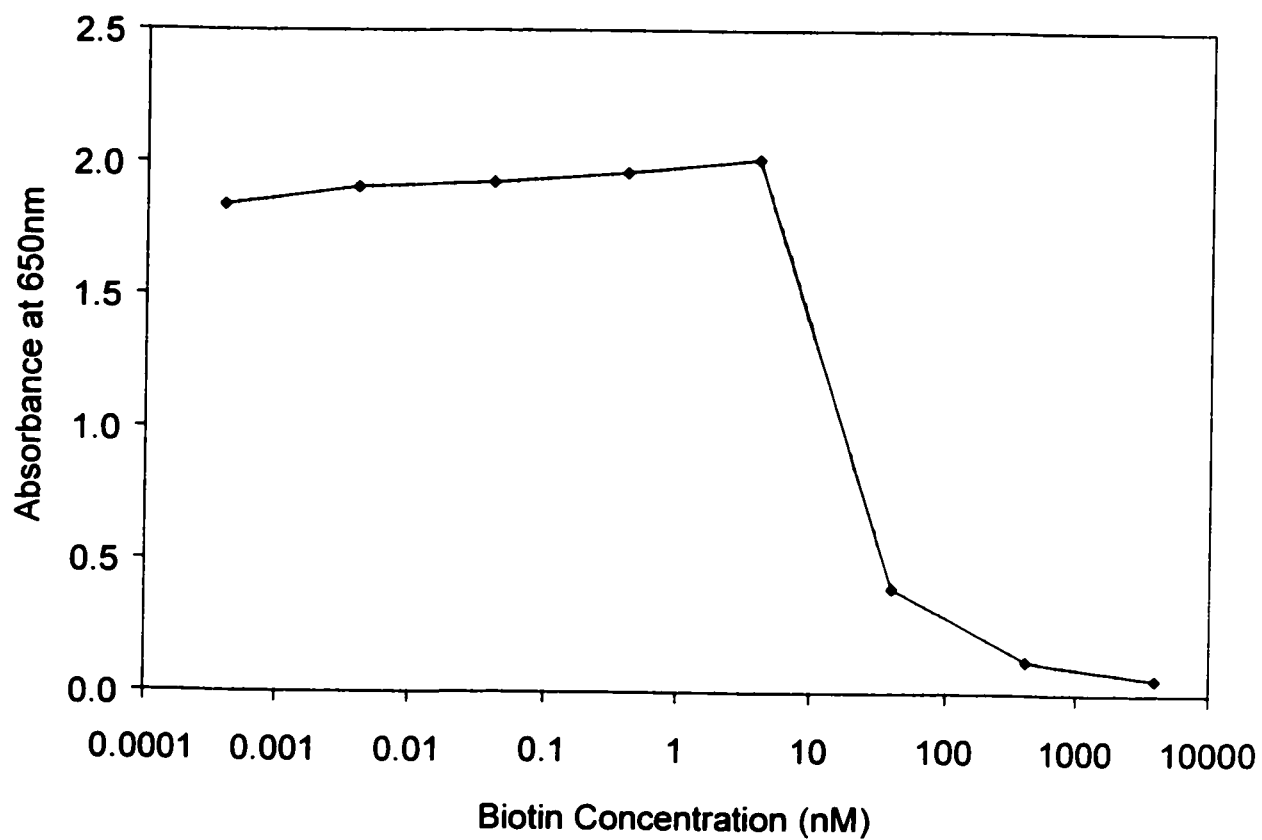


Figure 3.4 Biotin standard curve using an ELISA technique for 0.4pM–4μM.

The narrow increasing range is at 4nM–40nM.

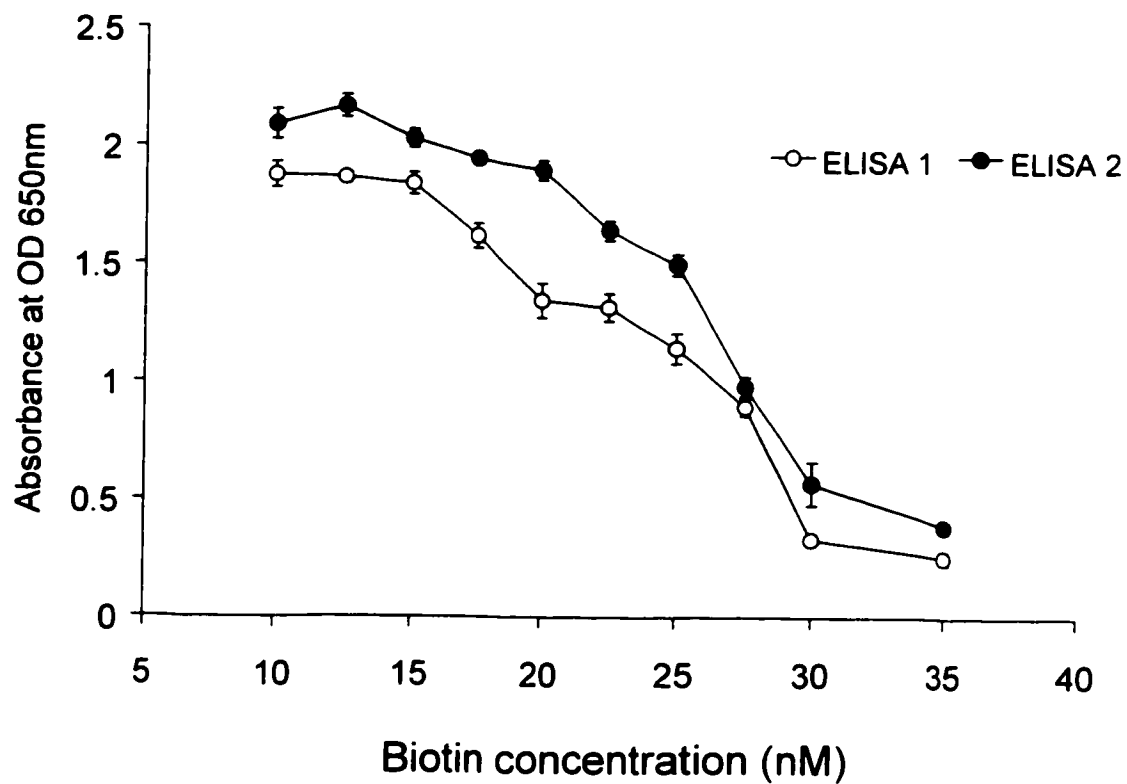


Figure 3.5 Biotin standard curve using an ELISA technique for biotin concentrations ranging from 10–35nM.

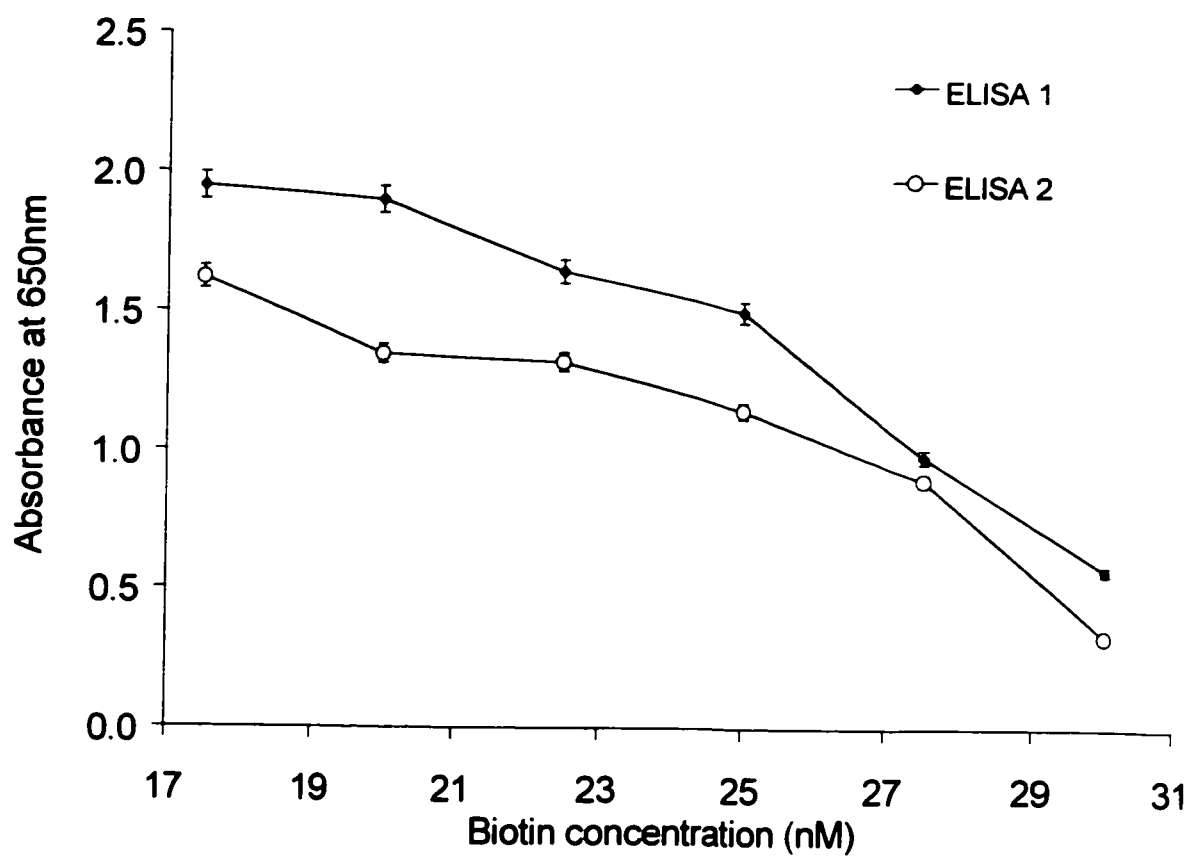


Figure 3.6 Biotin standard curves using an ELISA technique for biotin concentrations ranging from 17.5–27.5nM.

	Linear Range (nM)	Formula	R ²
ELISA 1	17.5—25	Y = -0.058 X + 2.60	0.9141
	17.5—27.5	Y = -0.066 X + 2.75	0.9518
	17.5—30	Y = -0.091 X + 3.27	0.8963
ELISA 2	17.5—25	Y = -0.064 X + 3.11	0.9452
	17.5—27.5	Y = -0.093 X + 3.70	0.8991
	17.5—30	Y = -0.112 X + 4.08	0.9249

Table 3.3 Comparison of the formula and R² value in different range of biotin standard curve using an ELISA technique.

Biotin contents in the unknown samples were estimated by extrapolating from a biotin standard curve in Figure 3.5. The average results are listed in Table 3.4. The concentration of biotin in the RPMI-1640 medium was determined using serial dilutions to move the biotin concentration into the linear portion (17.5–27.5nM) of the curve (Figure 3.6). The mean biotin concentration in RPMI-1640 medium was 825 ± 9.2 nM, which matched with the expected result $0.2\text{mg/L} = 819.7$ nM biotin in Sigma Chemical Company. When comparing biotin in mouse ascites using a HABA assay and an ELISA technique, the results of the HABA assay were not reliable because the biotin in mouse ascites was below the sensitivity of the HABA assay. Even using the more sensitive ELISA assay, the ascites levels were found to be <10nm in all four samples, where the sensitivity of the ELISA was 10nM.

Sample	Average Biotin Concentration
RPMI-1640 medium	825 ± 9.2 nM
Mouse ascites samples	
2-1	<10nM
2-2	<10nM
3-1	<10nM
3-2	<10nM

Table 3.4 Determination of biotin concentration in unknown samples using an ELISA technique.

In summary, the HABA assay is a simple method for biotin assay at the range of 1–20 μ M. The sensitivity or minimum detectable limit for this method was 1 μ M. Formula (2) can be directly used to calculate the biotin concentration in unknown samples instead of extrapolating a biotin standard curve. If the sample concentration is near to sensitivity limit (40 μ M) or ΔA is less than 0.034, the results of this HABA assay are not reliable. Biotin concentration in unknown samples should be above 40 μ M for accurate measurement.

The ELISA method is a more sensitive method than HABA assay. The sensitive region of the standard curve (Figure 3.5) range was 10–30nM. One disadvantage of this method is that the biotin standards should be run at the same time as the unknown samples because the ELISA is very sensitive method.

3.3.3 Biotin Uptake As a Function of the Biotin Concentration

The counting efficiencies of a liquid scintillation counter and 1450 Microbeta are $44.4 \pm 2.1\%$ and below 20% respectively. The results are shown on Table 3.5.

Measured activity(cpm)	Input activity(dpm)	Counting efficiency(%)
513	1110	46.2
528	1110	47.6
4701	11100	42.4
4716	11100	42.5
49132	111000	44.3
48358	111000	43.6
Mean		44.4 ± 2.1

Table 3.5 Calculation of the counting efficiency of liquid scintillation counter.

Mean counting efficiency is $44.4 \pm 2.1\%$. All samples have been corrected for background (15 cpm).

In Table 3.6, absolute uptake amounts are 218, 470, 1772 cpm and relative uptake percents are 0.414%, 0.092% and 0.036% respectively. The biotin uptake rates as a function of biotin concentration are shown in Figure 3.7. With the addition of cold biotin, the uptake of ^3H -biotin is reduced to near background levels when total biotin concentrations are greater than $5\mu\text{M}$. Therefore, only the first 2 data points for the ^3H -biotin plus cold biotin concentrations from Table 3.6 are plotted in Figure 3.7. The extra cold biotin concentration ($> 5\mu\text{M}$) can inhibit the uptake of ^3H -biotin and the effect was observed by others (Said HM *et al.*, 1998; Ma TY *et al.*, 1994; Debra W *et al.*, 1991). If we use the specific activity ratio to calculate the rate of biotin transport, the rate was found to increase similarly to research studies using intestine cell lines. The results are shown in Table 3.7 and Figure 3.8. The uptake percentage (0.2–0.4%) is low in ovarian cancer cells.

It appears that biotin uptake in ovarian cancer cells is a saturable and carrier mediated mechanism increasing as a function of concentration and inhibited by extra unlabeled biotin ($>5\mu\text{M}$). The ratio of cold biotin to hot biotin (no more than 20) was used for V_{max} and K_m determination. Biotin uptake amounts were corrected for counting efficiency and protein amounts. The biotin uptake rate vs. biotin concentration in SKOV cells is shown in Figure 3.7.

Uptake Activity cpm	Activity Added dpm	Uptake efficiency %
218	111000	0.414
470	1110000	0.092
1772	11100000	0.036

Table 3.6 Calculation of the uptake efficiency in SKOV cells

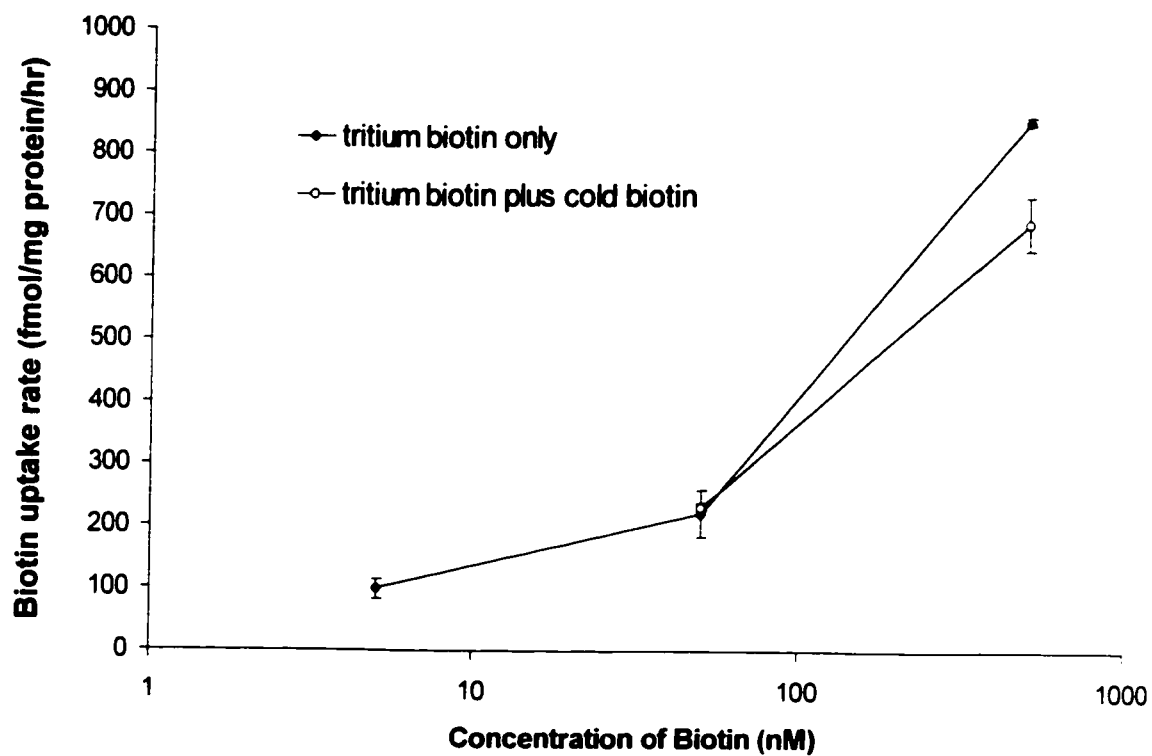


Figure 3.7 Biotin uptake rate vs. biotin concentration in SKOV cells. Error bars shown are due to biotin determination only.

Biotin concentration	5nM	50nM	500nM	5μM	10μM	20μM
Activity (without cold biotin)	240	524	1780	--	--	--
	196	416	1764	--	--	--
average activity	218	470	1772	--	--	--
SD	31.1	76.4	11.3	--	--	--
Activity (with cold biotin)	--	260	216	132	120	180
	--	244	96	188	108	192
average activity	--	252	156	160	114	186
SD	--	11.3	84.9	39.6	8.5	8.5
Activity (based on correction for specific activity)	--	504	1560	16000	22800	72000

NOTE: The unit of activity is cpm

Table 3.7 Original data for biotin uptake amount vs. biotin concentration in SKOV cells using a liquid scintillation counter. Without cold biotin, when the concentration of ³H-biotin increases, the uptake of biotin increases as well.

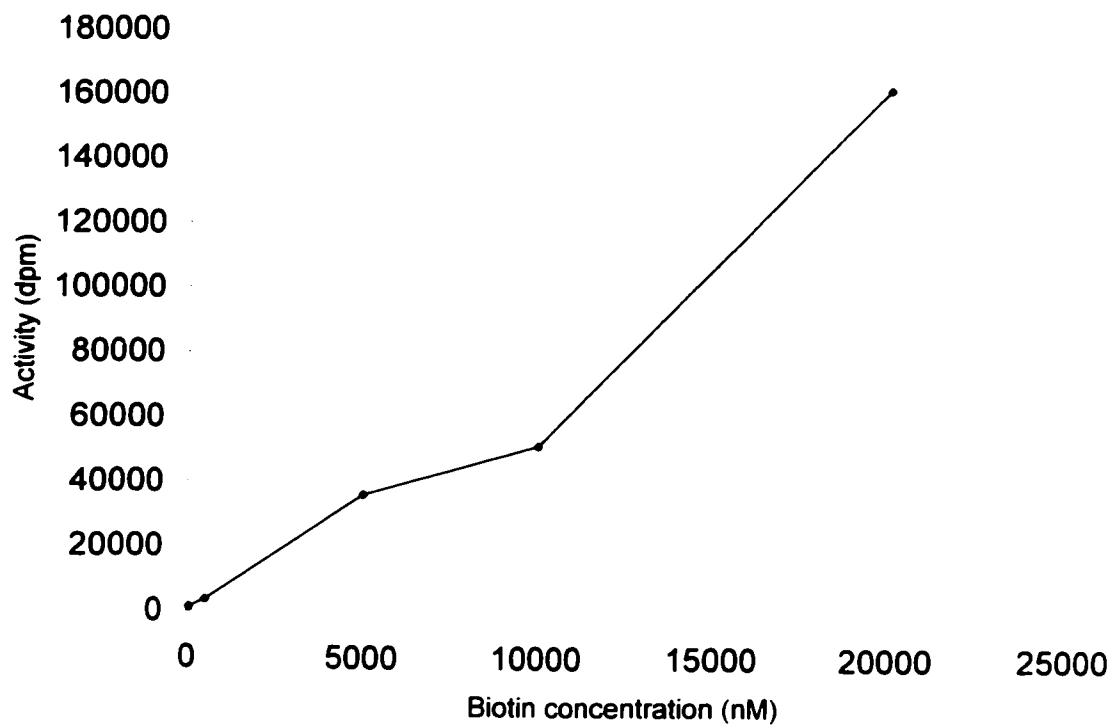


Figure 3.8 Biotin uptake vs. biotin concentration in SKOV cells (with cold biotin). Biotin uptake ratio with biotin concentration corrected for the cold biotin/hot biotin ratio.

3.3.4 Protein Assay With Bio-Rad Reagent

The protein assay standard curve is shown in Figure 3.9. The equation was obtained by a linear regression analysis (Microsoft, Excel 1997). Since this assay is sensitive, the standard curve was prepared for individual experiment instead of using an extinction coefficient.

The protein concentration and cell numbers were monitored using a protein assay and hemacytometer before and after the biotin uptake experiments. The protein concentrations were in the range of 0.1–0.2 mg protein/well and cell numbers were 10^5 – 10^6 cells/well.

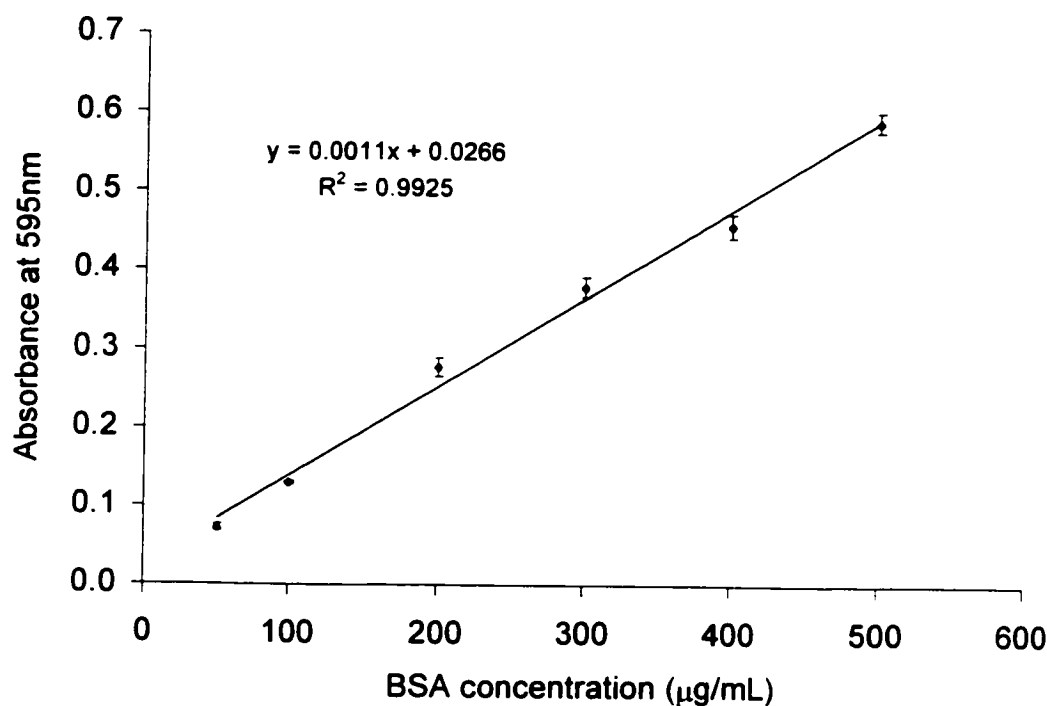


Figure 3.9 Standard curve for protein assay using Bio-Rad reagent.

3.3.5 Biotin Uptake As a Function of the Incubation Time.

The original data of biotin uptake amount vs. incubation time is shown in Table 3.8 and results are shown in Figure 3.10 for the OVCAR cells. The uptake amount of 1.5hr incubation was significantly different from that of 0.5hr incubation in OVCAR cells (ANOVA, $p < 0.05$). However, 4hr incubation was not significantly different from 1.5 hr incubation (ANOVA, $p > 0.05$). Increasing incubation time up to 24hr, uptake amounts were not significantly different compared to 1.5 hr incubation (ANOVA, $p > 0.05$). Therefore, the 1.5–2hr incubation was used for the uptake experiment. As shown in Table 3.9 and Figure 3.11, an incubation 1.5–2hr appeared adequate for the SKOV cells as well.

	Conc. of biotin (nM)	5	50	500	5000	50000	500000
Radioactivity (dpm) With cold biotin	Cold biotin 0.5hr	--	32.5	30	52.5	35	20
	Cold biotin 1.5hr	--	32.5	27.5	42.5	15	25
Radioactivity (dpm) Without cold biotin	0.5hr	17.5	45	70	--	--	--
	1.5hr	75	72.5	112.5	--	--	--
	4hr	35	60	117.5	--	--	--
	23hr	70	92.5	112.5	--	--	--

Table 3.8 Original data for biotin uptake amount vs. incubation time in OVCAR cells. Background is about 8 cpm. These data represent the mean of duplicate sample repeats.

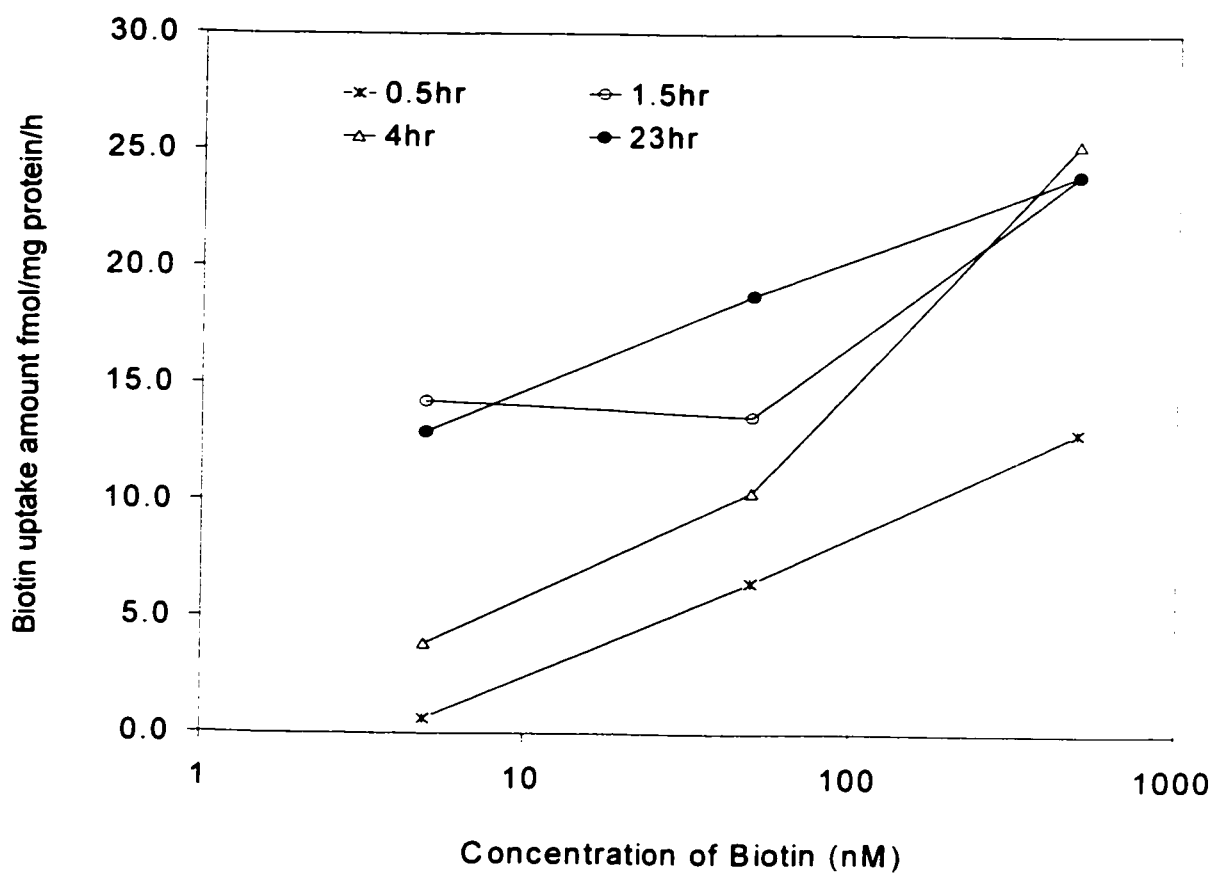


Figure 3.10 Biotin uptake rate vs. incubation time in OVCAR cell lines using a 1450 Microbeta. The 1.5–2hr incubation was enough for this uptake experiment.

Experiment Indication	(cpm)	Time	1	2	3	mean	SD
Experiment samples	50nM	4hr	702	892	856	874	25.5
		2hr	826	754	775	785	37.0
		1hr	632	531	516	560	63.1
		0.5hr	187	136	88	137	49.5
	5nM	4hr	80	--	--	80	0.0
		2hr	52	--	--	52	0.0
		1hr	31	74	--	53	0.0
		0.5hr	14	23	--	19	6.4
Negative controls	cell+no radioactivity	1hr	13	16	--	15	--
	no cells + 5nM	1hr	13	12	--	13	--
	no cells + 50nM	1hr	10	15	--	13	--

Table 3.9 Original data for biotin uptake amount vs. incubation time in SKOV cells using a liquid scintillation counter.

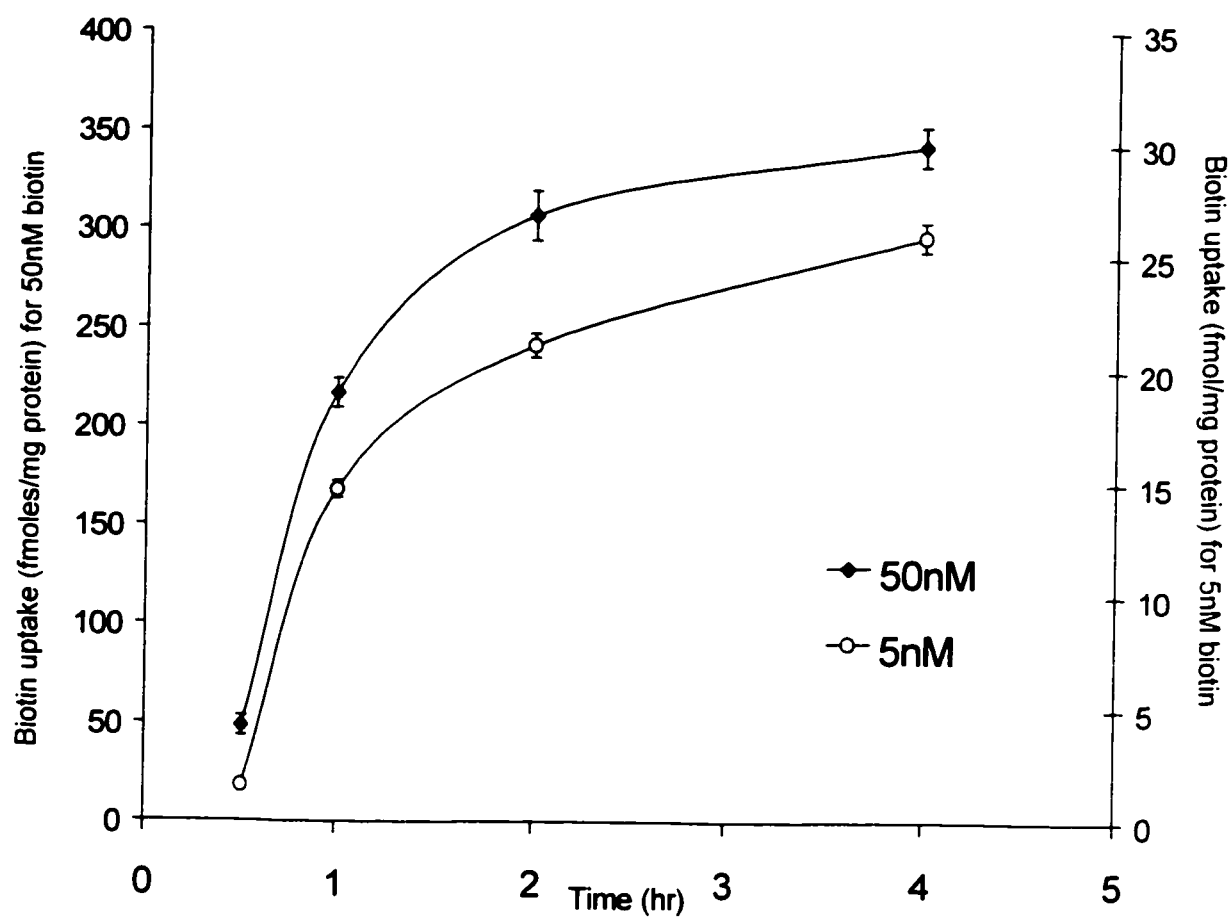


Figure 3.11 Biotin uptake kinetics vs. incubation time in SKOV cells using a liquid scintillation counter.

3.3.6 Determination of Vmax and Km

On the basis of previous studies, biotin concentration (50nM–800nM), 1 μ Ci/well activity, 10min incubation, and 6-well plates were chosen for Km and Vmax determination. The original counting activities were significantly higher than background (20cpm). The results are shown in Figure 3.12 and 3.13 for SKOV and OVCAR cells. The uptake activities were corrected for counting efficiency and protein assay results. The statistical analysis for linear regression was performed using the statistics program (Microsoft, Excel 1997). Vmax and Km are 51 ± 7.1 pmol/mg protein/10min and 1.9 ± 0.2 μ M respectively in OVCAR cell lines and 8.5 ± 1.3 pmol/mg protein/10min and 1.3 ± 0.4 μ M respectively in SKOV cell lines. The biotin accumulation in OVCAR cell is higher than that in SKOV cell using shown by their Vmax values. Additionally, the concentration of biotin that leads to half-maximal velocity in OVCAR cell is a little higher than that in SKOV cell. The transport mechanism appears to be a carrier mediated and saturable as a function of concentration as shown in Table 3.6. Biotin uptake amount was dependant on incubation time and biotin concentration.

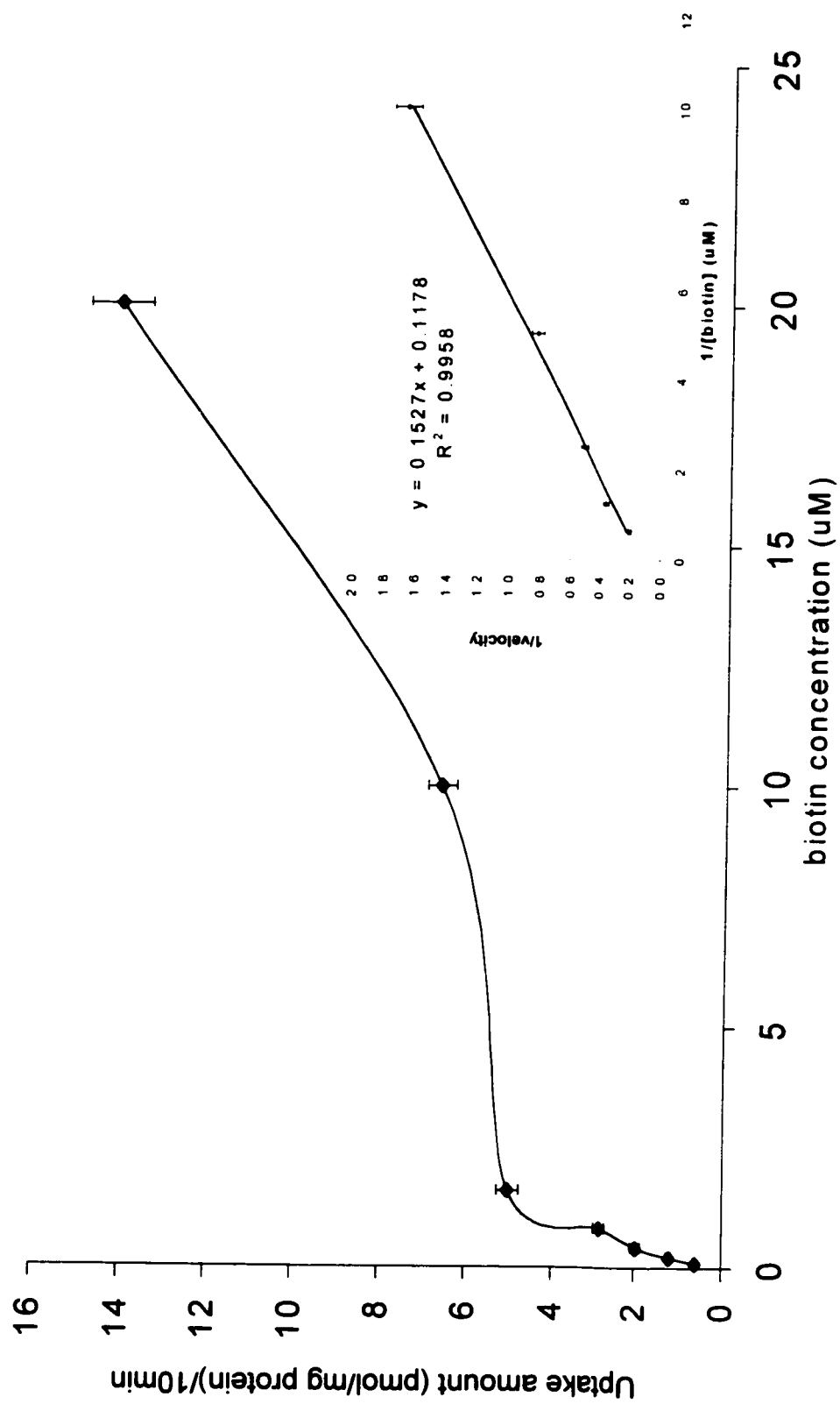


Figure 3.12 Determination of K_m and V_{max} in SKOV cell lines. The inset plot is $1/\text{velocity}$ vs. $1/[\text{biotin}]$

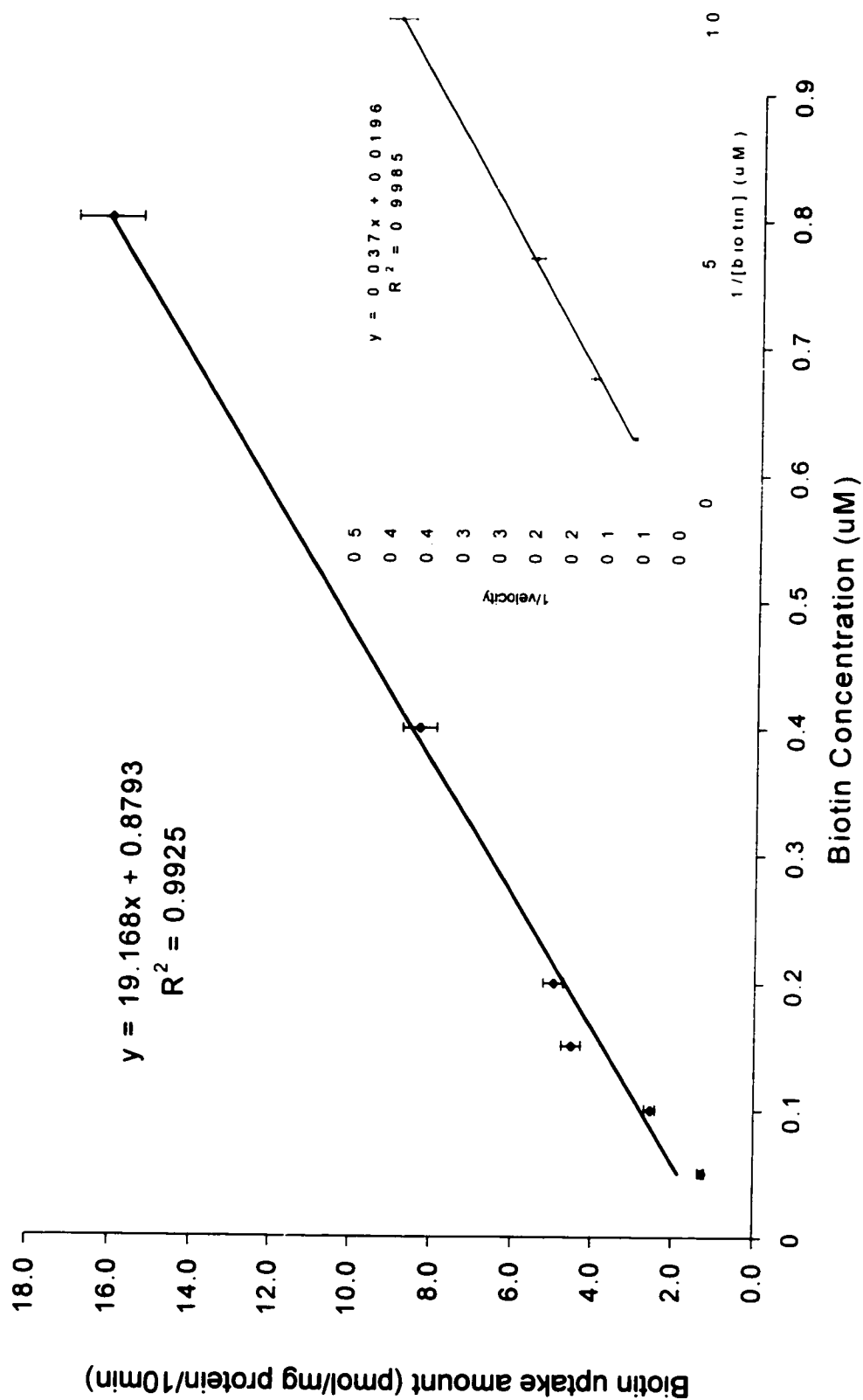


Figure 3.13 Determination of K_m and V_{max} in OVCAR cells. The inset plot is $1/\text{velocity}$ vs. $1/[biotin]$.

CHAPTER 4

BIOTINYLATED LONG-CIRCULATING LIPOSOMES AND *IN VITRO* TARGETING STUDIES USING CONFOCAL LASER SCANNING MICROSCOPY

4.1 INTRODUCTION

In this chapter, we propose to confirm the specific binding ability of biotinylated long-circulating liposomes to human ovarian cancer cells using biotinylated anti-CA125 monoclonal antibody as a pretargeting agent. The biotin-streptavidin system was used to connect this biotinylated Mab to the biotinylated liposomes and confocal laser scanning microscopy (CLSM) was used to monitor the binding characteristics (McQuarrie SA *et al.*, 2001; Xiao Z *et al.*, 2001).

4.1.1 Liposomes

Normally, phospholipids, cholesterol, and charged lipids are the main components of liposomes. Several methods have been used to prepare liposomes, including sonication (Zhang L *et al.*, 1997), French pressure (Brandl M *et al.*, 1990), detergent dialysis (Schwendener RA 1986), ether injection, ethanol injection (Betageri GV *et al.*, 1993), and extrusion (Hope MJ *et al.*, 1984). Many studies demonstrate that extrusion is a better protocol to prepare liposomes over the other techniques as

summarized below (Mayer LD *et al.*, 1985; Mayer LD *et al.*, 1986; Hope MJ *et al.*, 1984).

The disadvantage of sonication is moderate overheating. The disadvantage of French pressure is elevated pressures. These disadvantages result in degradation of phospholipids and problems in the stability of liposomes. Ether injection, ethanol injection, and detergent dialysis include organic solvents, detergents, surfactants, and emulsifiers, which cause problems in the stability and homogeneous size distribution of liposomes. Some advantages of extrusion are listed below:

- Lipid solutions are maintained in mild conditions, low pressure, with no organic solvents to damage the liposomes.
- The pore size of the polycarbonate filters is defined, facilitating homogeneous size distribution in a simple and rapid way.
- Extrusion can be used over a wide range of lipid concentrations (0–400mg/mL lipid) with high loading efficiencies (80%).

Different liposomes have specific targeting ability to different cell lines as described more completely in Section 1.6.2. In this chapter, we plan to confirm the specific binding ability of our biotinylated long-circulating liposomes to human ovarian cancer.

4.1.2 Confocal Laser Scanning Microscopy

Confocal laser scanning microscopy (CLSM) was first described by Marvin Minsky in 1957 (Marvin Minsky 1957). This invention did not obtain wide recognition until about 30 years later when CLSM was accepted as a potential tool in biological research on subcellular structure, function, and physiology (Marvin Minsky 1988).

Conventional light and electron microscopy have their own limitations. Light microscopy can view living cells, but with low resolution. The planes below and

above the focal plane are also illuminated. This wide focal plane obscures important structures of interest, particularly in thick specimens with overlapping structures. Electron microscopy can view ultrastructural details, but damages specimens and the samples need to be fixed (Brian M *et al.*, 1993).

CLSM has several advantages over conventional light microscopy and different uses than electron microscopy. The principles of CLSM are shown in Figure 4.1.

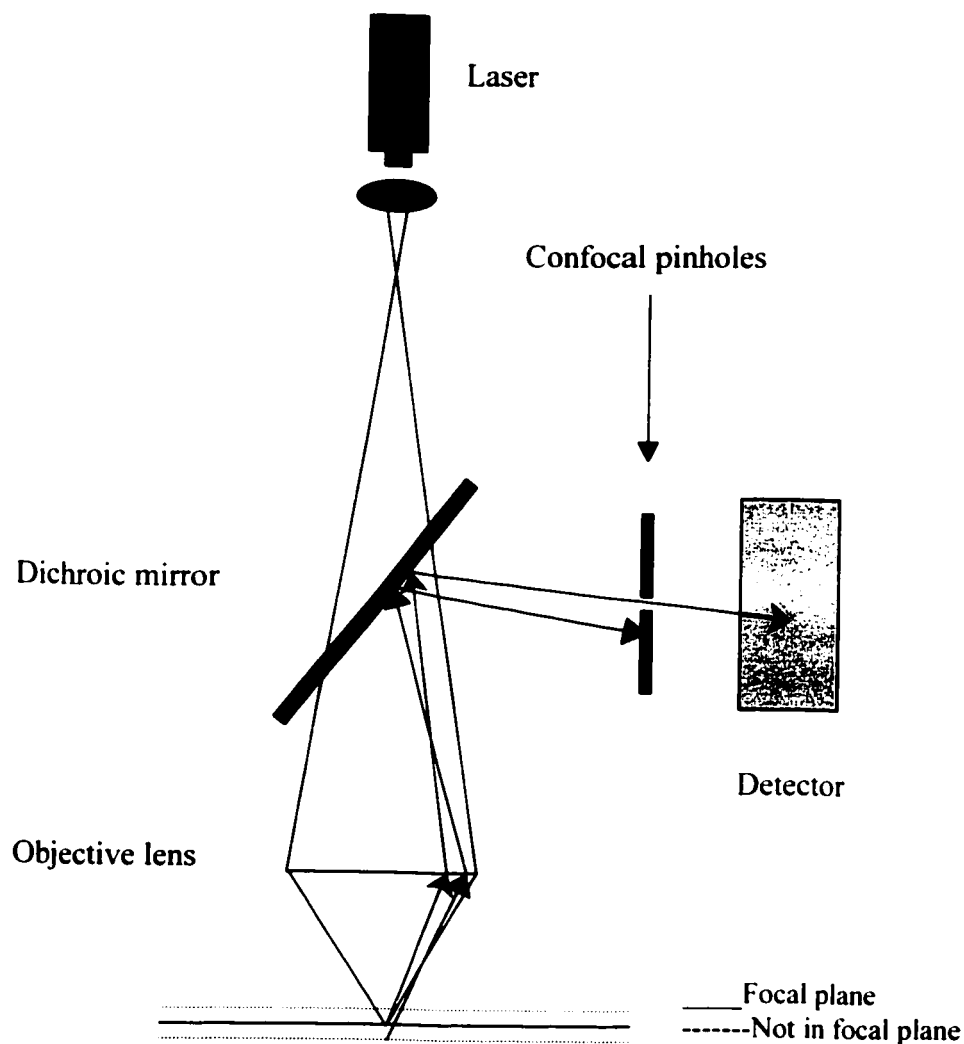


Figure 4.1 A schematic representation of confocal laser scanning microscopy

A laser provides the excitation light to pass through a dichroic mirror and objective lens, resulting in illumination of a small spot of a fluorescent dye-labeled specimen (focused spots as small as 0.25 μm in diameter and 0.5 μm deep). The fluorescent dye absorbs the excitation light and emits fluorescent light at a higher wavelength. The desired fluorescent light from the focal plane returns through the objective lens and is reflected by the dichroic mirror, passed through a pinhole, and collected by a photomultiplier detector. The scattered light outside the focal plane is reflected by the dichroic mirror but is obscure to the photomultiplier, since it does not pass through the pinhole. Thus, the light signals from the out-of-focus planes do not contribute to the image, resulting in high clarity and resolution.

The light signals are transformed into electrical signals by the photomultiplier detector. The photomultiplier has a photocathode that absorbs the photons and results in emission of electrons. The electrons are then accelerated under the high voltage to strike a series of dynodes resulting in production of a shower of electrons. Thus the light signals are amplified by the photomultiplier and subsequently converted into digital signals for display on a computer screen. The software programs allow us to analyze objects by their sizes, location and fluorescence intensity (Shotton DM 1989; White JG *et al.*, 1990). Additionally, CLSM can sequentially scan different parallel planes within the specimen with the help of the laser and objective lens. Stored images may be reassembled to obtain a three dimensional view of the specimen. Therefore, we can summarize the advantages of CLSM as shown below.

- It increases image resolution and clarity, especially for the thick specimens.
- CLSM can directly successively scan the specimen without resorting to thin sectioning and tissue fixation. Specimens can be optically scanned not only in the xy plane, but also in the xz and yz planes (Shotton DM 1989; Wilson T 1989). Thus a three dimensional view of the specimen can be reconstructed, which provides better observation of the structural components of living cells.

- The CLSM images can be analyzed by their sizes, fluorescence intensity, numbers of objects in the image, etc. With the help of the computer, quantitative studies are possible (Centroze V *et al.*, 1995).

4.1.2.1 Fluorescent Dyes

When a molecule is activated by light, it may emit photons of higher wavelength. Normally, the molecule absorbs energy and emits a lower energy, resulting in a longer emitted wavelength than the excitation wavelength. Many different kinds of fluorescent dyes can be used in confocal laser scanning microscopy (CLSM) if their emission wavelengths are sufficiently different. Among these, fluorescein and rhodamine are commonly used.

Fluorescein isothiocyanate (FITC) (excitation/emission at 490/520 nm) is a green fluorescent dye that is widely used in CLSM because its excitation maximum is close to the 488 nm spectral line of many lasers. Additionally, it may be highly purified and it has a high extinction coefficient (Goldsby RA *et al.*, 2000). Many fluorescent dyes are marketed by Molecular Probes, including fluorescein and sulforhodamine 101 (excitation/emission at 578/593 nm). Sulforhodamine B (excitation/emission at 565/586 nm) was selected for our studies. It has red fluorescence, strong absorbance, and good photostability (Torchilin VP *et al.*, 1992). When fluorescent dyes are coupled to antibodies, the emitted light can be detected by CLSM and the location of antibodies within biological specimens can be visualized.

4.2 MATERIALS AND METHODS

4.2.1 Preparation of Biotinylated Liposomes Encapsulated with Sulforhodamine B

4.2.1.1 Materials

50mM DSPC solution: 1,2-Distearoyl-sn-glycero-3-Phosphocholine (MW 790.15, Alabaster, AL) 790.15mg was dissolved in 20mL of chloroform to obtain 50mM DSPC clear solution.

50mM Cholesterol solution: Cholesterol (MW 386.66) 386mg was dissolved in 20mL of chloroform to obtain 50mM cholesterol clear solution.

5mM DSPE-PEG₂₀₀₀ solution: 1,2-Distearoyl-sn-Glycero-3-Phosphoethanolamine-N-Polyethylene glycol)-2000 (MW 2748.07, Alabaster, AL) 274mg was dissolved in 20mL of chloroform to obtain 5mM DSPE-PEG clear solution.

5mM DSPE-biotin solution: 1,2-Dioleoyl-sn-Glycero-3-Phosphoethanolamine-N-Biotin (MW 992.32, Alabaster, AL) 99mg was dissolved in 20mL of chloroform to obtain 5mM DSPE-biotin clear solution.

Sulforhodamine B solution: Sulforhodamine B 2 mg (Molecular Probes, Eugene, OR) was dissolved in 4mL water.

All above reagents were stored at 4°C.

4.2.1.2 Methods

Sulforhodamine B labeled liposomes were prepared using a commercial extruder (Lipex Biomembranes Inc, Vancouver BC, Canada). An 0.8mL aliquot of 50mM

DSPC solution and 0.4mL of 50mM cholesterol solution were mixed together to obtain a uniform lipid solution (molar ratio DSPC to cholesterol = 1:2). An extra 4mL of chloroform was added to facilitate formation of a thin film during evaporation. This homogeneous lipid mixture was transferred to a round bottom flask and organic solvent was removed under negative pressure by rotary evaporation for 2hr. A thin uniform lipid film was formed on the bottom of the flask and was stored in a refrigerator overnight to remove all chloroform solvent. Under heating and frequent vortexing, the lipid film was completely resuspended with 2mL of sulforhodamine B solution to produce multilamellar vesicles (MLV). This solution was stored in a refrigerator overnight to maximize encapsulation of sulforhodamine B prior to extrusion. The lipid suspension was extruded four times through 0.2 μ m polycarbonate filters (Nuclepore Corp. Pleasanton, CA), followed by extrusion 10 times with 0.1 μ m and 0.08 μ m polycarbonate filters stacked to facilitate production of homogeneous unilamellar vesicles (ULV) with an average diameter of about 100nm as determined by dynamic light scattering (BI-90 Particle sizer, Brookhaven Instruments Inc.). The extrusion temperature was controlled at approximately 50°C.

Biotinylated long-circulating liposomes containing sulforhodamine B were prepared using similar method as described above. A 1.6mL aliquot of 50mM DSPC solution, 0.8mL of 50mM cholesterol solution, 0.8mL of 5mM DSPE-PEG solution, and 0.16mL of 5mM DSPE-Biotin solution were mixed to obtain a uniform solution (molar ratio DSPC:Cholesterol: DSPE-PEG:DSPE-Biotin = 2:1:0.1:0.02). The other procedures are same as above.

4.2.2 Purification of Liposomes Using a Sephadex G50 Column

A Sephadex G50 column is used to separate molecules ranging from 1.5×10^3 – 3×10^4 Da. HEPES buffer (25mM HEPES in 140mM NaCl, pH 7.4) was used to equilibrate a Sephadex G50 column (bead height 7.5cm, diameter 2.8cm). The liposome suspension was carefully added to the top of column using a Pasteur pipette. HEPES buffer was layered on the column immediately after all liposome

suspension had completely flowed into the bead matrix. The liposomes were completely separated from unencapsulated dye due to their large size. Fractions were collected in 1mL aliquots and absorbance was monitored at 543nm.

4.2.3 Stability of Liposomes

Liposome fractions were diluted 10 fold using 25mM HEPES buffer and the size distribution of liposomes was monitored by dynamic light scattering (BI-90 Particle sizer, Brookhaven Instruments Inc.). Liposome leakage was quantified by Sephadex G50 column chromatography and ultracentrifugation. Liposome solutions were stored at room temperature for 4 days, followed by passage on a Sephadex G50 column. The procedure was the same as the purification procedure described above. Fractions were collected 1mL/tubes to quantify the liposome and free dye peaks at 543nm and to estimate the leakage of sulforhodamine B from the liposomes. Ultracentrifugation was used to separate the liposome suspension and quantify the absorbance of both supernatant and pellet.

4.2.4 *In Vitro* Targeting via the Biotin-Streptavidin System Using CLSM

4.2.4.1 Materials

- HBSS solution: one package of HBSS powder (9.5g) (Sigma, St. Louis MO) and 0.35g of NaHCO₃ were dissolved in 1L of distilled water and the pH was adjusted to 7.2. The solution was filtered through a 0.22µm membrane filter.
- Glycerol /PBS solution: glycerol was 1:1 diluted using PBS solution.

4.2.4.2 Methods

OVCAR-3 cell lines (CA-125 positive cell lines) were cultured in 75cm² flasks using RPMI-1640 medium containing 8% FBS and 1% penicillin-streptomycin. When the cells were in log phase growth, 4mL of 0.25% trypsin-EDTA (GIBCO, Grand Island, NY) was used to detach the cells followed by centrifuging at 1000rpm (95g) for

5min. The supernatant was discarded and the cell pellet was resuspended using fresh RPMI 1640 medium. Vortexing was used to resuspend the cell pellet if necessary. The cells were counted using 0.4% trypan blue and 10^5 cells/well were transferred to a Lab-Tek slide (Nalge Nunc, Naperville IL) to culture for 2–4 days. Cell growth was monitored with an inverted microscope and the medium was changed as necessary. After the cells were firmly adherent to the surface of the slide, the cells were carefully washed 3 times with HBSS to remove exogenous biotin. OVCAR-3 cell lines were incubated with $2\mu\text{g}$ of biotinylated Mab B27.1 in $600\mu\text{L}$ of HBSS at 37°C for 1hr to facilitate anti-CA125 Mab binding to CA125 antigen on the surface of the ovarian cancer cells. After washing 3 times with HBSS, $2\mu\text{g}$ of SA-FITC solution in $400\mu\text{L}$ of HBSS was incubated with OVCAR cells at 37°C for 30min to facilitate SA-FITC binding to the biotinylated Mab B27.1. After washing 3 times with HBSS, $400\mu\text{L}$ of biotinylated liposome solution were incubated at 37°C for 2hr, resulting in biotinylated liposomes binding to SA-FITC. After washing as above, one drop of 1:1 glycerol/PBS solution was added and the slides were coverslipped. Fluorescence distribution was monitored by CLSM (Zeiss LSM510, NLO, Jena, Germany). SKOV cells (CA125 negative cell line) were used as a negative control. All labeling procedures were the same as above. Another negative control was that OVCAR cell lines were incubated with SA-FITC and liposomes in the absence of the pretargeting biotinylated Mab B27.1. The settings of CLSM are listed below:

Beam Splitters	MBS:	HFT 488/543 primary beam splitter
	DBS1:	NFT 545 second beam splitter
		488/543 excitation wavelengths
	Ch1	LP 560
	Ch2	LP 505

Scan mode:	Plane 8 bit
Objective:	Plan-Neofluar 40×1.3 Oil
Pixel image format:	512×512
Pixel Time:	$2.24\mu\text{s}$

4.3 RESULTS AND DISCUSSION

4.3.1 Preparation of Liposomes

Several techniques are used to prepare liposomes and extrusion is the most advantageous one as described above. We used the extruder (Lipex Biomembranes Inc. Vancouver BC, Canada) to prepare liposomes. Several factors need to be optimized to produce the good characteristics of liposomes.

- Liposome constituents were dissolved completely in organic solvent to achieve a uniform lipid solution. The organic solvent was removed by rotary evaporation to obtain a lipid film as thin as possible. The residual solvent was completely removed by storing under vacuum or in a fume hood overnight. This is a critical procedure to achieve stable liposomes.
- The lipid film was resuspended by addition of an aqueous solution under vortexing and warming. The temperature of resuspension should be above the transition temperature (T_c or T_m) to facilitate encapsulation of an aqueous interior. Transition temperature is an important property of a phospholipid because phospholipid becomes fluid when the temperature is above the T_c point. Normally, vortexing and maintaining lipid suspensions overnight prior to extrusion are suggested to achieve homogeneous multilamellar vesicles (MLV) with high loading efficiency. Resuspending lipid in an ice bath or water bath alternatively may also increase the loading efficiency.
- MLV are forced through a defined polycarbonate film to yield homogeneous large unilamellar vesicles (LUV) and small unilamellar vesicles (SUV). Size distribution is close to that of the polycarbonate film, if multiple extrusions are done. For example, more than 10 times was used.

Stability is an important characteristic of liposomes. Some factors may compromise the stability of liposomes, including phospholipid degradation, hydrolysis or oxidation, liposome aggregates, fusion or leakage. Neutral buffers (HEPES buffer) are used to reduce lipid hydrolysis. Negatively or positively charged lipids are used to reduce liposome aggregation and fusion. Saturated fatty phospholipids with high T_c (DSPC $_{Tc}$ = 55°C) can be used to reduce leakage of the aqueous interior.

On the basis of the above considerations, biotinylated liposomes encapsulated with Sulforhodamine B were prepared by extrusion for *in vitro* targeting studies. Liposomes were purified using a Sephadex G50 column. Figure 4.2 shows the purification profile, indicating that liposomes were completely separated from the free dye peak. The loading efficiency is 14% and the calculation is shown below.

Loading efficiency (%)

$$\begin{aligned} &= (\text{Total absorbance of liposome peak} / \text{Total absorbance of dye}) \times 100 \\ &= (2.96 / 21.3) \times 100 \\ &= 14 \end{aligned}$$

Figure 4.3 shows the degree of leakage of liposomes after incubation of liposome suspension at room temperature for 4 days. The Sephadex G50 column was used to separate any free dye from the liposomes. The leakage was less than 2%. The calculation is shown below.

Leakage (%)

$$\begin{aligned} &= (\text{Total absorbance of free dye} / \text{Total absorbance of liposomes}) \times 100 \\ &= (0.014 / 0.74) \times 100 \\ &= 1.9 \end{aligned}$$

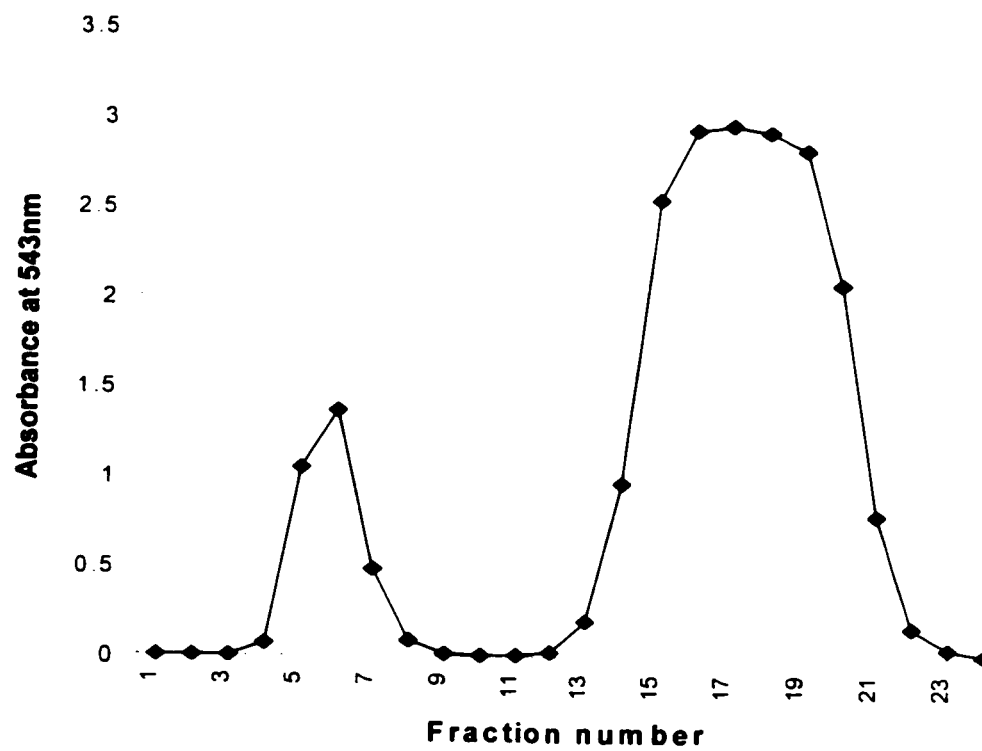


Figure 4.2 Purification of liposomes using a Sephadex G50 column. The first peak is the liposome peak and the second peak is free dye.

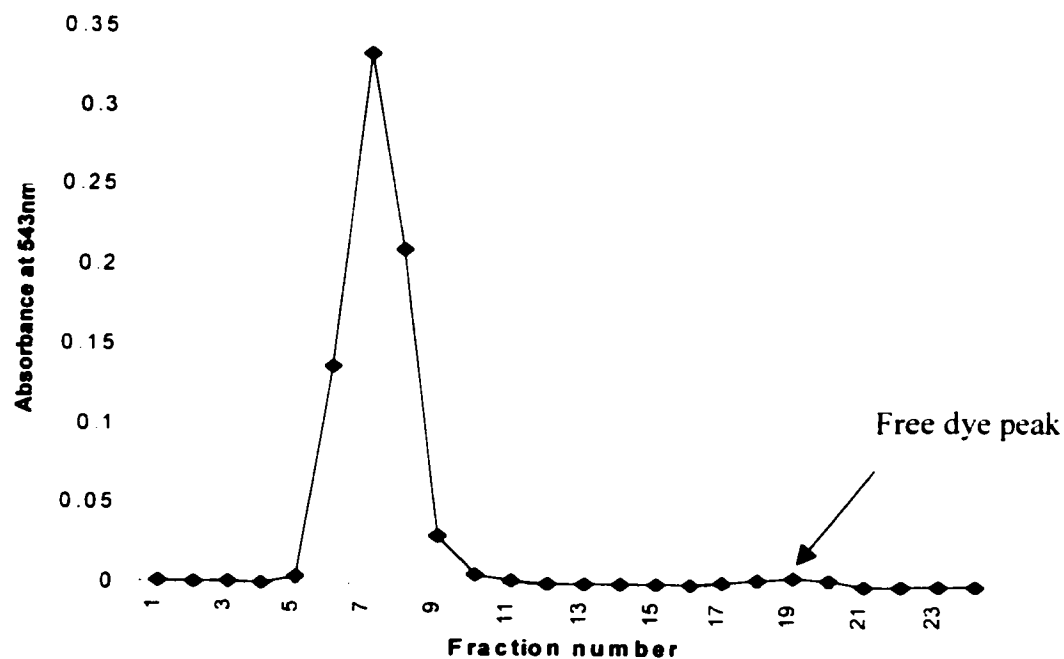


Figure 4.3 Stability of liposomes during storage at room temperature for 4 days. The free dye peak indicates that dye leakage is less than 2% after incubating at room temperature for 4 days.

4.3.2 *In Vitro* Targeting Study

The main project is a novel multistep radioimmunotherapy (RIT) for ovarian cancer. The long-term goal is to use bispecific monoclonal antibody (BsMab) with two paratopes (anti-CA125 and anti-biotin) to direct radionuclides encapsulated in liposomes to ovarian cancer micrometastases. Since the BsMab remained under development, we first used biotinylated anti-CA125 Mab to direct biotinylated liposomes to ovarian cancer cells in the *in vitro* study. Streptavidin was used to bridge two biotinylated reagents.

In the *in vitro* targeting study, biotinylated anti-CA125 Mab B27.1 targeted the CA125 antigen on the surface of OVCAR cells (CA125 positive cells). Streptavidin conjugated with FITC (SA-FITC, green label) was added as a second step in targeting. Green fluorescence was used to monitor the binding localization of the antibody (Figure 4.4). Since biotin has an extremely strong binding affinity to avidin ($K_d = 1.3 \times 10^{-15} \text{ M}$ at pH 5) (Green NM 1963), SA-FITC strongly bound to biotinylated Mab and resulted in green fluorescence on the surface of ovarian cancer cells (Figure 4.4). Streptavidin, the bacterial analog of avidin, is an analogous reagent of avidin to reduce nonspecific binding in many applications. Without biotinylated Mab B27.1, SA-FITC did not bind to the surface of ovarian cancer cells, resulting in no fluorescence (data not shown). Therefore, the green fluorescence on the surface of OVCAR cells indicated that biotinylated Mab specifically targeted the CA125 antigen on the surface of cells and SA-FITC bound to biotinylated Mab via biotin-streptavidin bridging. This result was confirmed by a sensitive ELISA as described in Section 2.2.6.2 and by flow cytometry.

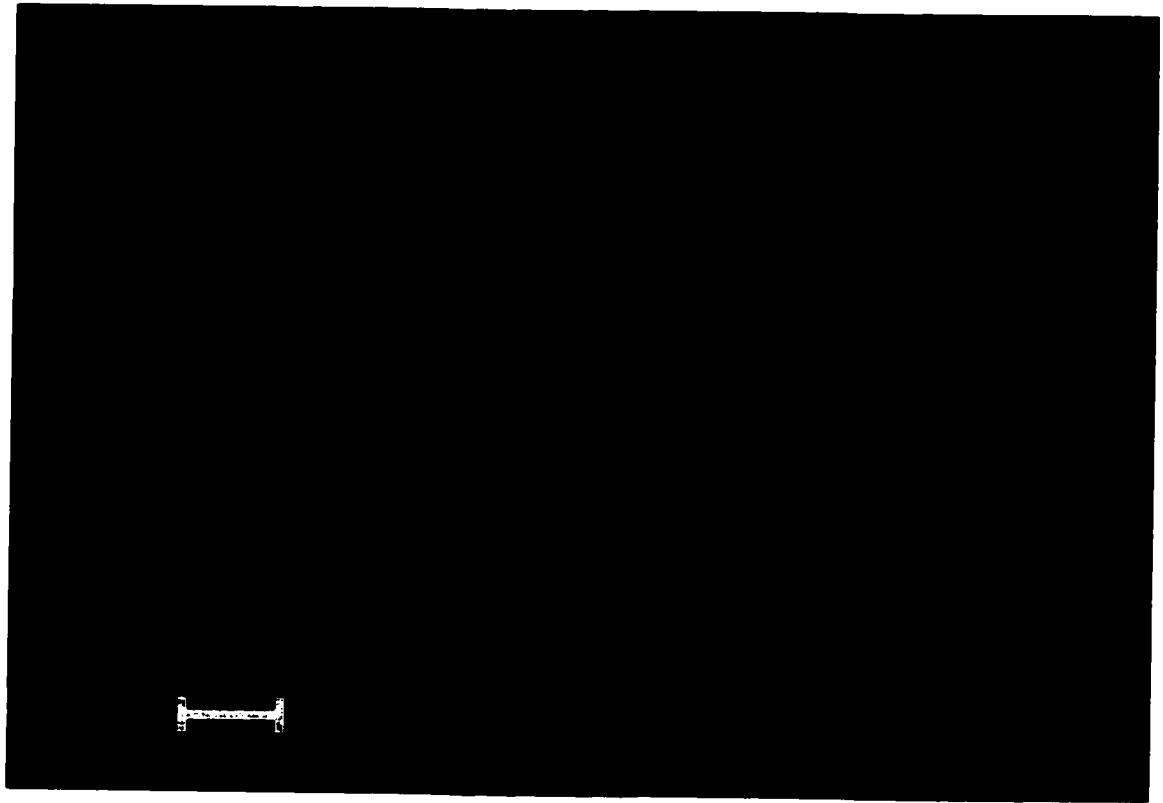


Figure 4.4 Biotinylated antibody specifically binds to the surface of OVCAR cells. The green label on the surface of OVCAR cells confirms that the biotinylated Mab B27.1 targets the OVCAR cells and directs SA-FITC (green label) to the surface of ovarian cancer cells via biotin-streptavidin cross-linking. The scale is shown on the image and average diameter of the cells is approximately 16 μ m.

Following binding of biotinylated Mab and SA-FITC to ovarian cancer cells, biotinylated liposomes containing sulforhodamine B (red label) bound to SA-FITC via the biotin-streptavidin bridge, resulted in red fluorescence on the cells' surfaces (Figure 4.5). The red dye was used to monitor the binding localization of the liposomes, as a surrogate for radionuclides, upon which the therapy was predicated. Without biotinylated antibodies, biotinylated liposomes do not bind to OVCAR cells, resulting in the lack of red fluorescence at the cell membrane (data not shown). Since the red dye signal was weak, a long incubation time (1hr, 2hr, overnight) was used to monitor liposome binding. The red dye shows a stronger signal with increasing incubation times (2hr and overnight). Additionally, biotinylated liposomes were incubated with SA-FITC for 2hr, following by monitoring this mixture by fluorescence microscopy. The green and red fluorescence at the same sites indicated that biotinylated liposomes could target SA-FITC via biotin-streptavidin cross-linking.

Thus the red fluorescence on the surface of OVCAR cells demonstrated that biotinylated anti-CA125 Mab could attract biotinylated liposomes to OVCAR cells via biotin-streptavidin cross-linking. Some preliminary images of internalized liposomes are shown in Figure 4.6 on the basis of a 12hr incubation. Uptake of liposomes is possibly due to receptor-mediated endocytosis, or by merger of the liposomes with the cell membrane. Since some radionuclides can achieve therapeutic efficacy from outside the cells, internalization of liposomes is not necessary in our radioimmunotherapy approach.

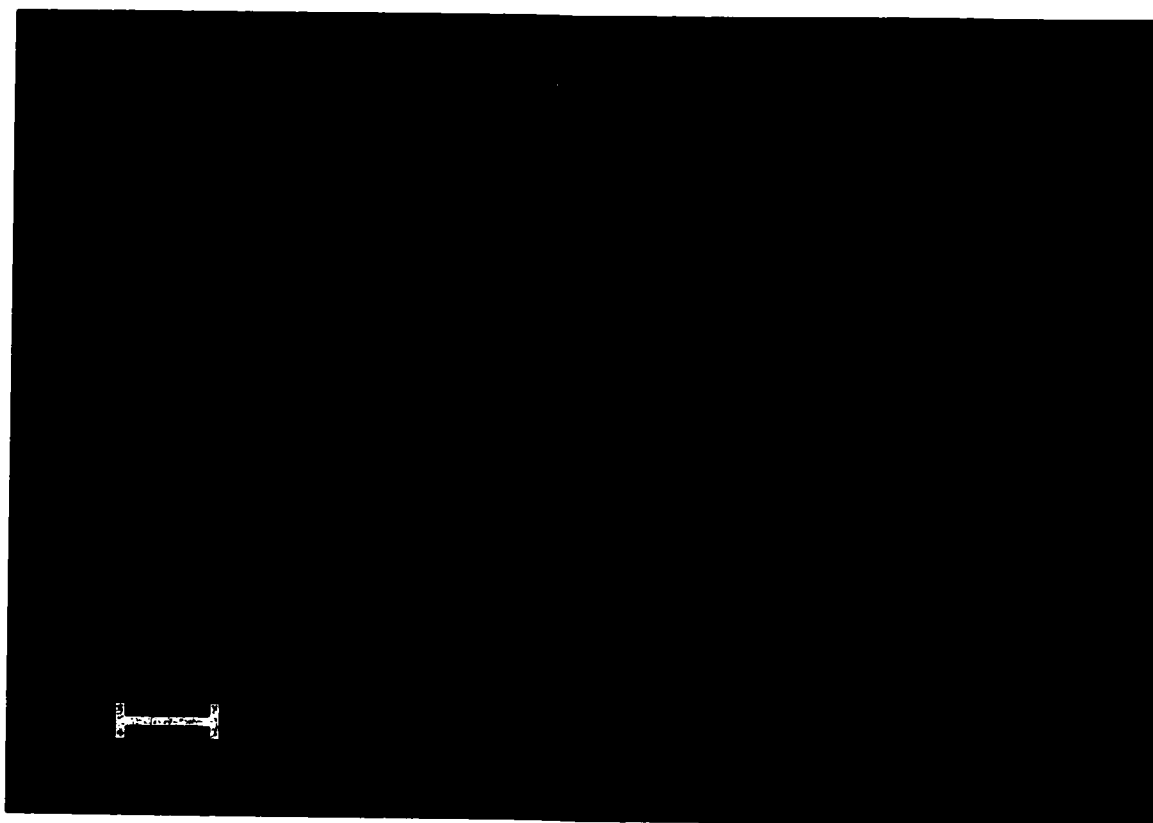


Figure 4.5 Biotinylated liposomes specifically bind to the surface of OVCAR cells. The red fluorescence on the surface of OVCAR cells is used to monitor the localization of liposomes, indicating that biotinylated liposomes encapsulated with sulforhodamine B (red dye) target the OVCAR cells via the cross-linking of the biotin-streptavidin system. The scale is shown on the image and average diameter of the cells is approximately 16 μ m.



Figure 4.6 Preliminary images of biotinylated monoclonal antibody and biotinylated liposomes. The biotinylated liposomes may be internalized to OVCAR cells after 12hrs incubation in images 1–3. The green fluorescence is used to monitor the location of biotinylated Mab and the red fluorescence is used to monitor the location of biotinylated liposomes. Image 4 is surface labeled after 2hrs incubation. The scale is shown on the image and average diameter of the cells is approximately 16–18 μ m.

CHAPTER 5

SUMMARY AND FUTURE WORK

SUMMARY

Our overall program is on the use of radioimmunotherapy approach as an adjuvant treatment for ovarian cancer. My specific project in this program is to mainly address if a) there is a biotin transport system in ovarian cancer cells that could be a potential alternate mechanism of uptake of biotinylated liposomes and b) free biotin in ascites and other body fluids would be a competitive inhibitor of the radioimmunotherapeutic strategy. Since the BsMab is under development, we first used biotinylated anti-CA125 monoclonal antibody as a pretargeting agent to tag the ovarian cancer, following by specific targeting of biotinylated long-circulating liposomes to the ovarian cancer cell *in vitro*. The following tasks have been completed in this thesis.

The Mabs B27.1 and B43.13 were successfully produced and subsequently purified using a Protein G column. Their immunoreactivity and relative affinities were confirmed by a modified ELISA technique and their purity was characterized by SDS-PAGE. The relative purity of Mab B27.1 and B43.13 are 88% and 91% as determined by “ImageJ image analysis” of SDS polyacrylamide gels. The relative affinity of Mab B27.1 for CA 125 was approximately 1.6 times higher than that of Mab B43.13. This is similar to the literature result of 1.6 times (Nustad K *et al.*, 1996).

Mabs B27.1 and B43.13 were biotinylated. The characteristics of biotinylated Mabs were determined using HABA assay, ELISA, and CLSM techniques. Since the concentrations of our Mabs were low (about 1mg/mL), a long incubation procedure (12hr) was used to biotinylate Mabs which is a modification of a previously described method (Coligan JE *et al.*, 1998). The HABA assay, ELISA, and CLSM all confirmed that antibodies had been labeled with biotin. The conjugation ratios of biotin/antibody are 7.4 and 5.9 for Mabs B27.1 and B43.13 respectively. The immunoreactivity of our biotinylated antibody was compromised by biotinylation (about 30%), but it was functional in the *in vitro* targeting studies. The NHS-LC-Biotin derivatizes the epsilon lysine residues and some of these may reside in the antigen-combining region of the antibody. This could be one possible explanation for the reduced immunoreactivity. Long-armed carbohydrate directed biotinylation reagents, such as biotin-LC-hydrazide, may be preferable for the future biotinylation protocol for our Mabs B27.1 and B43.13.

Since we use BsMab, the exogenous biotin may engage the biotin binding site of BsMab and result in inhibition of liposome targeting. In order to know if exogenous biotin has effects on our liposome targeting, we developed a sensitive method to determine the biotin content in ascites fluid. Since the HABA assay has low sensitivity (1 μ M, Green NM 1970), a more sensitive ELISA method was developed to determine biotin content. The biotin standard curve however had a narrow range of 10–30nM for determining biotin concentrations in unknown samples. The experimental limits of the biotin detection of the HABA assay and ELISA techniques were 40 μ M and 10nM biotin respectively in 50 μ L samples. Since the concentration of biotin in the mouse ascites bearing OVCAR cells was less than 10nM, it appears that free biotin will not be a problem with the targeting design.

Biotin transport was studied to estimate the effect of exogenous biotin and nonspecific binding of liposomes. Biotin transport kinetic constants were determined by a Michaelis-Menten plot. The Vmax and Km were 51 ± 7.1 pmol/mg protein

/10min and $1.9 \pm 0.2 \mu\text{M}$ respectively in OVCAR cells and $8.5 \pm 1.3 \text{ pmol/mg protein/10min}$ and $1.3 \pm 0.4 \mu\text{M}$ respectively in SKOV cells. The transport mechanism was carrier-mediated and saturable as a function of biotin concentration. Uptake amounts were dependent on incubation time and biotin concentration. Biotin uptake was inhibited significantly by a 100-fold excess of exogenous unlabeled biotin ($5 \mu\text{M}$). The free biotin in human plasma (0.5 nM – 10 nM , Guilarte TR 1985; Mock DM *et al.*, 1992, 1996) and my studies with mouse ascites (below 10 nM) are quite low. Therefore, free biotin may not be a significant factor in inhibiting the targeting of biotinylated liposomes in therapeutic applications.

Biotinylated long-circulating liposomes encapsulated with sulforhodamine B were prepared using a commercial extruder. After incubation for 4 days at room temperature, the leakage of the free dye was less than 2%. CLSM images confirmed our hypothesis, indicating that biotinylated anti-CA125 Mab can specifically target CA125 antigen on the surface of ovarian cancer cells. Through the biotin-streptavidin system, biotinylated anti-CA125 Mab could attract biotinylated liposomes to specifically bind to the surface of ovarian cancer cells. Hence, this pretargeting concept can be used to deliver therapeutic drugs and radionuclides to ovarian cancer intraperitoneally. Biotinylated antibody is essential to mediate liposomal binding. Since biotinylated liposomes did not bind the OVCAR cells in the absence of biotinylated Mab and streptavidin, we can reach a conclusion that biotinylated liposomes specifically bind to ovarian cancer cells via biotinylated Mab and probably there is no nonspecific binding in this *in vitro* targeting study. It appears that the biotin transporter is not an alternative route for nonspecific uptake of the therapeutic entity.

FUTURE WORK

Radioimmunotherapy is really on its early stage. During the past two decades, many investigators have directed their attention to this field and many advances have been reported, indicating that RIT is a promising therapeutic approach in selectively

killing cancer cells (Nicholson S *et al.*, 1995; Meredith RF *et al.*, 1996; Andersson H *et al.*, 2001). However, there are still no clinical applications of RIT. The most promising indication, non Hodgkin's lymphoma, is still in clinical trials and close to approval (Abrams PG *et al.*, 2000). Many challenges still exist in this approach. Among these challenges, the antigen accessibility maybe the greatest problem to make this approach fail in clinical trials (Mann BD *et al.*, 1984). Although monoclonal antibody has high affinity and specific binding ability to specific antigen, less than 0.1% antibody targeting could be found in several clinical trials no matter what administration modality is used (Mann BD *et al.*, 1984; Abrams G *et al.*, 2000). The reason is due to many combined factors, including HAMA (human anti-mouse antibody) response, antigen may be shed or not expressed on all malignant cells, poor vascularization in the solid tumor, and high interstitial pressure (Strand SE *et al.*, 1993; McQuarrie SA *et al.*, 2000). Since streptavidin is immunogenic and not ideal for therapy, the bispecific monoclonal antibody should be developed to cross-link biotinylated long circulating liposomes to ovarian cancer cells. However, the affinity of BsMab could be lower than that of the biotin-streptavidin system, which is the strongest noncovalent biological binding between a protein and a ligand. Currently, the most emergent project is to determine if our bispecific monoclonal antibody has a high tumor uptake. Some experiments should be conducted as described below.

- Bispecific monoclonal antibody with anti-CA125 and anti-biotin paratopes, or its fragment or chimeric or humanized BsMab should be developed and evaluated. Its affinity to CA125 antigen and biotinylated liposomes and its immunoreactivity can be evaluated using different ELISA techniques, including a fluorescent ELISA technique. If the affinity of BsMab is less than 10^7 M^{-1} , it will be inadequate for *in vivo* targeting. Two-dimensional gel electrophoresis should be used to evaluate its purity.
- Its *in vitro* targeting ability and its ability to cross-link biotinylated liposomes should be determined using CLSM. The nonspecific binding of BsMab and biotinylated liposomes to other cells should be determined using CLSM. If the

nonspecific binding exists, the BsMab or biotinylated liposomes should be modified until there is no nonspecific binding *in vitro*. Additionally, the internalization and shedding kinetics of BsMab should be determined to assure that BsMab remains on the surface of ovarian cancer cells for some time to facilitate the second step of therapy.

- Its *in vivo* targeting ability and its cross-linking biotinylated liposomes should be determined using animal experiments. Tumor uptakes of radiolabeled BsMab or radiolabeled liposomes should be higher than 20%.

If we can obtain a BsMab with high tumor uptake and also high affinity to cross-link radiolabeled liposomes *in vitro* and *in vivo*, our approach may be successful. Clinical trials are more complicated. Although some research data of IP RIT indicated good results *in vivo*, favorable clinical trial results with IP RIT are not numerous, especially for advanced stages of ovarian cancer (Epenetos AA *et al.*, 1987; Andersson H *et al.*, 2001; Markman M 1998). One possible explanation is that the tumor uptake ratio is approximately 20% in mouse and less than 0.1% in human beings (Abrams G *et al.*, 2000). There may be different CA125 levels on the surface of ovarian cancer cells and in body fluids in mouse compared to that in human beings. For our project, we used the liposomes to encapsulate the radionuclide, which may greatly benefit this approach to IP RIT for ovarian cancer. Liposomes were recognized as a potential drug delivery system and developed as a potential therapeutic vehicle within the past 20 years. However, more than 100 liposomal formulation are already on the market, which indicates their great potential in delivering different drugs. The advantages and different types of liposomes have been discussed in Section 1.6. Liposomes can load more radionuclides than Mabs and their inherent targeting ability should greatly improve the tumor irradiation of this IP RIT. Therefore, future work also includes preparation of different liposomes to achieve the best distribution in ovarian cancer with IP administration *in vivo*.

Since 5 year survival of early stage is high up to 50-90% while 5 year survival of advanced stage is only 15-20% with current therapeutic approaches (Landis SH *et*

al., 1999; Michael C *et al.*, 1994), we may explore techniques of early detection to provide the best chance for recovery from ovarian cancer. We can develop methods, including HPLC, SDS-PAGE, ELISA, etc to see the difference in the ascites of normal people, early stage ovarian cancer patients, and advanced stage ovarian cancer patients to further progress on diagnosis and therapy of ovarian cancer.

REFERENCES

- Abrams GP, Fritzberg RA. Radioimmunotherapy of Cancer. Marcel Dekker, Inc. NY (2000)
- Ahmad I, Allen TM. Antibody-mediated specific binding and cytotoxicity of liposome entrapped doxorubicin to lung cancer cells *in vitro*. Cancer Res. 52: 4817 (1992)
- Ahmad I, Longenecker M *et al*. Antibody-targeted delivery of doxorubicin entrapped in sterically stabilized liposomes can eradicate lung cancer in mice. Cancer Res. 53: 1484 (1993)
- Allen TM, Chonn A. Large unilamellar liposomes with low uptake by the reticuloendothelial system. FEBS Lett. 223, 42-46 (1987)
- Allen TM, Hansen C *et al*. Liposomes containing synthetic lipid derivatives of polyethylene glycol show prolonged circulation half-lives *in vivo*. Biochim. Biophys. Acta 1066, 29-39 (1991)
- Allen TM, Hansen C *et al*. Subcutaneous administration of liposomes: a comparison with the intravenous and intraperitoneal routes of injection. Biochem. Biophys. Acta. 1150, 9-16 (1993)
- Alvarez R, Partridge E *et al*. Intraperitoneal radioimmunotherapy of ovarian cancer with ¹⁷⁷Lu-CC49: A phase I/II study. Gynecol Oncol 65:94 –101 (1997)
- Andersson H, Palm S *et al*. Comparison of the therapeutic efficacy of ²¹¹At- and ¹³¹I-labelled monoclonal antibody MOv18 in nude mice with intraperitoneal growth of human ovarian cancer. Anticancer Res; 21(1A): 409-12 (2001)

- Armstrong R, Friedrich V *et al.* *In vitro* analysis of the oligodendrocyte lineage in mice during demyelination and remyelination. *J. Cell Biol.* 111, 1183-1195. (1990)
- Ayre SG, Garcia DP *et al.* Insulin, chemotherapy, and the mechanisms of malignancy: the design and the demise of cancer. *Medical Hypotheses*. Vol. 55, No. 4 pp. 330-334 (2000)
- Bangham AD, Standish MM *et al.* The action of steroids and streptolysin S on the permeability of phospholipid structures to cations. *J Mol Biol* 13: 138-144. (1965)
- Bartoli M *et al.* Interaction of calmodulin with striatin, a WD-repeat protein present in neuronal dendritic spines. *J. Biol. Chem.*, 273, 22248-22253 (1999).
- Bast RC, Jr., Feeney M *et al.* Reactivity of a monoclonal antibody with human ovarian carcinoma. *J Clin Invest*; 68: 1331-1337 (1981)
- Bast RC, Jr., Klug TL *et al.* A radioimmunoassay using a monoclonal antibody to monitor the course of epithelial ovarian cancer. *N Engl J Med* 309: 883-887 (1983)
- Baumgartner ER, Suormala T. Inherited defects of biotin metabolism. *BioFactors*. Volume 10, pages 287-290 (1999)
- Bayer EA, Rivnay B. "On the mode of liposome-cell interactions. Biotin-conjugated lipids as ultrastructural probes". *Biochim. Biophys. Acta* 550. 464-473 (1979)
- Behr JP, Demeneix B *et al.* "Efficient gene transfer into mammalian primary endocrine cells with lipopolyamine-coated DNA" *Proc. Natl. Acad. Sci.* 86. 6982-6986 (1989)
- Berger M, Wood HH. Purification of the Subunits of Transcarboxylase by Affinity Chromatography on Avidin-Sepharose. *J. Biol. Chem.*, 250, 927 (1975).

- Berghammer P, Obwegeser R and Sinzinger H. Nuclear medicine and breast cancer: a review of current strategies and novel therapies. *The Breast* Vol. 10, No. 3, pp. 184-197 (2001)
- Betageri GV, Jenkins SA *et al.* Liposome drug delivery systems. Technomic Publishing Company, Inc. Lancaster, Pennsylvania USA. (1993)
- Bodey B, Siegel SE *et al.* Human cancer detection and immunotherapy with conjugated and non-conjugated monoclonal antibodies. *Anticancer Research* 16(2):661-74. (1996)
- Bonjour JP. Biotin. IN: Handbook of Vitamins (machlin, L.J. ed.) Marcel Dekker, Inc. New York, NY. pages 393-427. (1991)
- Brain E. Huber Brian I Carr. Molecular and Immunologic Approaches. Futura Publishing Company Inc. (1994)
- Brandl M. Bachmann D *et al.* Liposome preparation by a new high pressure homogenizer Gaulin Micron LAB 40. *Drug Dev.Ind.Pharm.* 16(14), 2167-2191(1990)
- Brian Matsumoto. Cell biological applications of confocal microscopy. Academic Press, Inc. 1250 Sixth Avenue, San Diego, California (1993)
- Breitz HB, Fisher DR *et al.* Dosimetry of rhenium-186-labeled monoclonal antibodies: methods, prediction from technetium-99m-labeled antibodies and results of phase I trials. *J Nucl Med* 34:908 -917 (1993)
- Capstick V, MacLean GD *et al.* Clinical evaluation of a new two-site assay for CA125 antigen. *Int J Biol Markers* 6:129-135 (1991)

- Centroze V, Pawley J. In Handbook of Biological Confocal Microscopy (Pawley, J., Ed.), 2nd ed., pp. 559–567, Plenum, New York. (1995)
- Chalet L, Wolf FJ. Arch Biochem. Biophys. 106 1-5 (1964)
- Chalet L, Miller TW *et al.* Antimicrob. Ag. Chemother 3, 28-32 (1963)
- Chatterjee NS, Kumar CK *et al.* Molecular mechanism of the intestinal biotin transport process. American Journal of Physiology 277(4 Pt 1): C605-613: (1999)
- Chetanneau A, Barbet J. *et al.* Pretargetted imaging of colorectal cancer recurrences using an ¹¹¹In-labelled bivalent hapten and a bispecific antibody conjugate. Nucl. Med. Commun. 15, 972-980 (1994)
- Christian JH. Thomas Ovarian cancer chemotherapy: *Cancer Treatment Reviews*. Vol. 27, No. 2, pp. 99-109 (2001)
- Coligan JE, Kruisbeek AM *et al.* Current protocols in immunology. Volume 1.2.3. John Wiley & Sonc. Inc. Baltimore, (1998)
- Cullis PR, Mayer LD *et al.* "Generating and loading of liposomal systems for drug-delivery applications", Adv. Drug Del. Rev. 3, 267-282 (1989)
- David M, Gershenson MD *et al.* Ovarian Cancer. Churchill Living stone Inc. P3. (1998)
- Davis WC, Methods in molecular biology. Monoclonal antibody protocols. Human Presee Inc. Totowa. NJ (1998)

Dayhoff MO. In: Atlas of Protein Sequence and Structure, Volume 5. National Biomedical Research Foundation. Washington D.C (1972)

Debra Weiner and Barry Wolf. Biotin Uptake, Utilization, and efflux in normal and biotin-deficient rat hepatocytes. *Biochemical medicine and metabolic biology* 46, 344-363, (1991)

DeLange RJ, Huang TS. *J. Biol. Chem.* 246, 698-709 (1971)

Dewhirst MW, Tso CY *et al.* Morphologic and hemodynamic comparison of tumor and healing normal tissue microvasculature. *Int J Radiat Oncol Biol Phys* 17, 91-99. (1989)

Dianne MF, Debra VH *et al.* Differential Effects of Administration of a Human Anti-CD4 Monoclonal Antibody, HM6G, in Nonhuman Primates. *Clinical Immunology*. Vol. 92, No. 2, pp. 138-152 (1999)

Dijk J. van, Tsuruo T *et al.* Bispecific antibodies reactive with the multidrug-resistance related glycoprotein and CD3 induce lysis of multidrug-resistant tumor cells. *Int. J. Cancer* 44, 738-743 (1989)

Divgi CR. Status of radiolabeled monoclonal antibodies for diagnosis and therapy of cancer; *Oncology* 10(6):939-953. (1996)

Donovan JW, Ross KD. *Biochemistry* 12 512-517 (1973)

Duke M *et al.* The biotin/avidin-mediated microtiter plate lectin assay with the use of chemically modified glycoprotein ligand. *Anal. Biochem.*, 221, 266-272 (1994).

Egbaria K, Weiner N. Topical application of liposomal preparations. *Cosmetics & Toiletries* 106, 79-93 (1991)

- Ehrlich P. *Studies in immunity*. New York: John Wiley and Sons, 404-443 (1910)
- Epenetos AA, Munro AJ *et al*. Antibody-guided irradiation of advanced ovarian cancer with intraperitoneally administered radiolabeled monoclonal antibodies. *J Clin Oncol* 5:1890 –1899. (1987)
- Ernest JT, Aldina SS *et al*. Assessment of the antitumour activity of targeted immunospecific albumin microspheres loaded with cisplatin and 5-fluorouracil. toxicity against a rodent ovarian carcinoma *in vitro*. *Cell Biology International*. Vol. 25, No. 1, pp. 51-59 (2001)
- Felgner JH, Kumar R *et al*. "Enhanced gene delivery and mechanism studies with a novel series of cationic lipid formulations", *J Biol Chem* 269, 2550-2561 (1994)
- Fendrick JL, Staley KA *et al*. Characterization of CA125 synthesized by the human epithelial amnion Wish cell line. *Tumor Biol* 14: 310-318. (1993)
- Finkler NJ, Muto MG *et al*. Intraperitoneal radiolabeled OC 125 in patients with advanced ovarian cancer. *Gynecol Oncol* 34:339 –344. (1989)
- Fleisher D, Niemiec SM *et al*. "Topical delivery of growth hormone releasing peptide using liposomal systems: an invitro study using hairless mouse skin" *Life Sci*. 57 1293-1297 (1995)
- Forssen EA, Tokes ZA. "Use of anionic liposomes for the reduction of chronic doxorubicin-induced cardiotoxicity". *Proc. Natl. Acad. Sci. USA* 78, 1873-1877 (1981)
- Freitag S *et al*. Structural studies of the streptavidin binding loop; *Protein Science* 6 1157-1166 (1997)

- Friguet B *et al.* Measurements of true affinity constant in solution of antigen-antibody copmplexes by enzyme-linked immunosorbent assays. *J. Immunol Methods* 77: 305-319 (1985)
- Gabizon A, Papahadjopoulos D. Liposome formulations with prolonged circulation time in blood and enhanced uptake by tumors. *Proc Natl Acad Sci USA* 85, 6949-6953. (1988)
- Garrido MA, Valdayo MJ *et al.* Targeting human T lymphocytes with bispecific antibodies to react against human ovarian carcinoma cells growing in nu/nu mice. *Cancer Res.* 50, 4227-4232 (1990)
- Gershenson DM, Mcguire WP. Ovarian cancer. Churchill Livingstone Inc. NY. USA (1998)
- Gestin JF, Loussouarn A *et al.* Two step targeting of xenografted colon carcinoma using a bispecific antibody and ^{188}Re -labeled bivalent hapten. biodistribution and dosimetry studies. *J. Nucl. Med.* 42: 146-153. (2001)
- Giorgio Bolis, Giovanna Scarfone *et al.* Response and Toxicity to Topotecan in Sensitive Ovarian Cancer Cases with Small Residual Disease after First-Line Treatment with Carboplatinum and Paclitaxel *Gynecologic Oncology*, Vol. 80, No. 1, pp. 13-15 (2001)
- Goers J *et al.* *Immunochemical Techniques Laboratory Manual* P81-92, P147-162 (1993)
- Goldsby RA, Kindt TJ *et al.* *Kuby immunology*. Fourthe Edition. W.H. Freeman and Company. NY, USA, (2000)

- Gregoriadis G, Florence AT. Liposomes in drug delivery. *Drugs* 45: 15-28. (1993)
- Gregoriadis G, McCormack. Targeting of Drugs. Strategies for Stealth Therapeutic Systems. Plenum Press, New York (1998)
- Green NM. Avidin.3. The nature of the biotin binding site. *Biochem. J.* 89, 599-609. (1963)
- Green NM. A spectrophotometric assay for avidin and biotin based on binding of dyes by avidin. *Biochem. Journal*, 94, 23c-24c (1965).
- Green NM. Spectrophotometric determination of avidin and biotin. *Meth. Enzymol.* 18A, 418-424 (1970).
- Green NM. *Advances in Protein Chemistry*. Academic Press. New York. 29, 85-133. (1975)
- Gruner SM, Lenk RP *et al.* "Novel multilayered lipid vesicles: Comparison of physical characteristics of multilamellar liposomes and stable plurilamellar vesicles". *Biochemistry* 24, 2833-2842 (1985)
- Gularte TR. Measurement of biotin levels in human plasma using a radiometric microbiological assay. *Nutr. Rep Int.* 31, 1155-1163 (1985)
- Hakes TB, Chalas E *et al.* Randomized prospective trial of 5 versus 10 cycles of cyclophosphamide, doxorubicin, and cisplatin in advanced ovarian carcinoma. *Gynecol Oncol* 45:284 –289, (1992)
- Han X, Papadopoulos AJ *et al.* Tumor Lymphocytes in Patients with Advanced Ovarian Cancer: Changes during *in vitro* Culture and Implications for Immunotherapy: *Gynecologic Oncology*, Vol. 65, No. 3, pp. 391-398 (1997)

Harrington KJ, Rowlinson-Busza G *et al.* Biodistribution and pharmacokinetics of ^{111}In -DTPA-labelled pegylated liposomes in a human tumour xenograft model: implications for novel targeting strategies *British Journal of Cancer*. Vol. 83, No. 2, pp. 232-238 (2000)

Hashimoto K, Loader JE *et al.* "Iodoacetylated and biotinylation liposomes: Effect of spacer length on sulfhydryl ligand binding and avidin precipitability". *Biochim. Biophys. Acta* 856, 556-565 (1986)

Hedda H. Van Ravenswaay Claasen *et al.* Immunotherapy in a Human Ovarian Cancer Xenograft Model with Two Bispecific Monoclonal Antibodies: OV-TL 3/CD3 and OC/TR: Gynecologic Oncology, Vol. 52, No. 2, pp. 199-206 (1994)

Heegaard NHHH, Bjerrum OJ. Affinity electrophoresis for determination of binding constants for antibody-antigen reactions. *Anal Biochem.* 195: 319-326 (1991)

Hoffman WL, O'Shannessy DJ. *J. Immunol. Meth.* 112, 113-120, (1988)

Hofland H, Huang L. Inhibition of Human Ovarian Carcinoma Cell Proliferation by Liposome-Plasmid DNA Complex. *Biochemical and Biophysical Research Communications*, Vol. 207, No. 2, pp. 492-496 (1995)

Hope MJ, Bally MB *et al.* Production of large unilamellar vesicles by a rapid extrusion procedure. Characterization of size distribution, trapped volume and ability to maintain a membrane potential. *Biochimica et Biophysica Acta.* 812 55-65 (1985)

Horber DH, Schott H *et al.* Cellular Pharmacology of N^4 -hexadecyl-1-beta-D-arabinofuranosylcytosine (NHAC) in the human leukemic Cell Lines K-562 and U-937. *Cancer Chemother. Pharmacol.*, 36: 483-492, (1995)

Holland JW, Hui C *et al.* "Poly(ethylene glycol)-Lipid Conjugates regulate the calcium-induced fusion of liposomes composed of phosphatidylethanolamine and phosphatidylserine". *Biochemistry*, 35, 2618-2624 (1996)

Hope MJ, Bally MB *et al.* "Production of large unilamellar vesicles by a rapid extrusion procedure: Characterization of size, trapped volume and ability to maintain a membrane potential". *Biochim. Biophys. Acta* 812, 55-65 (1985)

Ignatowski TA, Bidlack JM. Differential kappa-opioid receptor expression on mouse lymphocytes at varying stages of maturation and on mouse macrophages after selective elicitation. *J. Pharmacol. Exp. Ther.* 290, 863-870 (1999)

Jain RK. Physiological barriers to delivery of monoclonal antibodies and other macromolecules in tumors. *Cancer Res.* 50: 814 (1990)

Jan AA, Kamps M *et al.* Uptake of Liposomes Containing Phosphatidylserine by Liver Cells *in vivo* and by Sinusoidal Liver Cells in Primary Culture: *In vivo-in vitro* Differences. *Biochemical and Biophysical Research Communications*, Vol. 256, No. 1, pp. 57-62 (1999)

Jeyakumar A, Cabeza R *et al.* Late Recurrence in Ovarian Dysgerminoma with Successful Response to Standard Adjuvant Chemotherapy: A Case Report and Review of the Literature. *Gynecologic Oncology*, Vol. 81, No. 2, pp. 314-317 (2001)

Juliano RL, Stamp D. "Pharmacokinetics of liposome-encapsulated antitumor drugs: Studies with vinblastine, actinomycin D, cytosine, arabinoside and daunomycin". *Biochem. Pharmacol.* 27, 21-27 (1978)

Kenemans P, Yedema CA, Bon GG, von Mensdorff-Pouilly S. CA 125 in gynecological pathology--a review. [Review]. *Eur J Obst, Gyn. Reprod Biol* 49(1-2):115-24. (1993)

- Kim S . Liposomes as carriers of cancer chemotherapy. *Drugs*. 46:618. (1993)
- Kim S. Liposomes as carriers for cancer chemotherapy: current status and future prospects. *Drugs* 46: 618-638. (1994)
- Kinsky SC, Nicolotti RA *et al*. Immunological properties of model membranes. *Ann. Rev. Biochem.* 46, 49, (1977)
- Klein JL. Kopher KA *et al*. Ferritin concentration and ^{131}I antiferritin tumor localization in experimental hepatome. *Int J. Radiat. Oncol. Biol. Phys.* 12:137. (1986)
- Knowles JR. *Annu. Rev. Biochem.* 58,195-221 (1989)
- Koeller Jim. Joseph Tami. Concepts in immunology and Immunotherapeutics. American Society of Hospital Pharmacists. (1990)
- Koller-Lucaae, SKM. Suter M *et al*. Metabolism of the new liposomal anticancer drug N^4 -octadecyl-1-beta-D-arabinofuranosylcytosine (NOAC) (NOAC) in mice. *Drug Metabolism and Disposition*,27: 342-3650. (1999)
- Kohler G, Milstein C. *Nature*; 256. 495-497: (1975)
- Kriangkum J, Xu B *et al*. Development and characterization of a bispecific single-chain antibody directed against T cells and ovarian carcinoma. *Hybridoma*; 19(1):33-41 (2000)
- Krieg PA, Milton DA. *Methods Enzymol.* 25, 397-415 (1987)

Kudelka A, Tresukosol D *et al.* Phase II study of intravenous topotecan as a 5-day infusion for refractory epithelial ovarian carcinoma. *J Clin Oncol* 14:1552–1557, (1996)

Lain S *et al.* *J. Virol* 65, 1-6 (1991)

Landis SH, Murray T *et al.* Cancer statistics. *Cancer J Clin* 49:8 –31. (1999)

Lanzavecchia A, Scheidegger D. The use of hybrid hybridomas to target human cytotoxic T lymphocytes. *Eur. J. Immunol.* 17, 105-111 (1987)

Lasic DD. "Liposomes: synthetic lipid microspheres serves as multipurpose vehicles for the delivery of drugs, genetic material and cosmetics". *American Scientist* 80, 20-31 (1992)

Leibel SA, Phillips TL. Textbook of radiation oncology. W.B. Saunders Company. Philadelphia. Pennsylvania USA (1998)

Leserman L, Machy P *et al.* "Targeted liposomes and intracellular delivery of macromolecules", *Prog. Clin. Biol. Res.* 343, 95-102 (1990)

Levi M, Sparvoli E *et al.* Biotin-streptavidin immunofluorescent detection of DNA replication in root meristems though Brd Urd incorporation: cytological and microfluorimetric applications. *Physiol. Plantarum* 79, 231-235 (1990)

Li L, Lishko LV *et al.* Liposomes can specifically target entrapped melanin to hair follicles in histocultured skin, *In vitro Cell. Dev. Biol.* 29A: 192-194 (1993a)

Li L, Lishko LV *et al.* Liposomes targeting high molecular weight DNA to hair follicles in histocultured skin: a model for gene therapy of the hair growth process. *In vitro Cell. Dev. Biol.* 29A: 258-260 (1993b)

- Lomant AJ, Fairbanks GJ. Mol Biol. 104. 243-261 (1976)
- Loughrey HC, Bally MB *et al.* "A non-covalent method of attaching antibodies to liposomes", Biochim. Biophys. Acta 901. 157-160 (1987)
- Ma TY, Dyer DL, and Said HM. Human intestinal cell line Caco-2: a useful model for studying cellular and molecular regulation of biotin uptake. Biochimica et Biophysica Acta, 1189: 81-88, (1994)
- Malik Juweid, Lawrence C *et al.* Prospects of Radioimmunotherapy in Epithelial Ovarian Cancer: Results with Iodine-131-Labeled Murine and Humanized MN-14 Anti-carcinoembryonic Antigen Monoclonal Antibodies. Gynecologic Oncology. Vol. 67, No. 3, pp. 259-271 (1997)
- Markman M. Intraperitoneal therapy of ovarian cancer. Semin. Oncol. 25, 356-360 (1998)
- Marvin Minsky, U. S. Pat. 3, 013, 467 (1957)
- Marvin Minsky. Memoir on Inventing the Confocal Scanning Microscope. Published in Scanning, vol.10 pp128-138, (1988)
- Masuho Y, Zzlutsky M *et al.* Interaction of monoclonal antibodies with cell surface antigens of human ovarian carcinomas. Cancer Res. 44: 2813-2819; (1984)
- Matsuoka Y, Nakashima T *et al.* Recognition of ovarian cancer antigen CA125 by murine monoclonal antibody produced by immunization of lung cancer cells . Cance Res, 47: 6335-6340, (1987)

- Matthay KK, Heath TD *et al.* Specific enhancement of drug delivery to AKR lymphoma by antibody-targeted small unilamellar vesicles. *Cancer Res.* 44, 1880-1886 (1984)
- Mattaj IW. *Cell* 73, 837-840 (1993)
- Mayer LD, Hope MJ *et al.* Solute distributions and trapping efficiencies observed in freeze-thawed multilamellar vesicles. *Biochimica et Biophysica Acta* 817 193-196 (1985)
- Mayer LD, Hope MJ *et al.* Vesicles of variable sizes produced by a rapid extrusion procedure. *Biochimica et Biophysica Acta* 858 161-168 (1986)
- Mayhew E, Lazo R *et al.* Characterization of liposomes prepared using a microfluidizer. *Biochem. et Biophys. Acta* 775, 169-174, (1984)
- McGinn KA, Haylock PJ. *Women's Cancers.* Hunter House Inc. Alameda CA (1998)
- McQuarrie SA, Riauka T *et al.* The effects of circulating antigen on the pharmacokinetics and radioimmunoscinigraphic properties of ^{99m}Tc labelled monoclonal antibodies in cancer patients. *J. Pharma. Pharmaceut Sci.* 1 (3) 115-125 (1998)
- McQuarrie SA, Xiao Z *et al.* Modern trends in radioimmunotherapy of cancer: Pretargeting strategies for the treatment of ovarian cancer. *Q. J. Nucl. Med.* 45: 160-6 (2001)
- Meier T, Fahrenholz F. *A laboratory guide to biotin-labeling in biomolecule analysis.* P2-27, Birkhauser verlag, PO Box 133, CH-4010 Basel, Switzerland (1996)

Merck Index, 11th Edition, Merck & Co. Rahway, NJ, p192 (1989)

Merck Index, 12th Ed. #920 (1996)

Meredith RF, Partridge EE *et al.* Intraperitoneal radioimmunotherapy of ovarian cancer with lutetium 177-CC49. J. Nucl. Med. 37(9): 1491-6. (1996)

Mezzanzanica D, Canevari S *et al.* Human ovarian carcinoma lysis by cytotoxic T cells targeted by bispecific monoclonal antibodies: Analysis of the antibody components. Int. J. Cancer 41, 609-615 (1988).

Mezzanzanica D, Garrido MA *et al.* Human T lymphocytes targeted against an established human ovarian carcinoma with a bispecific F(ab')₂ antibody prolong host survival in a murine xenograft model. Cancer Res. 51, 5716-5721 (1991)

Michaele C, Christian MD *et al.* Salvage Chemotherapy for Epithelial Ovarian Carcinoma. Gynecologic Oncology, Vol. 55, No. 3, pp. S143-S150 (1994)

Milstein C, Cuello AC. Hybrid hybridomas and the production of bispecific monoclonal antibodies. Immunol. Today 5, 299-304 (1984)

Milstein C, Cuello AC. Hybrid hybridomas and their use in immunohistochemistry. Nature 305, 537-540 (1983)

Mock DM, Malik MI. Distribution of biotin in human plasma. Most of the biotin is not bound to protein. Am J. Clin. Nutr. 56 427-432 (1992)

Mock DM *et al.* Present Knowledge in Nutrition. Washington D.C. ILSI Press, 220-236 (1996)

- Mock DM *et al.*. Eds. Nutrition in Health and Disease, 9th Edition. Baltimore: Williams & Wilkins, pages 459-466 (1999)
- Moller SA, Reisfeld RA. Bispecific monoclonal antibody directed lysis of ovarian carcinoma cells by activated human T lymphocytes, *J. Immunol. Immunother.* 33, 210-216 (1991)
- Moore GE, Gerner RE *et al.* Culture of normal human leukocytes. *JAMA.* 199, 519-524 (1967)
- Moore GE, Woods LK. Culture media for human cells PRMI 1603, RPMI 1634, PRMI 1640 and GEM 1717. Tissue culture association manual. 3 503-508. (1976)
- Nassander UK, Steerenberg PA *et al.* *In vivo* targeting of OV-TL 3 immunoliposomes to ascitic ovarian carcinoma cells (OVCAR-3) in athymic nude mice. *Cancer Res.* 52, 646-653. (1992)
- Nicholson S, Epenetos A. Adjuvant radioimmunotherapy of ovarian cancer: long-term survival data . *Anticancer Res.* 15(6A): 2435-6. (1995)
- Nimmo GR *et al.* Influence of antibody affinity on the performance of different antibody assays. *J. Immunol. Methods.* 72:177-187 (1984)
- Noujaim AA, Baum RP *et al.* Monoclonal antibody B43.13 for immunoscintigraphy and immunotherapy of ovarian cancer. In: Klapdor R (Ed.) *Current tumor diagnosis: Applications, clinical relevance, trends.* W Zuckschwerdt Verlag, Munich, pp 823-829 (1994).
- Nouwen EJ, Hendrix PG *et al.* Tumor markers in the human ovary and its neoplasms. A comparative immunohistochemical study. *Am J Pathol* 126: 230-242; (1987)

- Nustad K *et al.* Specificity and affinity of 26 monoclonal antibodies against the CA125 antigen. *Tumor Biology* 17:196-219, (1996)
- O'Brien TJ, Hardin JW *et al.* CA125 antigen in human amniotic fluid and fetal membranes. *Am J Obstet Gynecol* 155: 50-55, (1986)
- Olson F, Hunt CA *et al.* Preparation of liposomes of defined size distribution by extrusion through polycarbonate membranes. *Biochim. Biophys. Acta* 587. 522-539 (1979)
- Ostro MJ, Cullis PR. Use of liposomes as injectable-drug delivery systems. *Am. J. Hosp. Phar.* 46, 1576-1587 (1989)
- Paganelli G, Pervez S *et al.* Intraperitoneal radio localization of tumors pretargeted by biotinylation monoclonal antibodies. *Int. J. Cancer.* 45, 1184-1189 (1990)
- Parkin DM, Pisani P *et al.* Estimates of the worldwide incidence of eighteen major cancers in 1985. *Int J Cancer* 54:594 –606, (1993)
- Park JW, Hong K *et al.* Development of anti-p185HER2 immunoliposomes for cancer therapy. *Proc. Natl Acad. Sci.* 1327-1331. (1995)
- Papahadjopoulos D, Allen TM *et al.* *Proc Natl Acad Sci*, 88, 11460-11464 (1991)
- Perez P, Hoffman R *et al.* Specific targeting of human peripheral blood T cells by heteroaggregates containing anti-Ts crosslinked to anti-target cell antibodies. *J. Exp. Med.* 163, 166-178 (1986).
- Pratt WB, Ruddon RW *et al.* *The Anticancer Drugs*(second edition): Oxford University Press Inc. New York, 1994

- Pupa SM, Canevari S *et al.* Activation of mononuclear cells to be used for hybrid monoclonal antibody-induced lysis of human ovarian carcinoma cells. *Int. J. Cancer* 42, 455-459 (1988)
- Ramaswamy K. Intestinal absorption of water-soluble vitamins Focus on "Molecular mechanism of the intestinal biotin transport process". *American Journal of Physiology* , 277(4 Pt 1): C603-604 , (1999)
- Rao SV *et al.* Controlled layer-by-layer immobilization of horseradish peroxidase *Biotechnol. Bioeng.* 65, 389-396 (1999)
- Robert V, Higgins R *et al.* Is Age a Barrier to the Aggressive Treatment of Ovarian Cancer with Paclitaxel and Carboplatin? *Gynecologic Oncology*, Vol. 75, No. 3, pp. 464-467 (1999)
- Roland PY, Barnes MN *et al.* Response to Salvage Treatment in Recurrent Ovarian Cancer Treated Initially with Paclitaxel and Platinum-Based Combination Regimens: *Gynecologic Oncology*, Vol. 68, No. 2, pp. 178-182 (1998)
- Rongen H, Bult A *et al.* Liposomes and immunoassays review article. *Journal of Immunological Methods*, 204 105-133 (1997)
- Rose N, DeMacrio E *et al.* *Manual of Clinical Laboratory Immunology*. American Soc. Microbiology Press, Washington, D.C., (1997)
- Rosenfeld ME, Feng M *et al.* Adenoviral-mediated delivery of the herpes simplex virus thymidine kinase gene selectively sensitizes human ovarian carcinoma cells to ganciclovir. *Clin Cancer Res* 1:1571-1580, (1995)
- Ross SE, Carson SD *et al.* *BioTechniques* 4, 350-354 (1986)

- Russell NS, Bartelink H. Radiotherapy: the last 25 years. *Cancer Treatment Reviews*. Vol. 25, No. 6, pp. 365-376. Dec. (1999)
- Said HM, Alvaro Oratiz *et al.* Biotin uptake by human colonic epithelial NCM460 cells: a carrier-mediated process shared with pantothenic acid. *American Journal of Physiology*, volume 275: pages C1365-C1371, (1998)
- Scatchard G. The attraction of proteins to small molecules and ions. *Ann. NY Acad. Sci.* 51, 660-672. (1949)
- Scheinberg DA, Straus DJ *et al.* A phase I toxicity, pharmacology, and dosimetry trial of monoclonal antibody OKB7 in patients with non-Hodgkin's lymphoma: effects of tumor burden and antigen expression. *J. Clin Oncol.* 8: 792-803 (1990)
- Schwendener *et al.* *Biochim. Biophys. Acta* 1026: 69-79 (1990).
- Schwendener RA. The preparation of large volumes of homogeneous, sterile liposomes containing various lipophilic cytostatic drugs by the use of a capillary dialyzer. *Cancer Drug Deliv* Spring; 3(2): 123-9 (1986)
- Schwendener RA, Schott H. Lipophilic 1-beta-D-arabinofuranosyl cytosine derivatives in liposomal formulations for oral and parenteral antileukemic therapy in the murine L1210 leukemia model. *J. Cancer Res. Clin. Oncol.* 122: 723-726, (1996)
- Shek PN, Barber RF. Liposomes: A new generation of drug and vaccine carriers. *Mod. Med. Canada* 41, 314-382 (1986)
- Shalaby MR, Shepard HM *et al.* Development of humanized bispecific antibodies reactive with cytotoxic lymphocytes and tumor cells overexpressing the HER2 protooncogene, *J. Exp. Med.* 175, 217-225 (1992).

- Shotton DM. J. Cell Sci. 89, 129-150 (1989)
- Stamatos L, Leventis R *et al.* Interactions of cationic lipid vesicles with negatively charged phospholipid vesicles and biological membranes. Biochemistry 27, 3917-3925 (1988)
- Stewart JSW, Hird V *et al.* Intraperitoneal yttrium-90-labeled monoclonal antibody in ovarian cancer. J Clin Oncol 8:1941–1950. (1990)
- Steward MW, Lew AM. The importance of antibody affinity in the performance of immunoassays for antibody. I. Immunol. Methods. 78: 173-190 (1985)
- Stockler M, Wilcken NRC *et al.* Systematic reviews of chemotherapy and endocrine therapy in metastatic breast cancer. Cancer Treatment Reviews, Vol. 26, No. 3 pp. 151-168 (2000)
- Suresh MR, Cuello AC *et al.* Advantages of bispecific hybridomas in one step immunocytochemistry and immunoassays. Proc. Nat. Acad. Sci. USA 83, 7989-7993 (1986)
- Szoka F, Papahadjopoulos D. Comparative properties and methods of preparation of lipid vesicles (liposomes). Ann. Rev. Biophys. Bioeng. 9, 467-508 (1980)
- Talsma H, Crommelin DJA. Liposomes as Drug Delivery Systems. Part I: Preparation. Pharmaceutical Technology 16, 96-106 (1992)
- Talsma H, Crommelin DJA. Liposomes as Drug Delivery Systems. Part II: Characterization. Pharmaceutical Technology 16, 52-58 (1992)
- Talsma H, Crommelin DJA. Liposomes as Drug Delivery Systems. Part III: Stabilization. Pharmaceutical Technology 17, 48-59 (1992)

- Tannock IF, Lee C. Anti-cancer drugs. *British Journal of Cancer*. Vol. 84. No. 1 pp. 100-105 (2001)
- Tenereillo MG, Park RC. Early detection of ovarian cancer. *CA Cancer J Clin* 45:71– 87. (1995)
- Torchilin VP, Lukyanov AN *et al.* Interaction between oleic acid-containing pH-sensitive and plain liposomes. Fluorescent spectroscopy studies. *FEBS Lett* 305. 185-188 (1992)
- Tuxen MK, Soletormost G *et al.* Tumor markers in the management of patients with ovarian cancer. *Cancer Treat Rev* 21(3): 215-45 (1995)
- Van Hoesel Q.G.C.M., Steerenberg PA, Crommelin DJA. "Reduced cardiotoxicity and nephrotoxicity with preservation of antitumor activity of doxorubicin entrapped in stable liposomes in the LOU/M Wsl rat". *Cancer Res*. 44, 3698-3705 (1984)
- Vingerhoeds MH, Storm G *et al.* Immunoliposomes *in vivo* immunomethods 4, 259-272 (1994)
- Vivian E, von Gruenigen *et al.* *In vivo* Studies of Adenovirus-Based p53 Gene Therapy for Ovarian Cancer: *Gynecologic Oncology*, Vol. 69, No. 3, pp. 197-204 (1998)
- Wang MH, Claudine Rancourt *et al.* High-Efficacy Thymidine Kinase Gene Transfer to Ovarian Cancer Cell Lines Mediated by Herpes Simplex Virus Type 1 Vector *Gynecologic Oncology*, Vol. 71, No. 2, pp. 278-287 (1998)

- Webb MS, Harasym TO *et al.* "Sphingomyelin-cholesterol liposomes significantly enhance the pharmacokinetic and therapeutic properties of vincristine in murine and human tumour models", *Br J Cancer* 72, 896-904 (1995)
- Weber *et al.* *J. Am. Chem. Soc.* 114: 3197 (1992)
- Wei R, Wright LD. Heat Stability of Avidin and Avidin-Biotin Complex and Influence of Ionic Strength on Affinity of Avidin for Biotin. *Proc. Soc. Exp. Biol. Med.*, 117,341(1964).
- White JG *et al.* Optical microscopy for biology (B. Herman and K. Jacobson, eds.) pp1-18. Alan R. Liss, NY (1990)
- Wilchek M, Bayer EA. The avidin-biotin complex in bioanalytical applications. *Anal. Biochem.* 171, 1-32 (1988)
- Wilcheck M, Bayer EA. Avidin-biotin technology, in *Methods in Enzymology*. Vol 184, Academic New York pp 213-217 (1990)
- Wilson T. *Trends Neurosci.* 12, 486-493 (1989)
- Winkelstein A, Donnenberg A. Clinical Application of Flow Cytometry. *Human Immunology* Eds. Leffell, M. S., Donnenberg, A. D., and Rose, N. R. CRC Press, New York. (1997)
- Wolff B, Gregoriadis G. The use of monoclonal anti-Thy1 IgG1 for the targeting of liposomes to AKR-A cells *in vitro* and *in vivo*. *Biochim. Biophys. Acta* 802, 259-273 (1984)
- Woolley DW, Longsworth LG. Isolation of an antibiotin factor from egg white ; *J. Biol. Chem.* 142, 285-290 (1942)

Van,Gog FB, Visser GW *et al.* High dose rhenium-186-labeling of monoclonal antibodies for clinical application: pitfalls and solutions. *Cancer* 15;80(12 Suppl):2360.-70 (1997)

Voet Donald, Voet JG. Fundamentals of Biochemistry. John Wiley & Sons Inc. (1999)

Xiao Z. McQuarrie SA *et al.* A three step strategy for targeting drug carriers to human ovarian carcinoma cells in vitro. *J. Biotechnol.* (in press) 2001

Zempleni J. Mock DM. Biotin biochemistry and human requirements. *Journal of Nutritional Biochemistry.* volume 10: page 128-138 (1999)

Zhang LG, Hu JC *et al.* Preparation of Liposomes with a Controlled Assembly Procedure. *Journal of Colloid and Interface Science.* Vol. 190, No. 1, pp. 76-80 (1997)

Zigterman GJ. Snippe WJ *et al.* Adjuvant effects of nonionic block polymer surfactant on liposome-induced humoral immune response. *J. Immun.* 138, 220-225 (1987)

Zurawski VR, Jr., *et al.* Tissue distribution and characteristics of the CA125 antigen. *Cancer Rev.* 11-12: 102-118; (1988)